POLITECNICO DI TORINO

Master of Science Course

In Energy and Nuclear Engineering

Master of Science Thesis

REVAMPING AND OPTIMIZATION OF A GROUND MOUNTED GRID-CONNECTED PHOTOVOLTAIC PLANT

Tutor: Ing. Filippo Spertino *Candidate: Davide Fissore*

Academic year 2017/2018

Table of contents

0. Introduction

"Just as energy is the basis of life itself, and ideas the source of innovation, so is innovation the vital spark of all human change, improvement and progress"

—**Theodore Levitt**

Our society is based on progress; progress is aimed at improving the quality of life, but it is however closely connected to the need of energy.

Since world energy demand is expected to grow, year by year, the goal of the next future is to make this growth sustainable for the planet and all living species.

The aim of the introductory part of this treaty is to furnish a brief general overview of the global energy context and its possible evolution in the next future, strengthening the crucial role which renewable sources of energy can have in this sense, especially considering the preservation of the planet and of all its inhabitants.

0.1. Present and future of energy: world context

0.1.1. Primary energy mix

World demand of energy, in all its forms, can be usually accomplished by converting the energy from one form to another. The energy required in its original status is known as primary energy[1]; the amount of primary energy required is greater than the effective energy demand, due to unavoidable losses in these conversion processes.

Next graph shows the primary energy mix evolution with time.[2]

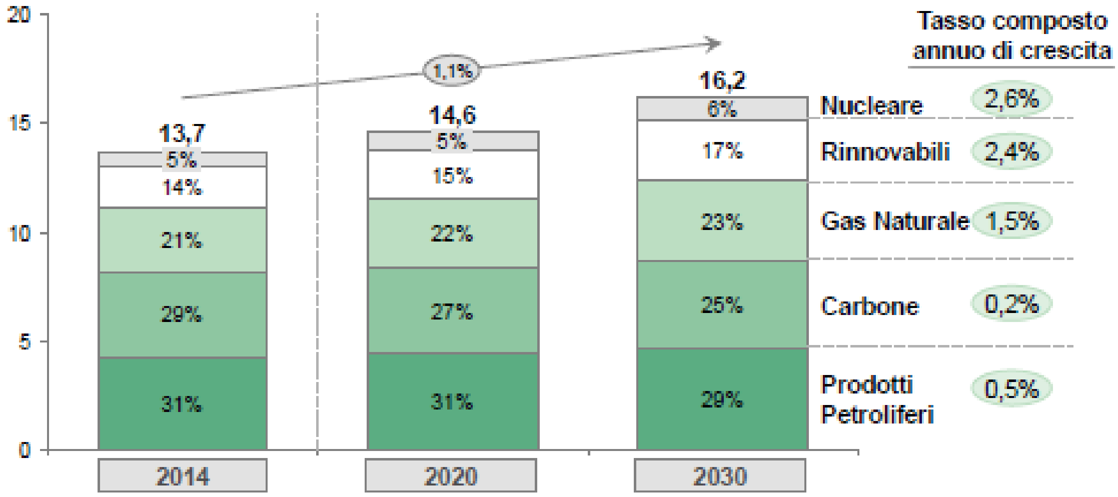

Figure 0.1 - Evolution of the global primary energy mix by source (Gtoe) - IEA, WEO 2016 (New Policies Scenario)

World energy mix, in terms of primary energy, represents how the global energy demand, expressed in Gtoe[3], is accomplished by source of energy. The graph has been traced according to the "New Policies Scenario", which imagines that all policies and strategies aimed at the fossil fuel plants phase-out and renewables subsidies settlement, that have already been announced or not, will take place. In other words, it is a scenario which favours a strong RES penetration in the energy market.

---

[1] Primary energy is energy in terms of primary matter (fossil fuels, solar power etc.).

[2] Previsions by IEA ("International Energy Agency"), publisher of annual reports (WEO –"World Energy Outlook") about world energy situation.

[3] Toe = Tonne of Oil Equivalent. 1 toe = 5347 kWh.

For each year of the analysis, primary energy mix is decomposed through percentages associated to all main primary energy sources available in the market.

According to IEA previsions, world primary energy demand is expected to grow from 13.7 Gtoe of 2014 to 16.2 Gtoe of 2030, with an annual growth rate of 1.1 %. Inevitably, to compensate the growth, all the main primary sources will subsequently see an evolution in request, but with different growth rates.

In particular, the graph highlights an important decrease of the role of traditional fossils, except for the natural gas, looking forward to decarbonisation[4]. This process would not be sustainable unless this energy "lack", caused by reduction of traditional fossils, is compensated by the growth of carbon-free technologies, such as renewables and nuclear.

Renewables sources have one of the highest growth rates in terms of share in primary energy (2.4%/year); for many countries, renewables have become the cheapest source of energy available in the market, and they convey two-thirds of global investments in power plants.

It is expected that electrical renewables[5], such as photovoltaic and wind, will see a reduction of LCOE ("Levelized Cost Of Electricity") of 40-70 % and 10-25 % respectively by 2040, especially thanks to technological developments of the grid and of battery systems. At the same time, also thermal renewables[6] will grow, and acquire a greater share in overall heat production by 2030.

The same growth rate is expected to be also for nuclear energy, especially for Asian countries, despite the technology is quite old and widespread.

[4] The decarbonisation of the power sector means reducing its carbon intensity; that is, the emissions per unit of electricity generated (often given in grams of CO2 per kWh).
[5] For direct production of electricity (PV, wind, hydro, etc.).
[6] For heat production (geothermal, solar, bio-energy, etc.).

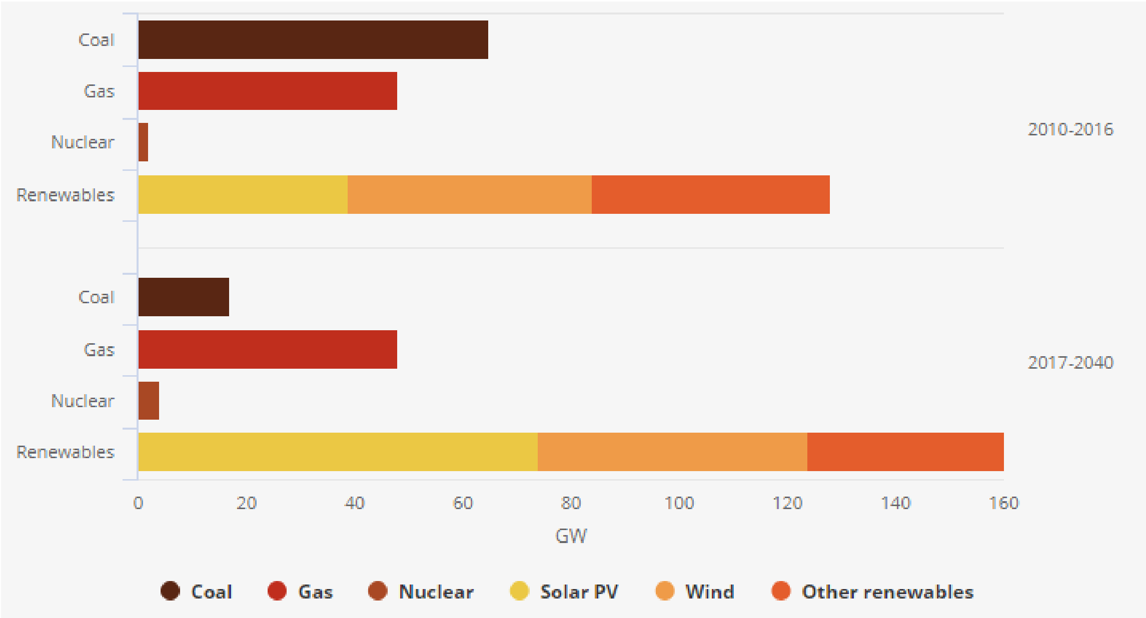

Figure 0.2 - Global annual net capacity additions by type (GW) - IEA WEO (2017) New Policies Scenario

The previous histogram reports the average annual growth in installed capacity of all the main energy technologies for the period 2010-2016, and speculates the trend for the period 2017-2040, according to the new policy scenario.

What is evident is the crucial role of renewables, and the subsequent decaying importance of coal and other traditional fossils as energy source.

Coal annual net capacity addition is expected to fall dramatically from 65 GW of 2010-2016 to 17 GW of 2017-2040 and, if natural gas remains almost constant, renewables are expected to compensate, by enhancing their shares.

The highest growth regards solar PV: annual additions will almost double, from 39 GW of 2010-2016 to 74 GW of 2017-2040. Especially thanks to China and India development, it is expected to become, by 2040, the principal low-carbon source in terms of installed capacity. This very impressive growth can be partly explained considering that solar PV is both a concentrated (in huge installations) and a distributed source (from traditional houses to large industrial plants), therefore it has a wider market to exploit.

0.1.2. Energy demand

Energy demand concerns the request of energy of the final users, which is generally in a different form with respect primary energy, so as to be more usable.

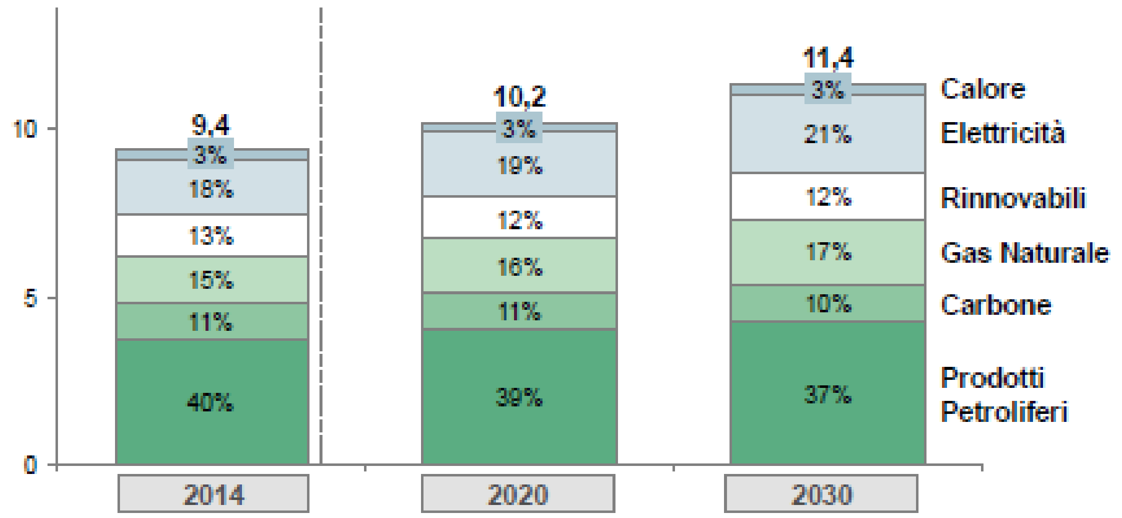

Figure 0.3 - Evolution of the gross final consumption by source (Gtoe) - IEA, WEO 2016 (New Policies Scenario). The term renewables include only RES for heat and transportation; electrical renewables are included into the electricity term.

Previous graph shows how the end-user demand is accomplished and will be accomplished, by source of energy, in the next 20 years. A negative trend of traditional fossils would be balanced by a rise of natural gas and especially electricity (considering all ways of production).

According to the very last IEA WEO report (2017), electricity rise for end-uses at 2040 is expected to be of 40% with respect current share, which is comparable to the growth which has undergone oil in the last 25 years.

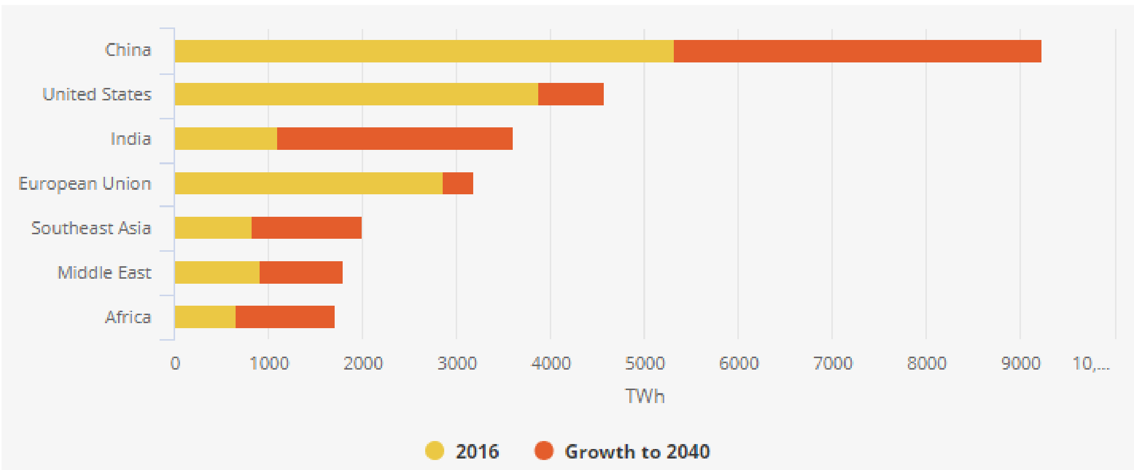

Figure 0.4 - Electricity demand by selected region

The greatest growth will be present in countries in rapid industrialization, such as India and China. The last one, not surprisingly, has become the world's leading producer of photovoltaic modules.

The electrification of the demand means that electricity will be far more rooted in the end-user life in different aspects. Sectors in which electricity importance would raise the most are mobility and heat production, traditionally associated to fossils or other types of RES.

Historically, transportation has been a sector in which traditional fossils are still now the major actors: changing the situation will be a very tough challenge for the next future, especially from a social and economic point of view. E-mobility, i.e. electricity as a source for transportation, is the new frontier. IEA expects the global electric car fleet to expand from 2 million of 2016 to almost 280 million of 2040.

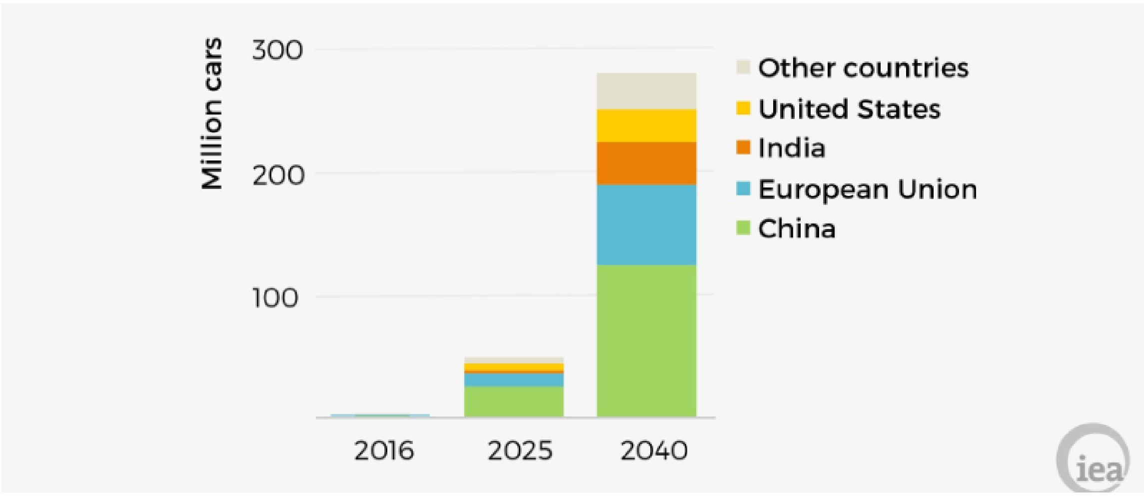

Figure 0.5 - Electric car fleet, 2016-2040

0.2. The Italian situation

Italy, in the very last years, has undergone an important growth in the renewable area, especially in the electrical sector. This growth has brought renewables till the 17.5 % of share on gross final consumption in 2015[7], which has enabled the country to overcome in advance the 20-20-20 target of 17 % of renewable overall penetration for 2020.

Italian statistics are very favourable, especially if compared with the other major European countries.

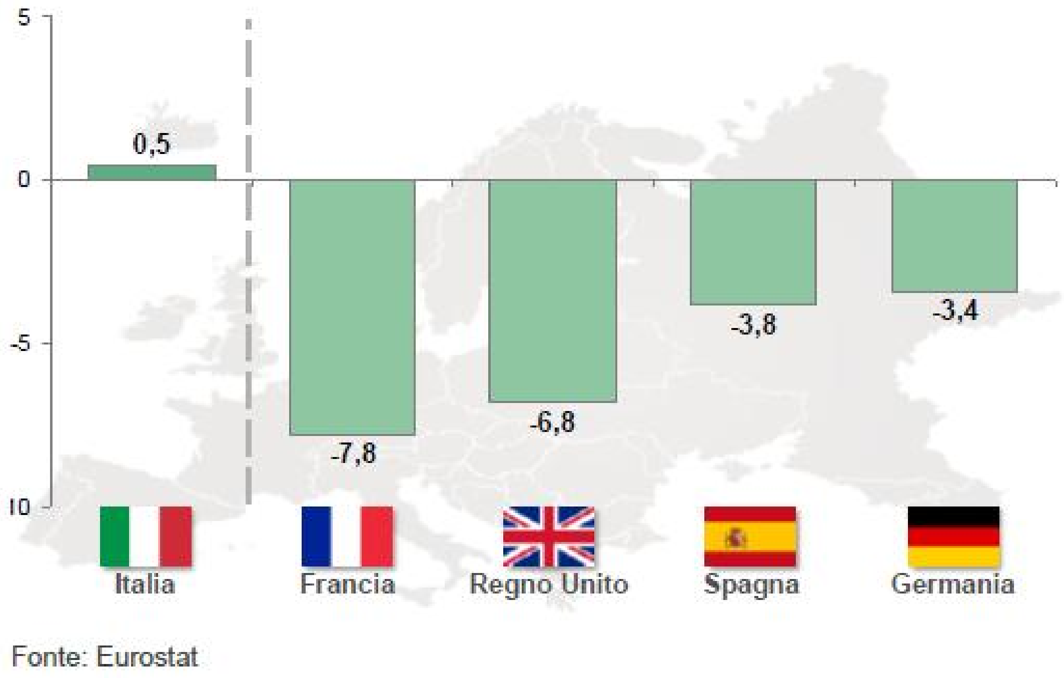

Figure 0.6 - Renewable penetration (2015) vs. 2020 target

Fig 0.6 shows the renewable penetration[8] in 2015, in comparison to the same indicator with the 2020 target's value, for the major European countries.

The contradiction inherent to the presented situation concerns the fact that, in Italy, there is a bigger disequilibrium between RES energy employment sectors; electrical and thermal renewables are the most widespread, and the main authors of the rapid achievement of the European goals, especially thanks to very generous settlement policies which have encouraged their development. On the other side, RES penetration in other sectors, like transportation, is clearly under average with respect other European countries.

[7] Eurostat shares 2015 – Short Assessment of Renewable energy sources.
[8] Amount of energy produced by all types of renewables to the total energy demand.

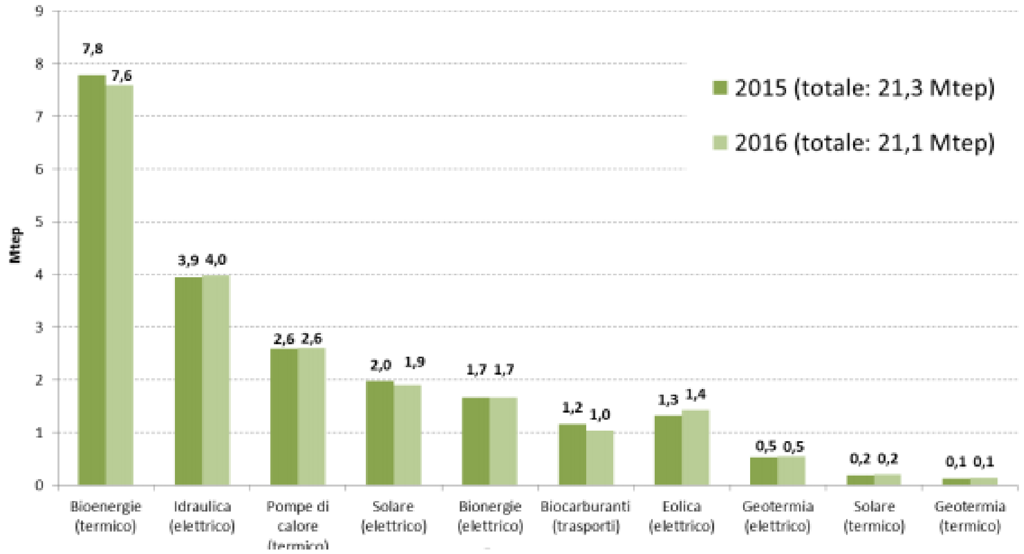

Figure 0.7 - Contribution of individual sources to gross final consumption of RES energy

The graph shows how the 17.5% of share of RES on gross final consumption is achieved; in front of an overall consumption of 132 Mtep, 21.1 Mtep are guaranteed by renewables, especially of thermal and electrical type.

For what concerns electrical renewables, they were the real workhorse for achieving the 20-20-20 goal; in 2015, the 33.5 % of the Italian final consumption of electricity was covered by renewables.

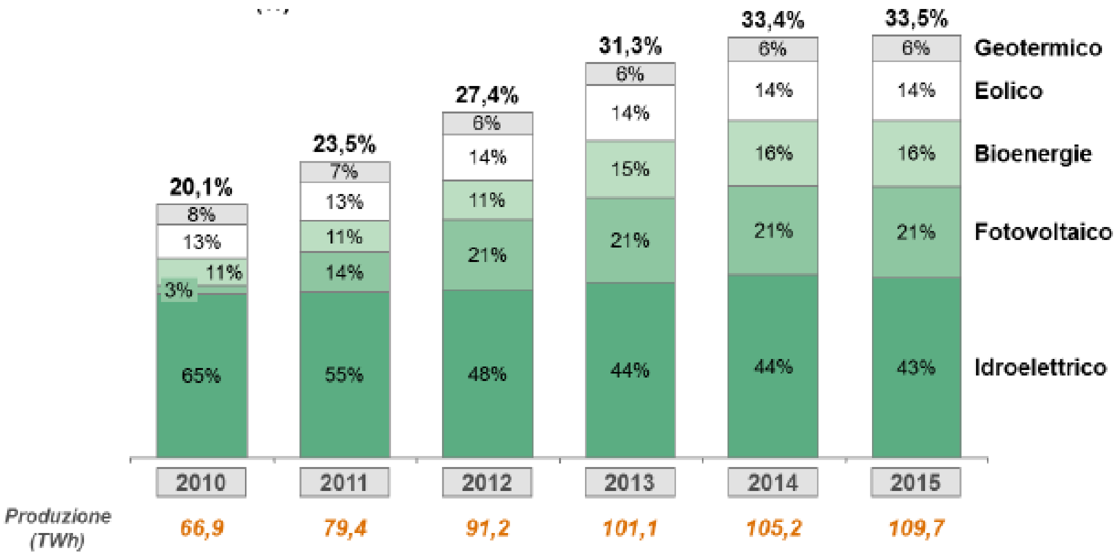

Figure 0.8 - Contribution of renewable sources to gross domestic electricity consumption (2010-2015) - Eurostat

Historically, the major Italian renewable source is hydro; nevertheless, PV and wind are the ones which have the greatest unexplored potential. Indeed, new hydro power plants are very difficult to set and authorize, due to the saturation of their market.

It can be easily noticed the very fast growth of PV technology in the last years; the fact was due especially to the extremely generous public support mechanisms of the beginning of the 10s ("Conto Energia").

0.3. Italian future scenario

The last treaty in terms of energy planning for Italy is the "National Energy Strategy" (SEN) of 2017, which has established a series of actions to be achieved by 2030.

Figure 0.9-SEN 2017 logo

One of the main goals of the strategy is the necessity to "reach and overcome, in a sustainable way, the environmental targets of decarbonisation set at European level by the COP 21[9] ". Certainly, renewable sources of energy, together with energy efficiency, are the protagonist's deputies to act in this sense.

The National Strategy, in terms of renewables, places clear guidelines:

- reach 28 % of RES on total consumption by 2030, compared to 17.5 % of 2015;
- electrical renewables at 55% to 2030 compared to 33.5% in 2015;
- thermal renewables at 30% to 2030 compared to 19.2% in 2015;

[9] The 2015 United Nations Climate Change Conference, COP 21 or CMP 11 was held in Paris, France, from 30 November to 12 December 2015. It was the 21st yearly session of the Conference of the Parties (COP).

- renewable transport at 21% to 2030 compared to 6.4% in 2015.

It is recognized that "*the development of renewable sources is functional not only for reducing emissions but also the containment of energy dependence and, in the future, reduction of the electricity price gap compared to the European average*".

Since, in Italy, environmental compatibility and landscape protection are strictly connected, the National Strategy favours repowering (revamping) of existent RES plants and gives priority to abandoned area, in order to possibly diminish the environmental impact caused by the exploitation of new terrains.

Abstract

The goal of the following work is the correct re-design of a medium scale photovoltaic plant, in order to increase its energetic and, consequently, economic performances (revamping); an existent 1 MW grid-connected plant located in Racconigi (CN), of ground mounted type, will be considered the case study for the revamping operation to which making reference for the whole treatment.

After a brief overview on PV technology, the case study plant will be described in its original configuration.

Plant's productivity concept will be defined, and some methods of estimation will be applied in order to determine its value before and after the intervention, so as to estimate the potential energy gain of the revamping operation.

Shifting the attention from the generator to components, in particular PV modules, main anomalies affecting the panels will be analysed; making reference to the ones characterizing the existent case study installation, a deeper examination will be exposed. An experimental I-V curve of the existent modules will be obtained with proper instrumentation and compared to the theoretical one; thermographic analysis will be also carried on in order to further characterize existing problems. Furthermore, a final experimental estimation of plant's efficiency will be performed and described, to characterize the plant as a whole.

The final part of the elaborate will be devoted to the description of the revamping operation for the plant under analysis. A complete design for the case study will be set: the plant will be redesigned, starting from the existent structures of the current design. Exploiting previous results, a further estimation of plant's productivity will be given. Finally, a financial analysis (business plan) of the investment will be carried on so as to estimate the advantages of the whole process.

The work will be made in collaboration with the Entec Spa company, in Savigliano (CN), which is in charge for the labour.

1. Photovoltaic technology

In the first chapter, photovoltaic technology will be synthetically described; a picture of the state of the art will be presented, starting from Sun energy and arriving to the description of all the components which can be found inside a PV plant. The situation and distribution of these systems inside the Italian energetic panorama will be also introduced.

1.1. Basic definitions

PV technology converts directly solar energy into electricity. The analysis should consequently start from the primary source, i.e. solar energy.

1.1.1. Solar energy

Solar energy is, to all effects, the origin of all the energy and life on Earth. Fossil fuels, biomass, wind power, hydroelectricity: all these forms of energy are indirectly derived from the Sun. PV is, on the contrary, a direct usage of the solar energy, converting the incident radiation into electricity.

1.1.2. Solar radiation

The Sun, as source of solar energy, is a sphere of intensely hot gaseous matter with a diameter of 1.39×10^9 m and at an average distance of 1.5×10^{11} m (150 million km) from the Earth.

The Sun behaves approximately as a black body, i.e. an ideal radiation emitter, with an effective black body temperature of 5’800 K.

It is a continuous fusion reactor[10], producing energy in the interior of the solar sphere, at a temperature of many millions of °C.

[10]Nuclear fusion consists in the union of two light molecules, such as hydrogen’s isotopes, and a subsequent release of energy in form of heat.

Figure 1.1 –The Sun

The correspondent electromagnetic radiation g(λ) [$Wm^{-2}\mu m^{-1}$] (monochromatic power density), which arrives till the external part of Earth atmosphere, has a spectral distribution which ranges from the ultraviolet to the infrared, following the Planck law

$$g(\lambda)_{bb} = \frac{C_1 \cdot \lambda^{-5}}{e^{\frac{C_2}{\lambda \cdot T}} - 1} \qquad (1.1)$$ [11].

Deriving the function with respect wavelength, the maximum results located in the visible range, for a wavelength λ near 0.5 μm, considering a black body similar to the Sun in terms of superficial temperature.

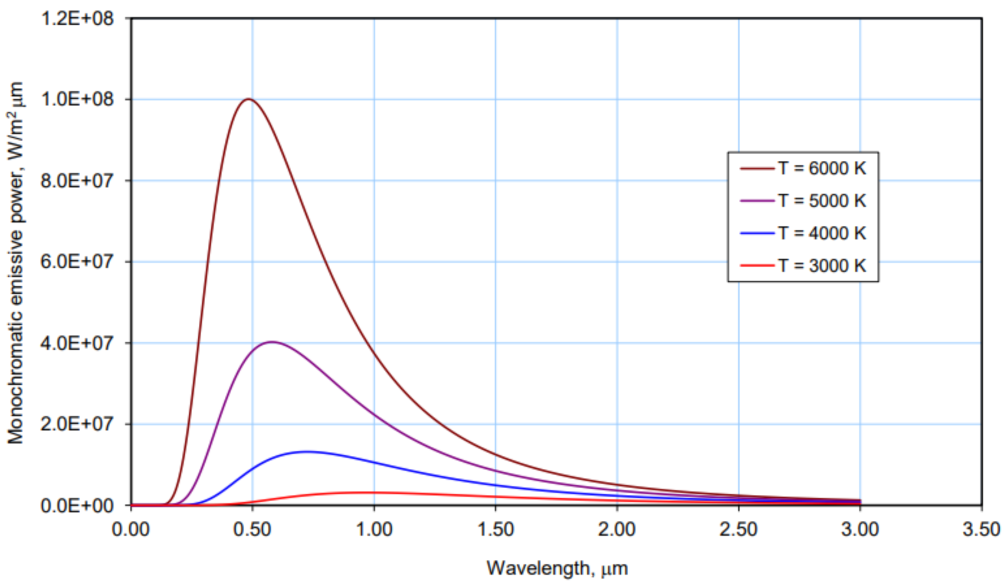

Figure 1.2 –Black body monochromatic emissive power as a function of wavelength and temperature

[11] λ is the wavelength, expressed in μm, T the temperature in K, C1 and C2 are two constants.

With increasing black body temperature, according to Wien's law, the maximum monochromatic power density g(λ) is reached for lower wavelengths, with an absolute value which increases as the equivalent black body temperature increases.

The power density, in W/m^2, which can be found on a unitary area (irradiance) outside the atmosphere, at mean earth-sun distance, and perpendicular to the Sun rays, is called Solar Constant G_o; it is value is approximately 1'367 W/m^2[12]. This value can be assumed constant, since variations linked to the power emitted by the Sun, or due to the change of the Earth-Sun distance, lead to a negligible discrepancy of the 3.3 %.

Due to the presence of the atmosphere, solar irradiance going across interacts with molecules; there are two principal mechanisms of interaction:

- *Absorption*: it involves only few spectral bands (discrete phenomenon), due to three-atoms molecules, such as water (H_2O), carbon dioxide (CO_2), active mainly in the IR, and Ozone (O_3), especially in UV band;
- *Scattering*: it is a continuous phenomenon due to molecules of N_2 and O_2. According to Rayleigh theory, scattering is a function of the wavelength ($\sim\lambda^{-4}$); the most scattered molecules are those with shorter wavelength.

Radiation reaching the earth is strongly variable, depending on several factors such as apparent Sun motion, meteorological conditions, atmosphere average composition etc. It can be subdivided into three contributions:

- *Beam radiation* (G_b): radiation not scattered or absorbed, which reaches the surface following a straight line, from the Sun disk;
- *Diffuse radiation* (G_d): part of radiation which has been scattered by light molecules. It appears distributed all over the sky. Averagely, it represents the 20% of the total radiation, depending on the climate conditions;
- *Reflected radiation* (G_ρ): part of the incident radiation is reflected by earth's surface, and it is still able to reach a receiver. Its value is a function of the albedo (ρ) parameter, in turn function of the type and color of the interested surface. The maximum value, near the unity, is reached for white surfaces (e.g. snowy lands).

[12] Value adopted by the World Radiation Center (WRC).

The total (global) irradiance reaching a terrestrial receiver can be estimated as:

$$G = G_b + G_\rho + G_d \left[\frac{W}{m^2}\right] \tag{1.2}$$

An important parameter used to characterize the spectral distribution of the radiation entering the atmosphere is the Air Mass (AM), which is defined as the ratio between the length of path through the atmosphere followed by beam radiation and the length of path that would be crossed if the sun were at the zenith.

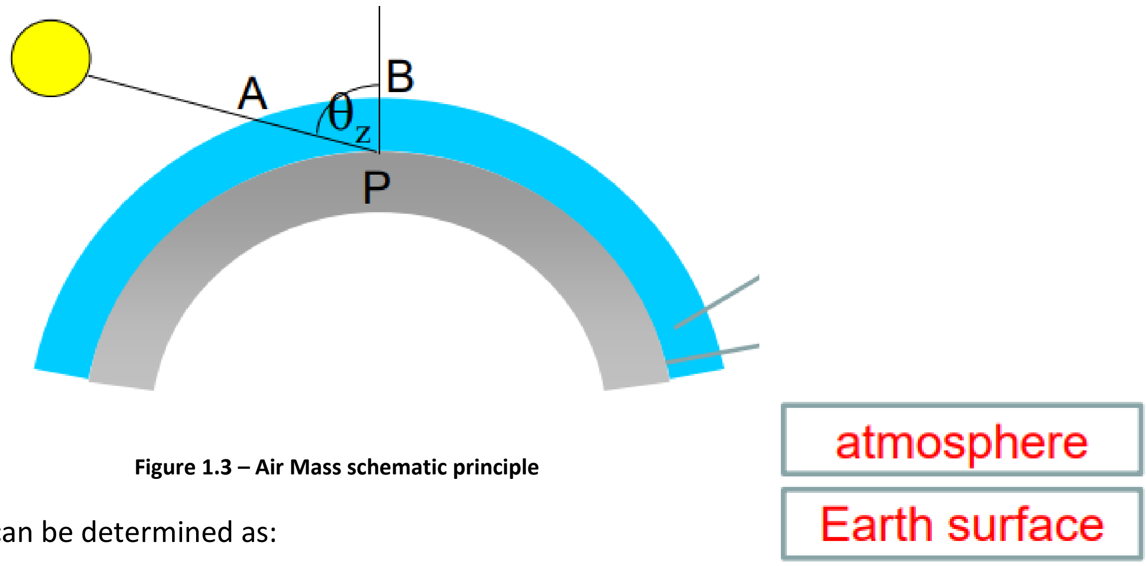

Figure 1.3 – Air Mass schematic principle

AM can be determined as:

$$AM = \frac{AP}{BP} = \frac{1}{cos(\theta_z)} \tag{1.3}$$

, where θ_Z is the zenith angle, i.e. the angle between the perpendicular to the surface and the Sun rays' direction. The more this parameter is high, the less would be radiation reaching the surface.

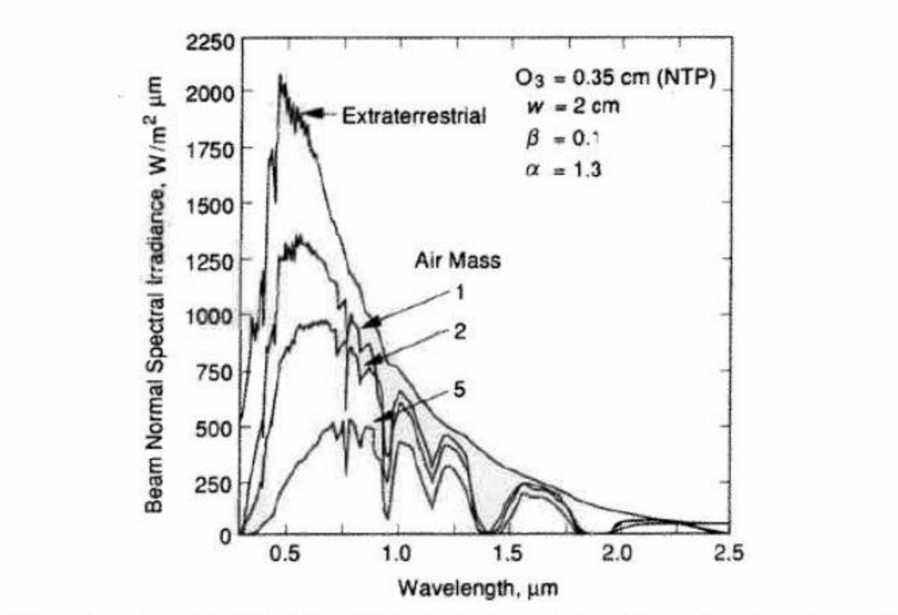

Figure 1.4 – Beam normal irradiance as a function of air mass and wavelength

As convention, the value of the extra-atmospheric Air Mass is equal to 0; this value is useful for PV satellite applications. The standard value for terrestrial applications is AM 1.5; with this spectral distribution, together with a solar irradiance of 1’000 W/m^2 and an ambient temperature of 25°C, PV cells and modules are tested (STC–Standard Test Conditions).

1.2. Photovoltaic's historical background

Photovoltaic, compared to other more traditional electricity generating technologies, such as fossils or hydroelectricity, it is a relative new entry, with the first practical photovoltaic devices demonstrated in the 50's.

PV research was boosted in the 60's thanks to space industry, requiring an alternative power supply, with respect the traditional grid power, suitable for satellite applications. These first space solar cells were far costlier than they are today; they were considered only as a scientific variation with respect the development of silicon transistor of the time, and not as an alternative energy source suitable for society.

It is precisely the oil crisis of the 1970s that opens the door to alternative energy sources to traditional fuels for the supply of electricity, somehow also independent on the network itself. Photovoltaic was able to enter and proliferate in this context, especially thanks to their advantage with respect the remote power supply area, being more manageable and usable; indeed, they could be utilized for small scale transportable applications (such as calculators, watches etc.), as well as remote power applications.

In the 1980s, thanks to great efforts on research aimed at the development of silicon cells, these devices began to increase their efficiency. In 1985, silicon solar cells achieved the symbolic 20% efficiency.

In the next decade, photovoltaic industry experienced constant growth rates, between 15% and 20%, mainly supported by the remote power supply market.

Nowadays, solar cells are familiar not only as a mean for providing power and as an indispensable tool for those who do not have grid access, but they also mean a significant diminution of the impact on the environment caused by conventional electricity generation in developed industrial countries. More applications than ever before are "photovoltaically powered", from multi-MW power stations to the common solar calculators, also thanks to the very last environmental policies, aimed at the reduction of atmospheric CO_2 concentrations, against global warming.

1.3. Solar Cell: structure and basic principles

PV technology, as said before, enables to transform directly solar energy coming from the Sun into electrical energy, with 6-21 % efficiencies, through the photovoltaic effect, namely the property of some semiconductor materials of generating electricity if hit by light.

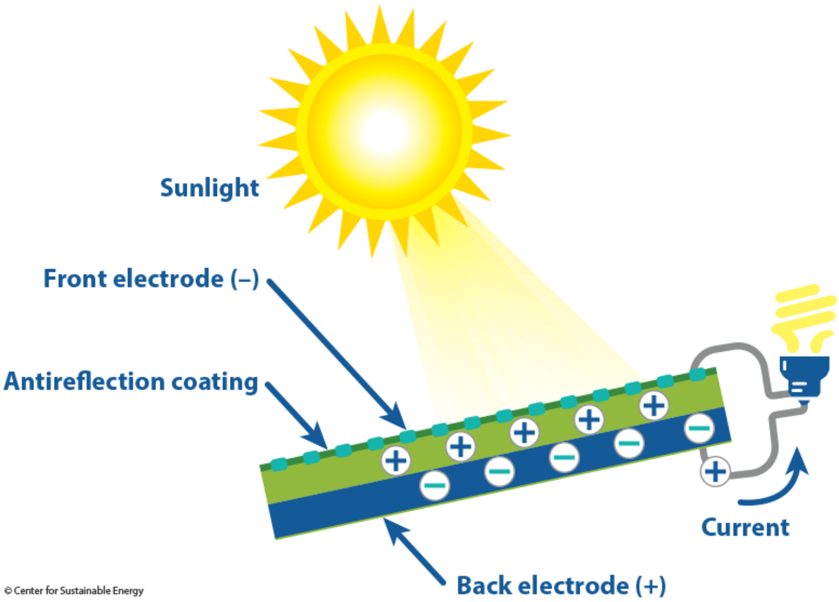

Figure 1.5 – Basilar operation of the solar cell

1.3.1. Cell's types

Solar cells can be essentially distinguished accordingly to the type of material adopted:

- *Mono-crystalline silicon*: higher performances, with very pure silicon. Cells are of dark blue colour and octagonal shape;
- *Polycrystalline silicon*: most common type of solar cell. They have a square shape, and a lighter blue coloration;
- *Amorphous silicon (thin films)*: less efficient. A very subtle film of silicon (few micrometers) is deposited over a plastic/glazed surface. Very light and cheap modules, useful for particular architectonic applications;
- *Other types of modules*: CIS (Copper – Indium – Selenide) and CIGS (Copper - Indium – Gallium – Selenide); CdTe (Cadmium – Telluride) and CdS (Cadmium Sulphide).

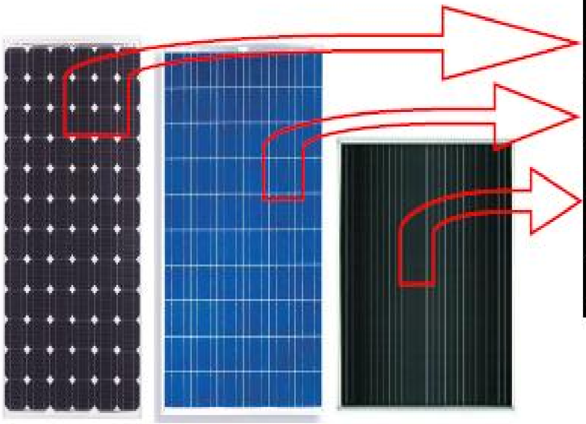

Technology	Efficiency
m-Si ; m-Si/a-Si	15-21 %
p-Si	14-16 %
a-Si ; a-Si/µc	6-10 %
CIS/CIGS	11-13 %
CdTe/CdS	13-15 %

Figure 1.6 - Main PV modules technologies in comparison

Definitely, a solar cell can be profitably represented as semiconductor diode, with square (p-Si), pseudo-square (m-Si) or rectangular (a-Si and CIS) shape, depending on the material adopted. The cell is composed of two electrodes; averagely, its thickness ranges from the order of few µm for a-Si, to hundreds of µm for crystalline silicon cells.

All considered, silicon is the best material for the solar cell. It is a tetravalent semimetal, and the second element in the world for abundance. In its crystalline form, it is of grey colour and it has a sheen similar to metals.

Figure 1.7 - Mineral silicon

1.3.2. PN junction

Focusing the attention on silicon cells, the upper electrode, smaller and transparent, it is type N doped, i.e. it presents impurities of phosphorous, which is an element belonging to the fifth group of the periodic table; the inferior layer is P doped, with impurities of boron, of the third group of the periodic table.

The interface between the two electrodes is called depletion region; in its correspondence, an electric field is formed, due to electron's diffusion from N to P, and opposite diffusion of holes. Therefore, a positively charged layer is formed on the superior layer, while a negatively charged layer is created on the inferior layer.

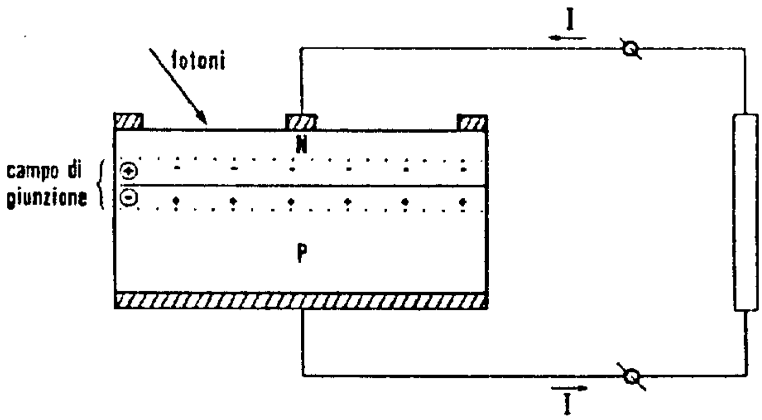

Figure 1.8 - Silicon solar cell's junction structure (PN junction)

The depletion region, with positive charges on the N side and negative charges on the P side, has no mobile carriers; fixed charges of the doped atoms create a potential barrier which opposes to an ulterior flux of electrons and holes.

If an external bias is applied, the equilibrium can be broken. In particular:

- *Forward Bias (direct polarization)*: positive voltage is applied to the P-side, and negative to the N-side. Consequently, the potential barrier is reduced, and a relevant current flow through the junction (diffusion current);
- *Reverse Bias (inverse polarization)*: an opposite voltage direction increases the potential barrier. A very small inverse saturation current flows through the junction.

The junction effect can be described through the Shockley model:

$$I = I_o \cdot \left(e^{q \cdot \frac{U}{m \cdot k \cdot T}} - 1\right) \tag{1.4}$$

, where:

- I_0 is the saturation current [A];
- T is the absolute temperature [K];
- q is the electron elementary charge [C];
- M is the junction's quality factor;
- K is the Boltzmann's constant $[m^2 kg\ s^{-2} K^{-1}]$.

1.3.3. Spectral response

PV conversion of energy is based on the particle nature of the light; according to Planck's law, photons transport a certain amount of energy:

$$E_{ph} = \frac{h \cdot c}{\lambda} \tag{1.5}$$

, where:

- h is the Planck's constant [Js];

- c is the light speed [m/s];

- λ is the light wavelength [m].

Only photons with sufficient energy, i.e. with an energy greater than the energy gap E_g between valence and conduction bands (only a part of the solar spectrum has the necessary energy), can be converted into electricity from the cell. In this case, when a photon enters in the semiconductor (silicon), it can be absorbed, given that it has sufficient energy, and promote an electron to conduction band, forming, as a direct consequence, an electron-hole couple.

Different technologies of PV cells, considering the most common silicon tech (poly-crystalline p-Si, mono-crystalline m-Si and amorphous a-Si), have different spectral responses S(λ) [A/W], therefore different sensibility bands to light depending on the wavelength. The larger it is, the higher is the amount of useful solar radiation which can be converted.

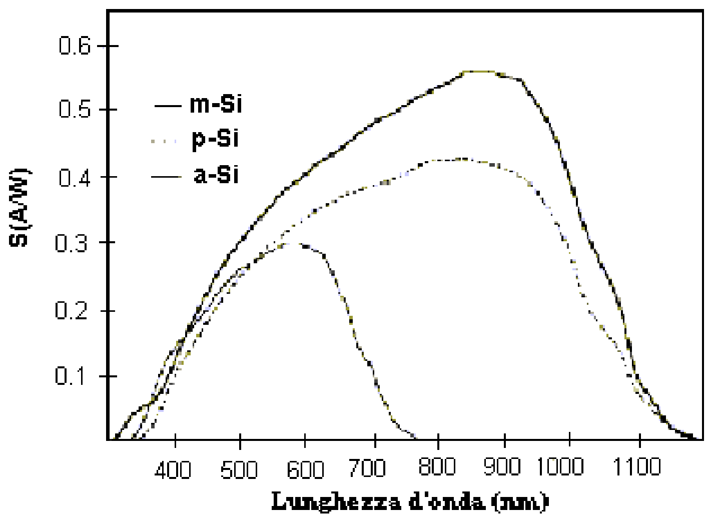

Figure 1.9- Spectral response for different PV technologies

Since, in most of the cases, the electron-hole couple created by the photon has an energy which is greater than the energy gap, this excess of energy is lost in form of heat, and it cannot be recovered neither converted into useful power.

To estimate the electrical power produced, the electron movement, induced by photons, is known as photo-generated current. Each photon has a contribution of an electron to the current, which can be estimated as:

$$I_{ph} = q \cdot N \cdot A \quad (1.6)$$

, where q is the electron charge, A is the semiconductor's area, while N is the number of incident photons per unit area.

In terms of current density:

$$J_{ph} = \frac{I_{ph}}{A} = \int g(\lambda) \cdot S(\lambda) d\lambda \quad (1.7)$$

, where S is the spectral response, and g is the spectral irradiance (W/m^2/μm). Average values of photogenerated current density for common solar cells are 40-50 mA/cm^2.

If the current generated by the cell is directly proportional to the number of incident photons per unit area, i.e. to the solar irradiance, voltage is determined by the electrostatic energy of separated charges, which cannot overcome the E_g limit, numerically equal to the maximum voltage.

For different materials, there are different current-voltage characteristics; semiconductors with greater energy gap, such as a-Si (1.7 eV), generate a greater voltage with respect, for instance, m-Si (1.1 eV), but they present a smaller spectral response, and, as a result, a smaller current density. Since the power is the product of current and voltage, the best solution is a trade-off between the two parameters.

1.3.4. Solar cell model

Solar cell can be modeled with the following equivalent circuit:

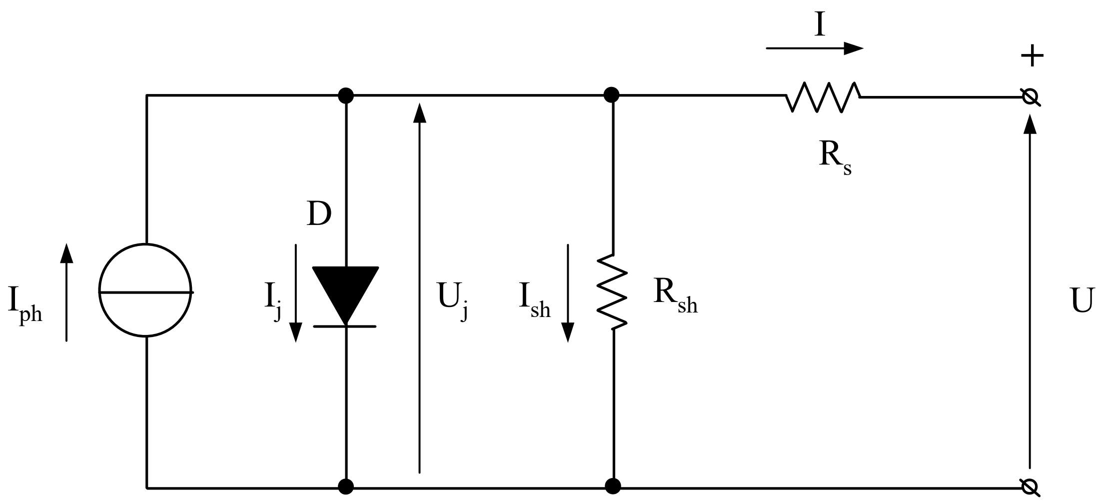

Figure 1.10 -Equivalent solar cell's circuit

It can be represented as an ideal current source, whose current is directly proportional to the solar irradiance, and a diode posed in anti-parallel; two resistors are then introduced in order to take into account possible dissipative effects. In particular:

- R_{sh} is the shunt resistance, connected in parallel to the current source, taking into account superficial dispersion currents[13];
- R_s is the series resistance, and it takes into account electrodes resistances, contact resistances and semiconductor volume resistance.

Through Kirchhoff's law, the global current I and voltage U at PV cell's clamps can be determined as:

$$I = I_{ph} - I_j - \frac{U_j}{R_{sh}} \quad (1.8)$$

[13] Superficial dispersion currents reduce the amount of current effectively flowing into the junction and the voltage of the solar cell, "weakening" the cell itself.

, where I_j is the junction current modeled through Shockley, and U_j is the voltage across the junction.

For voltage, instead:

$$U = U_j - R_s \cdot I \tag{1.9}$$

Voltage can also be determined as a function of current, through Shockley model:

$$U = \frac{m \cdot k \cdot T}{q} \cdot \ln\left(\frac{I_{ph} - I \cdot \left(1 + \frac{R_S}{R_{sh}}\right) - \frac{U}{R_{sh}} + I_o}{I_o}\right) - R_s \cdot I \tag{1.10}$$

With fixed values of irradiance and temperature, the previous expression can be graphed on the I-V plane, building the I-V curve (or characteristic) of a solar cell. Every point of the diagram represents the electrical power P as a product of current I and voltage U.

The remarkable points that distinguish the diagram are:

- *Short circuit condition*: current is equal to the short circuit current (I_{sc}), while voltage is zero;
- *Open circuit condition*: current is zero, while voltage is equal to open circuit voltage (U_{oc});
- *MPP ("Maximum Power Point")*: the product current per voltage is the maximum.

The fill factor can be defined as the ratio between the maximum power practically obtainable and the maximum theoretical power:

$$FF = \frac{U_m \cdot I_M}{U_{OC} \cdot I_{SC}} \tag{1.11}$$

In general, this value is around 0.8

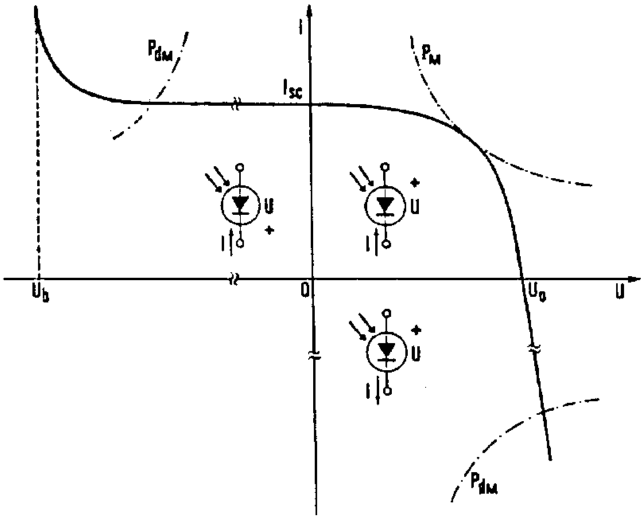

Figure 1.11 - Solar cell I-V curve

The complete I-V curve of a solar cell can be represented into four quadrants. The normal operating points are in the first quadrant, in which the cell operates like a generator. In the II and IV quadrants, respectively due to inverse voltage and inverse current, cell's behavior resembles a load behavior. These two working conditions are acceptable if and only if the thermal limit (corresponding to a cell's temperature of 85 °C, represented with two branches of hyperbola), is not overcome. Furthermore, there is also a threshold for the maximum inverse voltage, which should be limited to the breakdown voltage (U_b), in order to avoid instantaneous cell's failure.

1.3.5. I-V curve dependence on irradiance and temperature

Cell's I-V curve is strongly dependent on irradiance and temperature. In particular:

- *Variation with solar irradiance*:

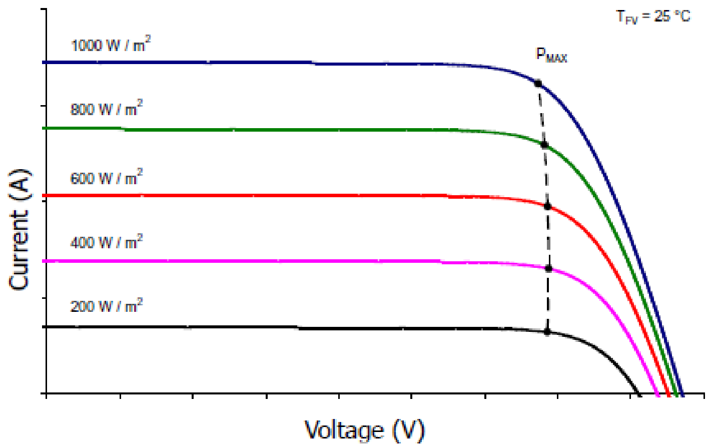

Figure 1.12 - Solar irradiance dependence

Since photo-generated current is directly proportional solar irradiance, there is a strong dependence of the current, while voltage almost remains constant. The short-circuit current is directly proportional to irradiance, while open circuit voltage has a logarithmic dependence (much more smoothed); only for very low values of irradiance, voltage changes abruptly. The MPP locus variation is reported through the dashed line.

The variation of current can be modeled through the following equation:

$$I_{SC}(G,T) = I_{SC}(STC) \cdot \frac{G\left(\frac{W}{m^2}\right)}{1000} \cdot (1 + \alpha_{Isc} \cdot \Delta T_C) \qquad (1.12)$$

, where α is the thermal coefficient of current.

- *Variation with ambient temperature*:

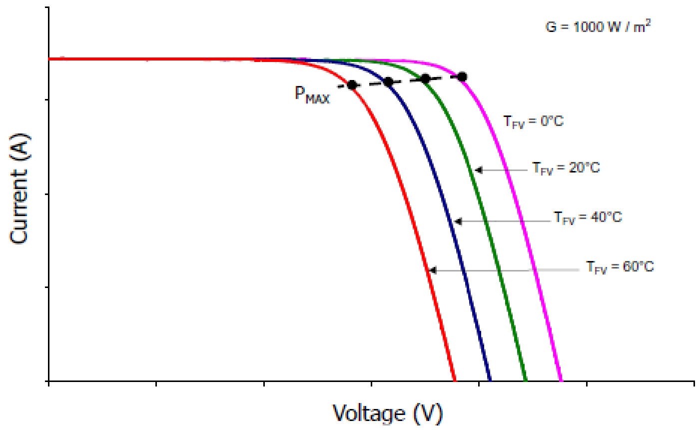

Figure 1.13 - Ambient temperature dependence

With constant irradiance, a positive temperature variation causes very small variations on the photo-generated current, and consequently on the short-circuit current; due to the E_g negative variation, there is a strong increment of diffusion current I_j in the diode, at which corresponds a decrease of the open circuit voltage U_{oc}.

The variation of voltage can be modeled through the following equation:

$$U_{OC}\,(T_C) = U_{OC}(STC) \cdot (1 + \beta_{Uoc} \cdot \Delta T_C) \qquad (1.13)$$

, where β is the thermal coefficient of voltage.

As a good approximation, it is assumed that short-circuit current depends only on irradiance, while open-circuit voltage only on cell’s temperature.

1.3.6. Solar cell conversion losses

There are several factors which causes losses inside a cell:

- Shading and reflection (10%): due to the presence of the frontal contacts. They can be minimized by enhancing the useful surface, i.e. minimizing the amount of contacts posed in the frontal side;
- Photon's excess of energy (30%): the energy which a photon has in addition to the one requested to create an electron-hole couple is lost in form of heat;
- Photon's lack of energy (20%): part of the incident photons does not have the necessary energy to create an electron-hole couple, therefore they are absorbed in form of heat;
- Electron-hole recombination (2%): depending on the quality of the material adopted, and so on the amount of impurities present, the couple can recombine and lose its energy in form of heat;
- Losses due to shunt and series resistances (Rs and Rsh) (20%).

All considered, final conversion efficiency of a solar cell is between 10-20%; differently from traditional generators, the solar cell has an input power independent on the absorbed power, constant for a given location and meteorological conditions.

Since normal loads requires voltages and currents much greater than the ones which can be developed by a single solar cell, it is necessary a series/parallel connection between cells. The total voltage/current of the connection is determined by the sum of each connected cell, depending on the type of connection.

1.3.7. Mismatch problems

When solar cells are connected together, some problems can rise depending on the connection and on the features of the linked cells.

- *Series connection*: if N_s cells are connected in series (string of cells), and one of the cell has defects/is shadowed, then the resulting I-V curve of the generator presents:

$$U_{OC} = \sum_i U_{OCi} \quad (1.14)$$

$$I_{SC} \cong (I_{SCi})_{MIN} \quad (1.15)$$

In other words, the resulting connection present a short circuit current equal to the one of the weak cell, causing a strong decrement of power, which is always different from the sum of each single cell's power.

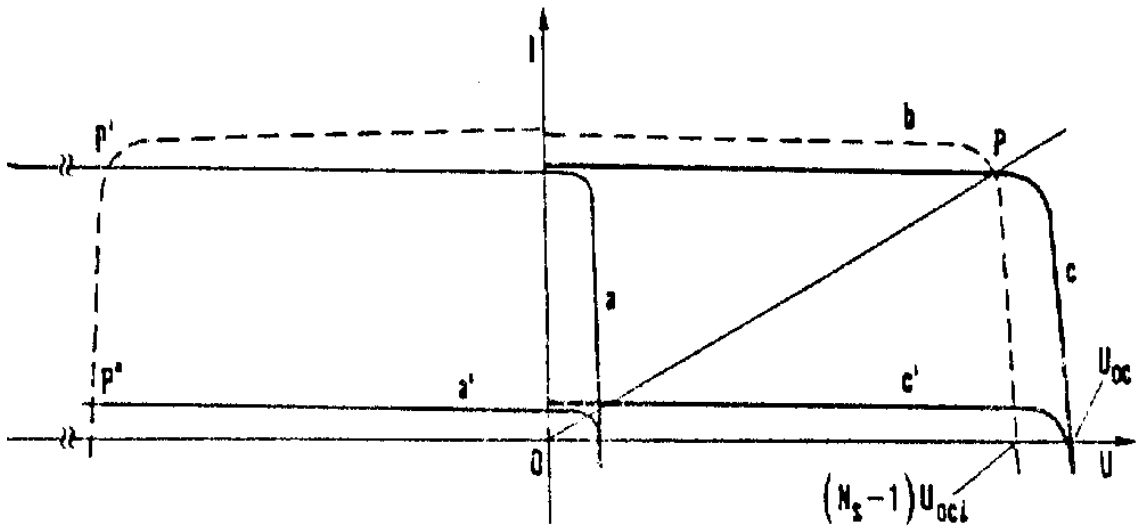

Figure 1.14 - I-V curve of solar cells in series

Worst condition is short-circuit condition; in this case, the weak cell is bond to absorb all the inverse voltage of the other group of cells. If the voltage overcomes the breakdown voltage, the cell can face immediate failure. This condition, which makes the weak cell to operate like a load, and therefore heat up, can be avoided thanks to the insertion of a diode in anti-parallel, called bypass diode, which does not allow the cell to operate like a load and restores the short circuit current to the value of the (Ns-1) good cells, limiting the resulting abrupt decrement of power. Usually, for terrestrial applications, bypass diodes are connected to groups of nearly 36 cells.

- *Parallel connection*: if a group of cells is connected in parallel, and one of the cell has problems (like highlighted before), then the whole group can be influenced. In this case:

$$I_{SC} = \sum_i I_{SCi} \tag{1.16}$$

$$U_{OC} \cong (U_{OC})_{MIN} \tag{1.17}$$

Worst condition is open-circuit condition, when the weak cell is forced to absorb the current of the good cells; in general, a diode in series (blocking diode) is adopted in order to avoid the problem. The condition of parallel of solar cells is quite uncommon.

In order to avoid completely mismatch problems, solar cells connection should include most likely cells with similar constructional features, and in a way such that the illumination is spread almost uniformly to the whole group.

1.4. PV modules

Figure 1.15 – PV module

Many cells electrically connected and encapsulated together, generally in series, form a PV module, generally with 60-72 cells. In order to obtain the solar cell connection, ribbon connections are welded to the main busbars, which are consequently welded to the back electrode of the adjacent cell.

PV modules have several technical and economic advantages:

- High reliability and long life (>25 yrs.);
- Absence of noise and air pollution during operation;
- Low maintenance costs;
- Production of electricity, in most of the cases, directly where it is needed;
- Possibility of recycling without wastes at the end of life.

The typical structure of a PV module is the following:

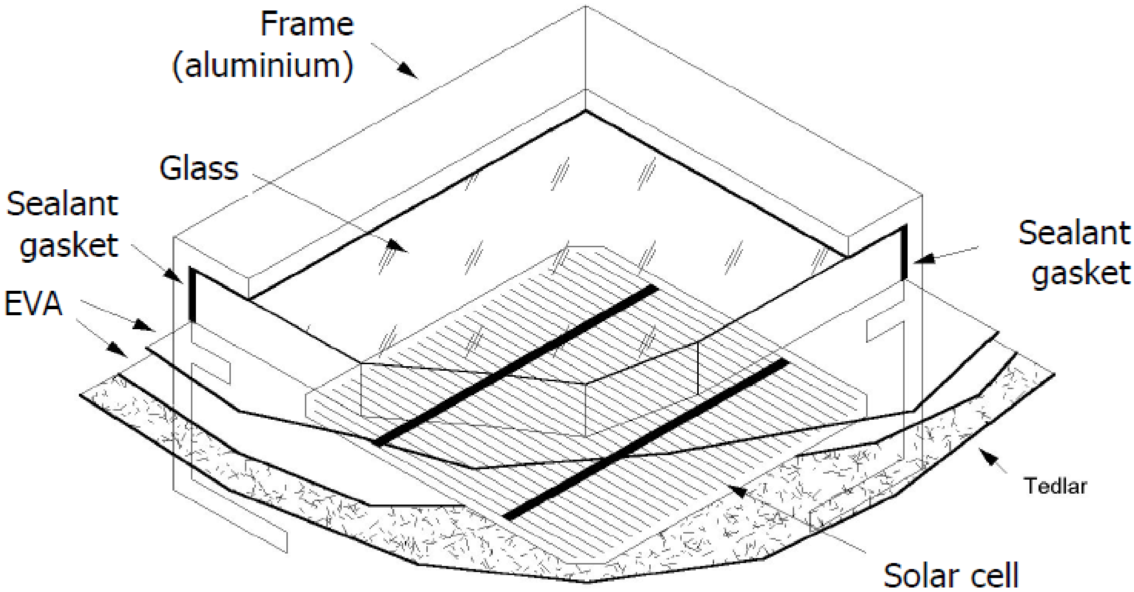

Figure 1.16 - PV module structure

1. Tempered glass, 3-4 mm thick, at high transmittance;
2. EVA (Ethylene – Vinyl – Acetate), used for the encapsulation of the solar cells, to make them more flexible and elastic. It guarantees the electrical insulation of the cells, avoiding the penetration of humidity, but it cannot withstand high temperatures;
3. PV cells;
4. EVA (second layer);
5. Tedlar (or Mylar): plastic material with good properties as UV ray's barrier and resistance to ageing caused by weathering;
6. Aluminium frame;
7. Junction box: contains bypass diodes (usually 3, one per group of 20-24 cells) and connection terminals.

The global conversion efficiency of the module is defined in STC (Standard Test Conditions), i.e. irradiance 1'000 W/m^2, air mass AM 1.5 and ambient temperature 25°C; it ranges from 7 to 16%, according to the type of module and material adopted. Each module, in its own datasheet, presents several other features reported, such as:

- Nominal power [W_p], nowadays between 270-320 W_p;
- Short circuit current [A];
- Open-circuit voltage [V];
- MPP voltage and current values. Their product gives the nominal power.

Since STC are laboratory conditions, NOCT ("Normal Operating Cell Temperature") conditions are also given. The NOCT temperature is the temperature at which a PV module, subjected to an irradiance of 800 W/m^2, with an ambient temperature of 20 °C and a wind speed of 1 m/s, works. In general, its value is around 40-50 °C. Through NOCT data, cells temperature, in every condition of ambient temperature and irradiance, can be easily determined through a linear approximation of the cell's behaviour:

$$T_C = T_a + \frac{NOCT-20\ (°C)}{800\left(\frac{W}{m^2}\right)} \cdot G\ \left(\frac{W}{m^2}\right) \tag{1.18}$$

The I-V curve of a module is similar to the one of a cell, only with scaled values for current and voltage, depending on the number of series connected cells.

1.5. PV generator

In order to produce a sufficient amount of power and, consequently, energy, PV modules should be connected together.

In general, a PV generator is the combination of series of modules and parallel of the series. The range of power of a PV generator ranges from few kW for domestic applications (usually, 10-12 PV modules), to several MW of power; these powers are usually exploited thanks to the combination of 4000-5000 modules.

PV strings are defined as series of a certain number of modules. Their length usually depends on the inverter (DC-AC converter) to which are connected. Generally, a certain number of strings N_p of N_s modules are then put in parallel before being connected to an inverter. The input of the inverter presents certain voltage and current ranges of acceptability; therefore, N_s and N_p are limited numbers.

As said before, each module has inside, in general, 2 or 3 bypass diodes; parallel connection of strings can present also mismatch problems. Consequently, blocking diodes for strings can be adopted, in order to prevent damages in case of eventual unevenness in the generator.

These diodes, in general, can be avoided, since the total reverse current flowing the string in case of mismatching conditions has a value which ranges from 0.5 I_{sc}, for N_p=2, to 1 I_{sc}, for N_p -> +oo. Its value can be determined through the intersection of the I-V curve of the weak cell (it behaves like a load; therefore the I-V curve is symmetrical with respect the voltage axis) with the one of the good cells.

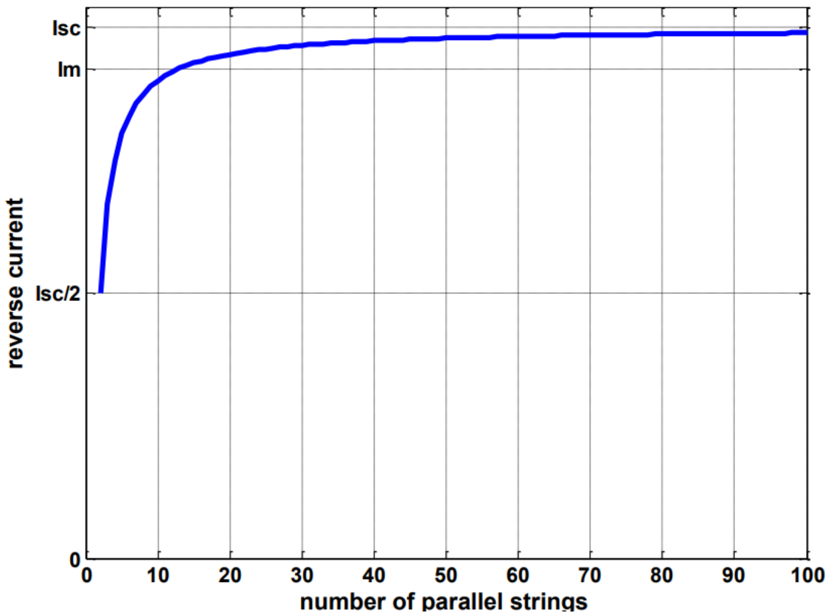

Figure 1.17 - Reverse current in mismatched parallel strings

The optimal working point of the load corresponds with the MPP of the I-V curve of the complete PV generator; differently from traditional generators, in the PV case, it is the load which should be adapted in order to better fit the generator characteristic. This combination is generally performed through the electronic converter MPPT ("Maximum Power Point Tracker").

1.6. Other components

In order to make usable the produced energy, other components are required.

- Inverter

The most important are the electronic converters from DC to AC (inverters). A PV generator produces electricity in direct current (DC), but the majority of the users are fed with alternating current (AC).

Figure 1.18 - Small size inverter

Depending on the power, inverters can be distinguished as single-phase inverters (the smallest) or tri-phase inverters.

The waveform of the output voltage is an index of the quality of an inverter; the cheapest type of inverter generates a square wave, with high harmonic content. The harmonic content on the output wave defines the “quality” of the output signal; if it is higher, the signal is worse, and has a shape which is different from the optimal one.

Sinusoidal inverters present an output signal which is sinusoidal, with very low harmonic content; through the adoption the PWM (“Pulse Width Modulation”) technique, based on the comparison between a triangular and a sinusoidal waveform, they generate the output signal. Modulation index, defined as the ratio between sinusoidal amplitude and triangular amplitude, is the main regulation parameter adopted for the PWM; generally, it is between 0.2 and 1, that is, the sinusoidal amplitude is lower than the triangular one.

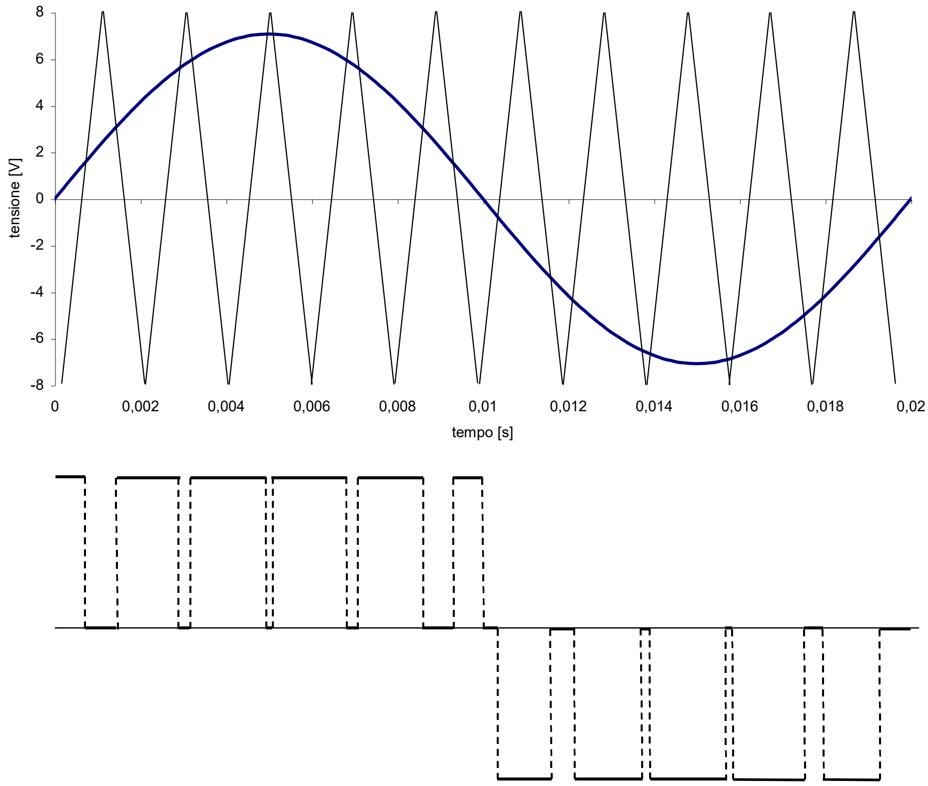

Figure 1.19 - PWM operation

In order to inject active power into the grid, line-commutated (thyristors) inverters or self-commutated (transistors) inverters, with transformers for galvanic separation from the grid, can be implemented. The first type of inverter is the oldest and cheapest, but presents several problems, like a higher harmonic content, and a grid dependent switch-on. Transistor inverters, independent from the grid signal, can be distinguished according to the type of transformer to which are connected. Also, transformer less inverters can be found in commerce, with very high efficiency but with more safety problems.

Most recent inverters include also the MPPT, i.e. a DC-DC electronic converter useful to optimize the utilization of the PV generator, when varying irradiance and temperature. Indeed, it is able to extract the maximum PV power and bring it to the load, with different values of voltage and current. In general, it is posed before the DC-AC converter.

These converters operate following some MPP searching algorithms. The most common is "Perturb & Observe"; a small variation of voltage ΔV is imposed, and a subsequent variation of power ΔP is measured: if this variation is positive, voltage is again varied in the same direction, otherwise it is reversed.

The working principle of a DC-DC converter can be represented in the I-V plane.

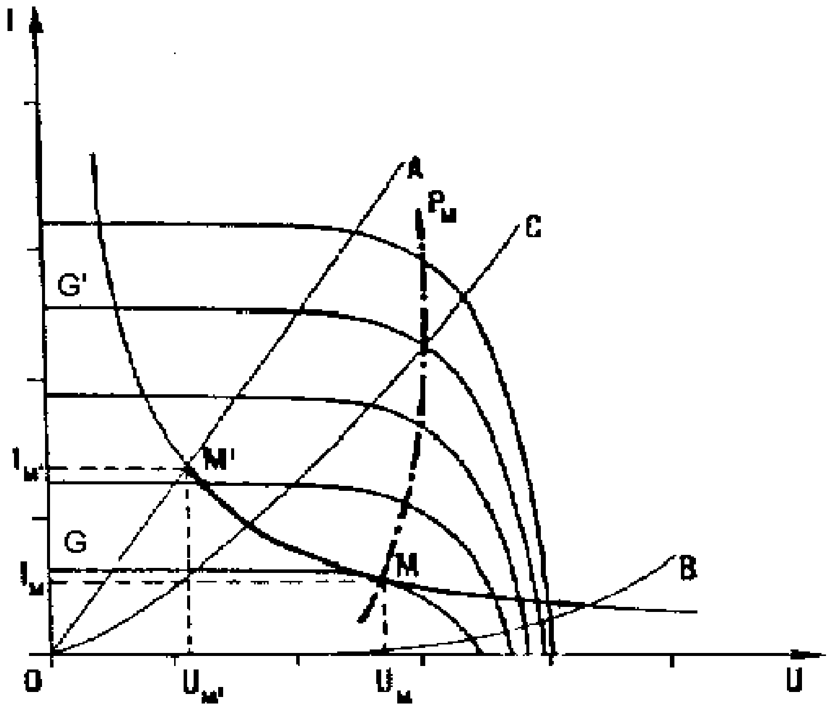

Figure 1.20 - MPPT operational principle

Let's consider OA as the load curve of an ideal user connected to the PV plant; its intersection with the I-V curve of the generator gives the working point. Since the operational point is different from the MPP (U_m;I_m), to anyway recover the maximum power, the load should operate at (U_m';I_m'), i.e. exactly at the intersection with the constant power hyperbola. The MPPT, therefore, operates in input with (U_m;I_m) to extract the maximum power, and in output with (U_m';I_m'). In this case, since the output voltage U_m is lower than the input one (U_m'), MPPT operates like a step-down converter. Considering instead load curve OB, the operation is reversed: it acts like a step-up converter, enhancing the input voltage.

Main specifications for grid connected inverters are:

- High conversion efficiency $\eta_{DC\text{-}AC}$ (>90%) and low no-load losses (<1%);
- Power factor greater than 0.9;
- Low harmonic content;
- MPPT presence, with efficiencies greater than 97%;
- Capability of limiting DC input power from the PV generator;
- Automatic switch-off in case of overvoltages or overfrequencies of the grid;
- Automatic switch on and off for low irradiance values.

Typical behaviours of the inverter and MPPT conversion efficiencies can be represented as a function of the % of rated AC power.

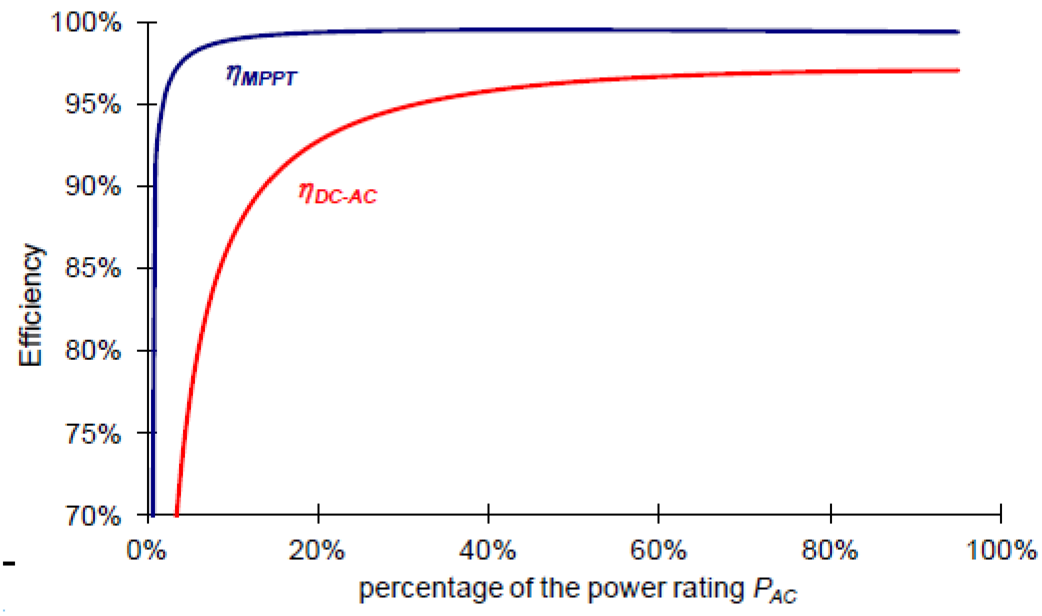

Figure 1.21 - Inverter and MPPT efficiency as a function of percentage of power rating

Inverters and MPPT efficiencies are quite constant and very high for a wide range of power rating (i.e. ratio between the actual power and the nominal power).

Other components present inside a PV plant are:

- Field switchboard DC**:** it puts in parallel the different strings composing the PV plant. It contains the overvoltage arresters, useful to protect modules and inverter from overvoltage discharges, due to possible fulminations on the incoming line. Furthermore, it presents fuses to protect modules and cables from overvoltage, and the main switch;
- Field switchboard AC: it contains a magnetermic switch that, together with the main switch on the DC side, can secure the inverter for possible maintenance. An SPD (Surge Protection Device) protects from possible overvoltage from the grid.
- Production counter (GSE)**:** located downstream the inverter, it is useful to measure the electrical energy produced by the plant;

- Exchange counter**:** bidirectional counter, useful to measure the complete energy exchange both in exit (energy sold to the grid) and in entrance (energy absorbed from the grid).

Figure 1.22 - Energy counter

For plants of power greater than 20 kW, other components are necessary:

- Interface device: sensor able to detect characteristic parameters of the grid (in particular, voltage and frequency). If these parameters are no more guaranteed, it releases the switch to which is connected;

Figure 1.23 - Interface device

- Transformer: assures a galvanic (electrical) insulation between the PV plant and the grid, and enhance the voltage level according to grid connection type;

Figure 1.24 - Insulation transformer

- General device: located downstream the production counter, it is a magnetermic switch necessary to disconnect contemporary both the user and the PV plant. It has breaking capacity adequate to the short-circuit current of the installation point, taking into account the contribution of the photovoltaic generator. It is explicitly requested by Enel connection guides.

In order to monitor the plant production, usually remote-control devices (data-loggers) are placed. They are small electronic devices equipped with micro-processors and a memory for data acquisition. They can be connected to the web via pc or through an internal SIM card.

Figure 1.25 - Remote control device (datalogger)

1.7. Plant's overview

Resuming:

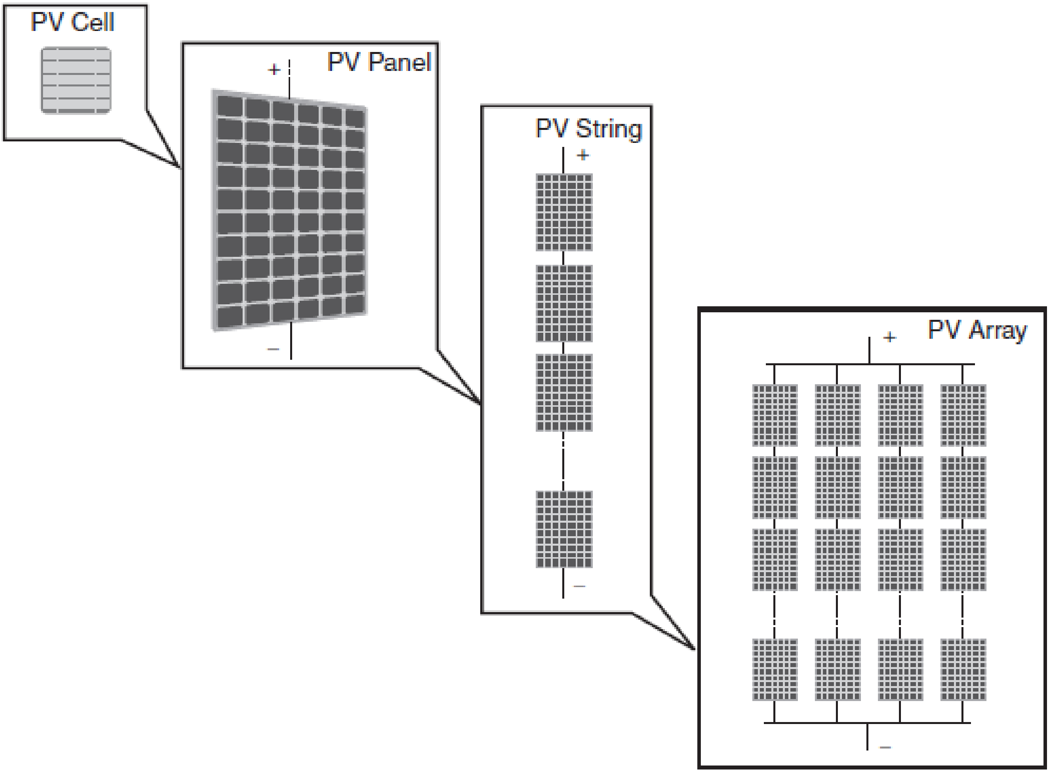

Figure 1.26 - From a solar cell to a PV system

Depending on what will be the final usage of the electricity generated, there are different systems of photovoltaic plants:

- Stand-alone: usually with batteries, for the accumulation of the surplus of electrical energy. It is typical when the user has not the possibility of grid connection;
- Grid-connected: surplus energy is injected into the grid and accounted by energy counters. Grid can be used as storage of energy, which can be subsequently re-absorbed, when necessary, by the users.

Most common plants are surely in grid connection; stand-alone systems are typical of isolated areas, which cannot be reached by the electric grid.

The general schematic of a grid connected plant is now reported.

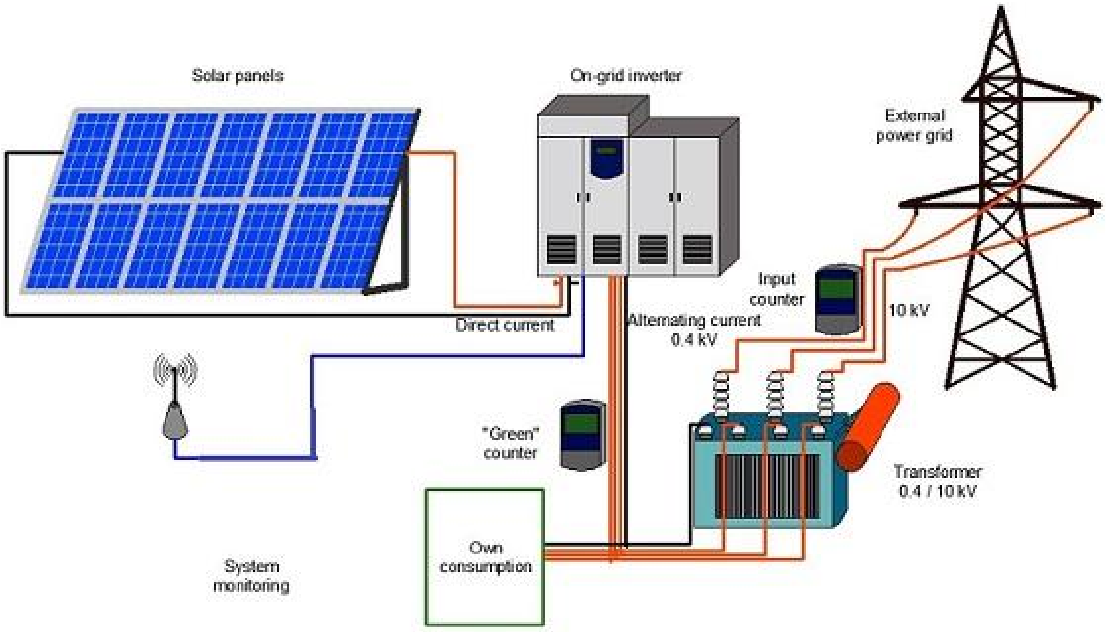

Figure 1.27 - Basic schematic of a grid-connected PV plant

They can be further classified into:

- Centralized PV plants: bigger plants, till some MW of power, useful to serve directly in medium voltage. Usually are ground-mounted;
- De-centralized (distributed) plants: projected in order to fed residential users at low voltage level. They are integrated with the grid, injecting the energy in excess which is not directly consumed by the users. For these plants, at the interface with the grid, counters should be present in order to quantify the energy sold and bought from the grid.

1.8. PV in Italy: today's panorama

In Italy, RES have an important role in the energetic panorama of the country. As said before, the major contribution to the 17.5 % of share covered by RES today is due to electrical renewables, which are responsible for 33 % of the final need of electricity.

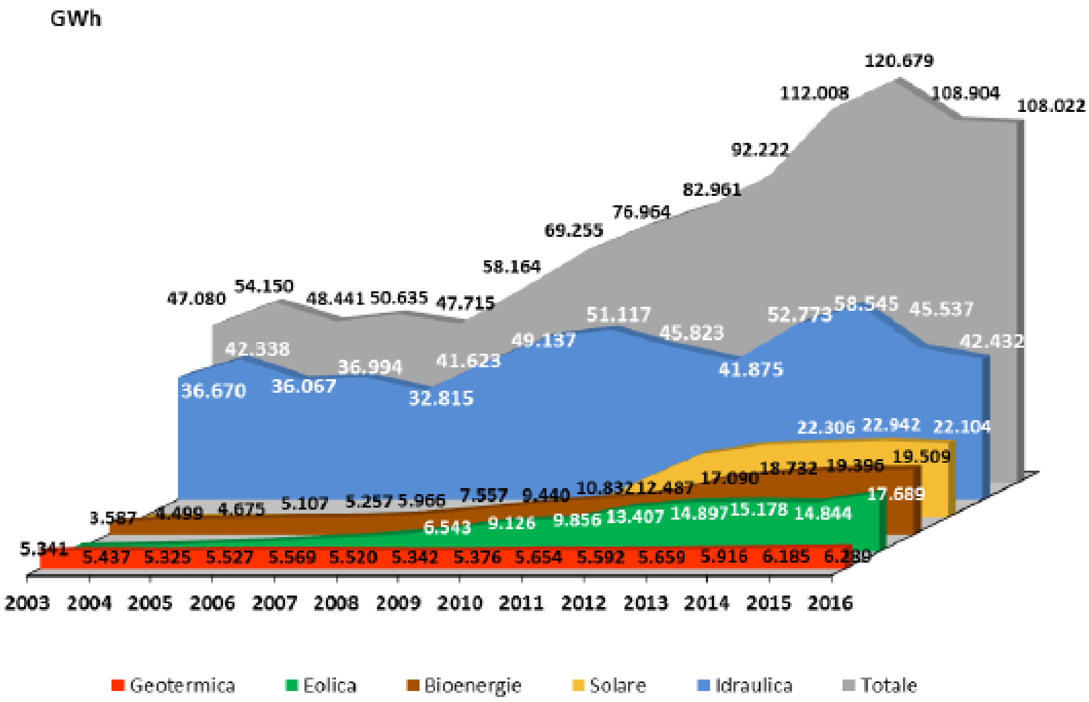

Figure 1.28 - Energy production from renewables (GWh) in Italy

The two major contributions to RES electricity production in Italy comes from hydro and solar.

According to GSE[14] statistical report of 2016 about solar photovoltaic technology, at the end of 2016, in Italy, were installed around 732'000 photovoltaic plants, with a global power of 19.3 GW. The majority of these plants (>90 %) were of small size (P < 20 kW).

The rapid growth, especially at the beginning of the 10's, was favoured by the presence of very positive incentives ("Conto Energia"); many plants injecting all the energy produced into the grid at a very favourable price (almost 300 €/Mwh) were erected.

After the cessation of these support mechanisms, the majority of PV plants installed was associated to a user, both of domestic and industrial type, usually stipulating a SSP contract ("Scambio sul Posto") with GSE, in order to inject into the grid all the surplus energy produced by

[14] GSE = "Gestore dei Servizi Energetici"; Italian public holding which sustain renewables development supplying incentives for the electrical production and promoting a sustainable development with awareness campaigns on the efficient use of energy.

the plant, to all effects using the network as a hypothetical electrical storage, and then recovering the same amount of energy at a favourable price with respect the one intended to traditional energy purchase.

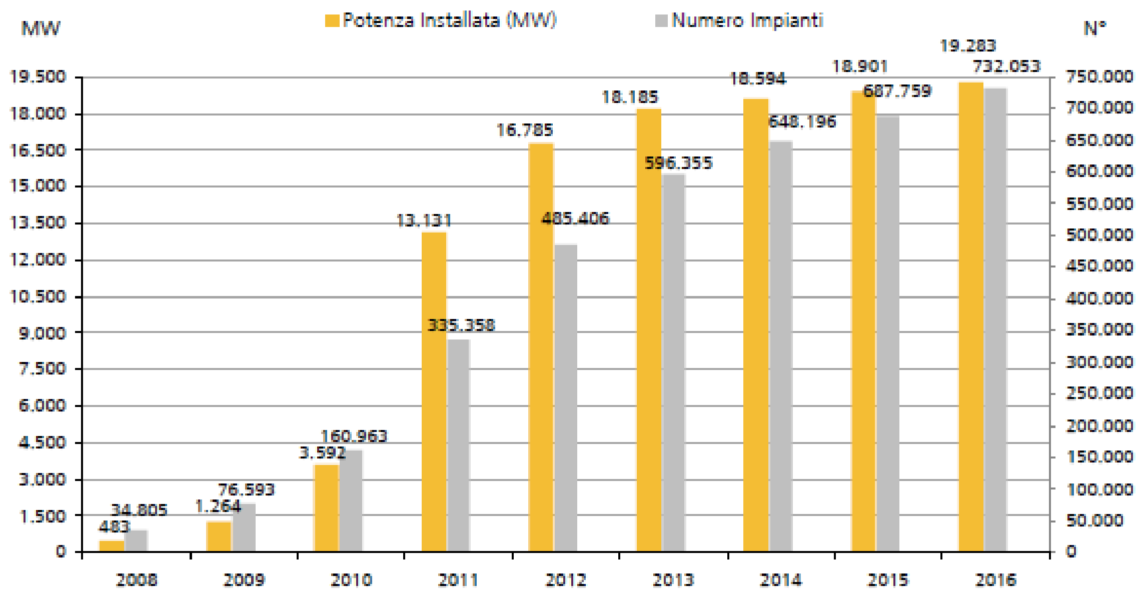

Figure 1.29 - Evolution in power and numerosity of PV plant in Italy (2008-2016)

It is evident how the presence of support mechanism has “doped” the growth of the technology; after the cessation of the last “Conto Energia” (2013), the evolution in power and numerosity has been less rapid, but still present.

The average size of an Italian PV plant is around 26 kW in degrowth; most of the plants are connected in LV grid (400 V), despite the majority of the power resides in MV grid (15’000V). In general, the distinction between voltage levels is associated to the plant’s power; a higher voltage level guarantees higher capability of power transmission, reducing losses.

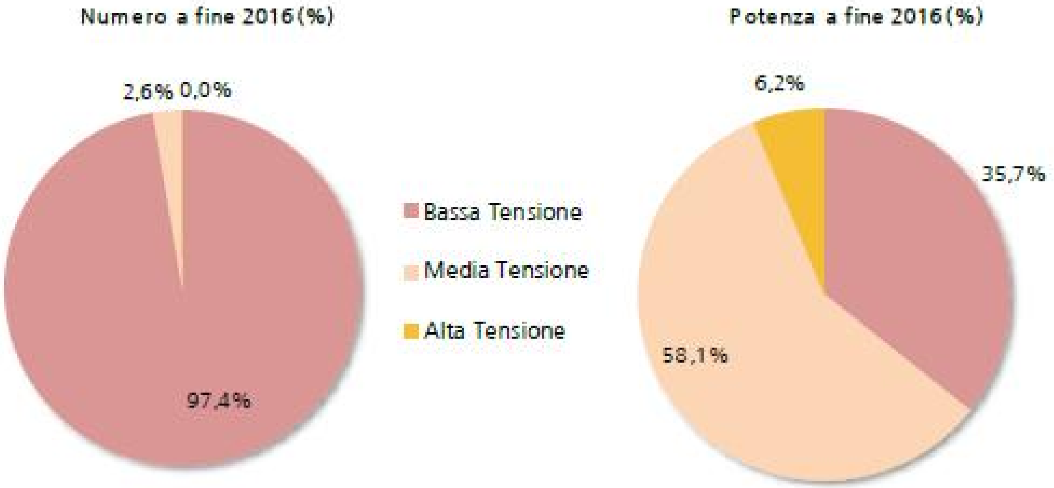

Figure 1.30 - PV plants for connection voltage

The productivity of a PV plant is strongly influenced on the available radiation, and therefore on the place of installation. As a proof, fig.1.34. reports the yearly sum of global irradiation (kWh/m^2) in Italy for different tilt angles of modules: horizontal, i.e. zero tilt angle, and optimal tilt. As a first approximation, the optimal tilt angle (β°) depends on the latitude of installation (ϕ); for modules which are not subject to any kind of shading, the optimal tilt can be found as:

$$\beta_{opt} = \phi - 10° \quad (1.19)$$

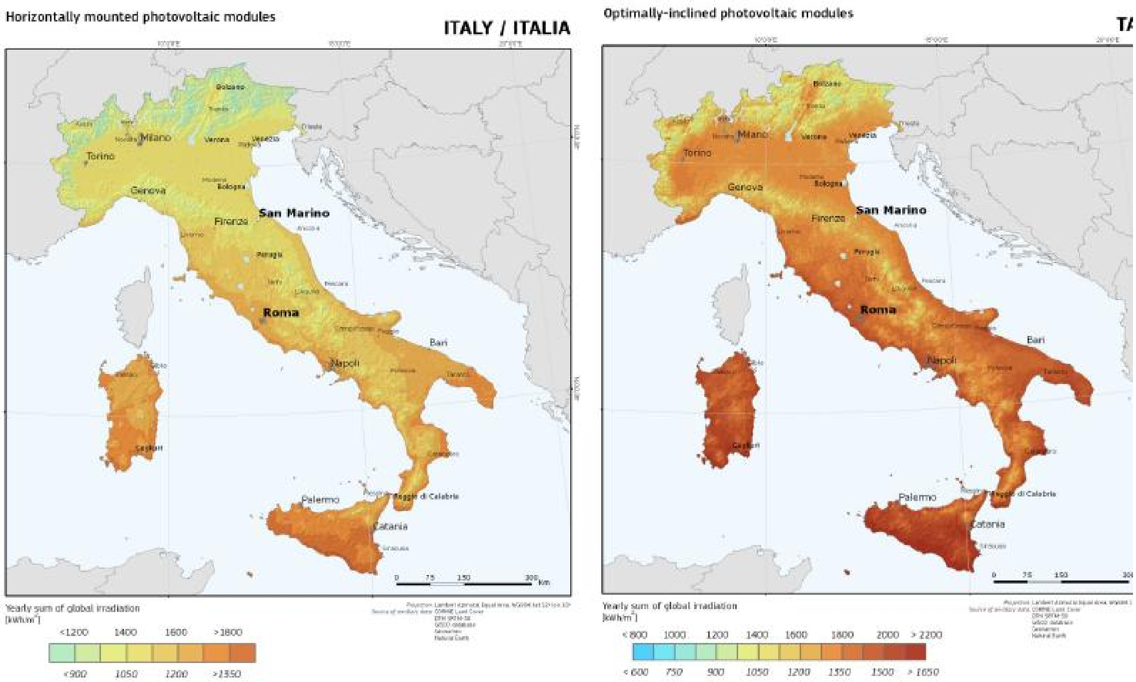

Figure 1.31- Available solar radiation for horizontal and optimally inclined modules- Italy

Regions which have the greater numerosity of PV plants installed are in North Italy (54 % of the total), especially in Lombardia and Veneto.

Despite that, the region which has most of installed power is Puglia, which has also the highest power density (power per unit surface, kW/m^2).

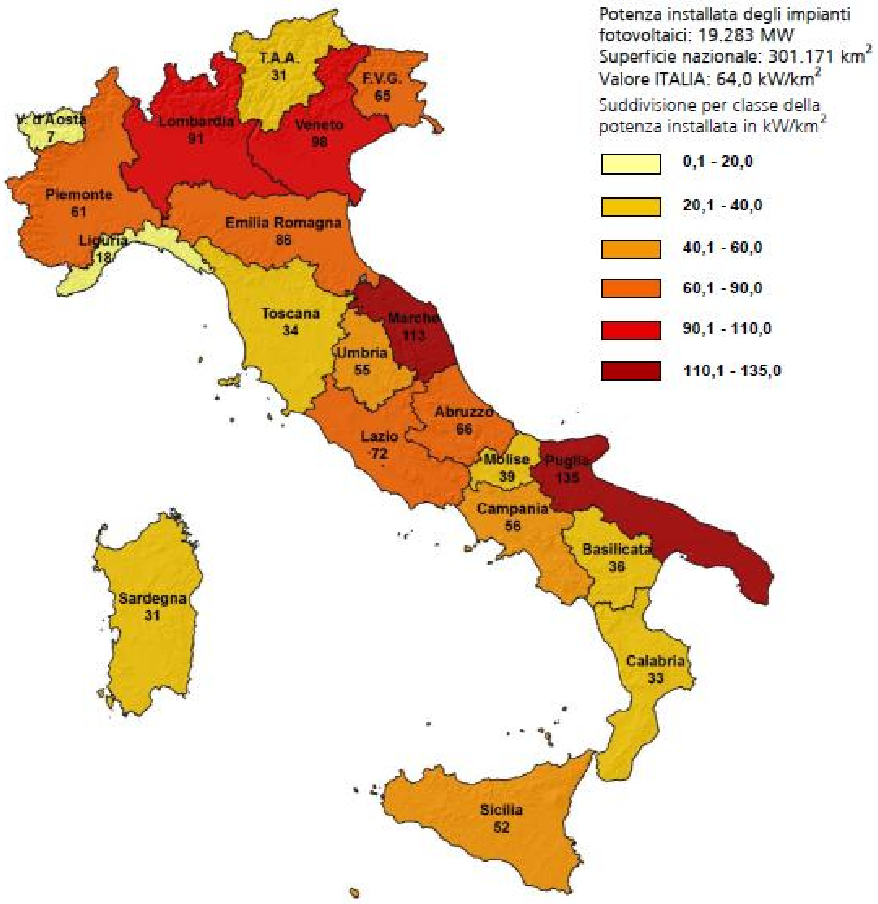

Figure 1.32 - Installed PV power per unit surface (kW/m^2)

Considering the average power per capita, the national average is 318 W/inhabitant; greater values can be found in central Italy.

Energy production by PV is strongly influenced by installed power and place of installation. As the power, it has grown considerably since the beginning of the 10's, thanks to incentives.

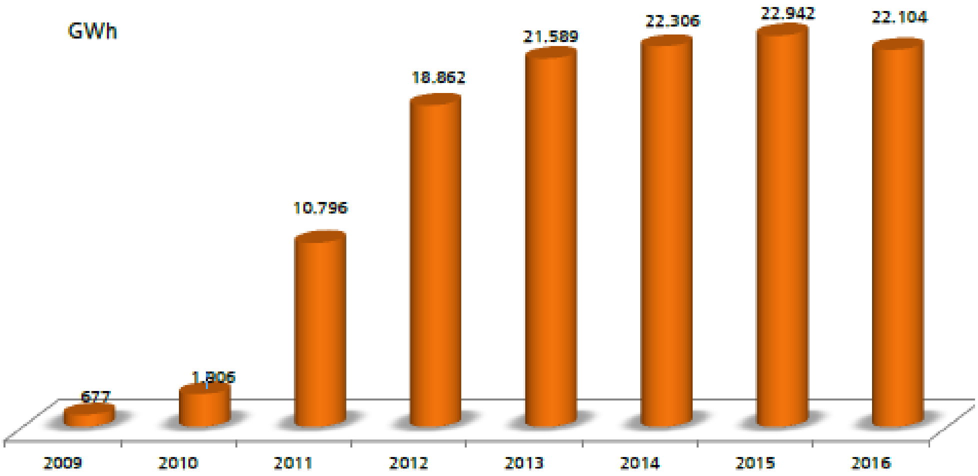

Figure 1.33 - Yearly production (GWh) by PV

Southern regions present a higher number of hours equivalent per year, therefore the production of PV plants located there is considerably superior to the ones of north Italy. Nevertheless, since the numerosity of PV plants is higher in the north, except for Puglia, the greater contribution to national yearly energy production comes from northern regions.

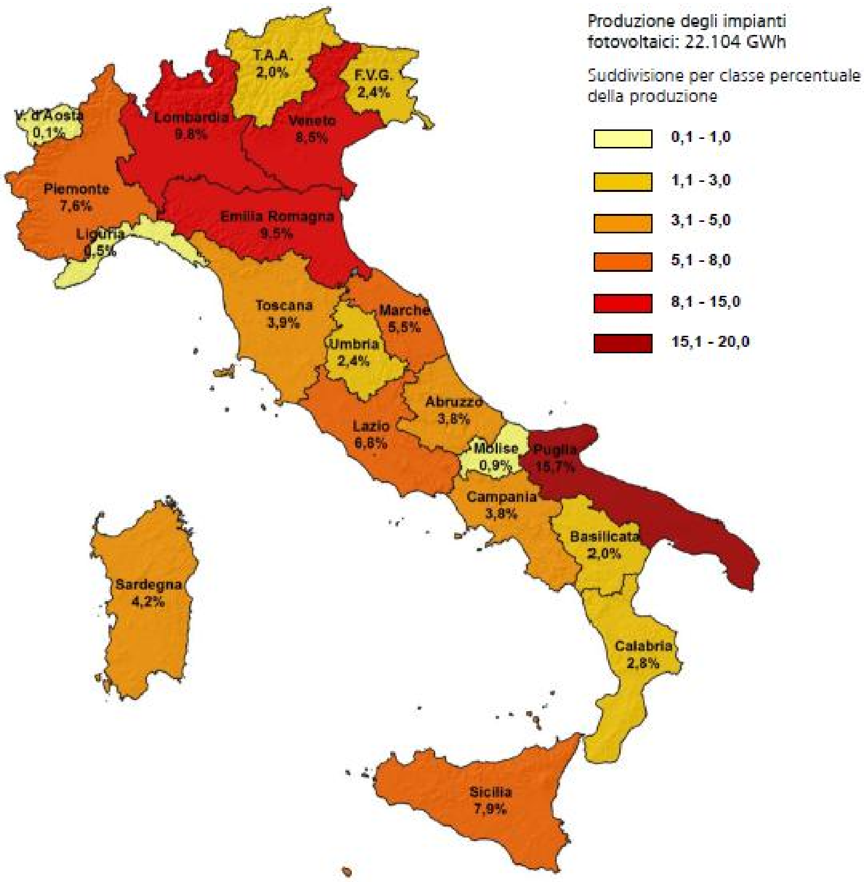

Figure 1.34 - Yearly production from PV (2016)

The final yield of a plant (or equivalent hours of functioning), expressed in kWh/kW_p, can be a useful parameter to consider both the efficiency of the systems involved and the solar irradiance level (kWh/m^2) of the location considered. Indeed, lower efficiency or lower irradiance (due to the place climate or to the presence of sources of shadowing) can compromise plant's productivity and affordability and are symptoms of a bad design.

The value of final yield characterizing all the PV plants built in Italy presents a decreasing trend with time. Main reasons for this result are the change in irradiance and, mostly, the increasing share of small PV plants, which have generally lower efficiencies with respect bigger plants.

Considering main applications sectors of PV technology, most of Italian plants are at service of domestic appliances, while industry sector presents the majority of the installed power. The reason for the mismatch numerosity-power is essentially due to the average size of the systems, much greater for industry than domestic sector, because of the different energy requests; less plants but bigger for industry sector, the opposite for domestic.

2. Project: PV plant

The aim of the second chapter is to furnish a general overview about the main steps for the correct design of an efficient PV system, starting from the input data (such as energy demand of the users, available area) to the final project.

The last part of the chapter will be devoted to the description of the plant under study (case study plant).

2.1. PV plant design

Several types of photovoltaic plants can be distinguished, depending on the site of installation or on the users to which are connected, and again depending on whether or not there is a connection with the network.

As said previously, the attention will be focused on grid connected PV plants. Inside this category, a further subdivision can be applied, depending on the typology of installation. Mainly, distributed (usually roof mounted) or centralized (usually ground mounted) PV plants can be considered for grid connection.

According to the type considered, design parameters and procedures can be very different for the two cases.

In the following paragraph, the differences in the approach if considering the two types of plants, when present, will be highlighted.

2.1.1. Sizing

Generally, the starting point is the PV plant sizing. During this phase, the designer should interact with the customer, in order to understand its needs.

The power to be installed, in general, is determined according to:

- Available area;
- Annual energy demand of the customer;
- Payback time of the investment.

Considering grid-connected plants, the goal is the maximization of the annual production, since possible surplus and deficit of energy, in specific moments, can be compensated by the grid. The situation is different for stand-alone PV plants, in which production should be maximized during central year months, for which the consumption is higher.

In the case of distributed plants, normally associated to a user, plant sizing is performed mostly accordingly to the electrical bill of the customer; in general, the size of the plant must be determined so as to cover entirely energy needs of the customer. The energy in excess is then sold to the grid.

In Italy, for these types of plants, the regulation of exchange and withdrawal of energy with the network follows the SSP scheme (“Scambio sul Posto”), which is a contract stipulated with the GSE that allows the excess energy to be fed into the grid, and, simultaneously, to withdraw from the grid an amount of energy equal to that entered, at a price lower than the standard market value. The possible excess of user’s energy request with respect the amount injected can be also covered from the grid, at standard prices.

The investment can be considered convenient also nowadays (without specific incentives), considering the growth of the electricity price (standard price) for household consumers with time.

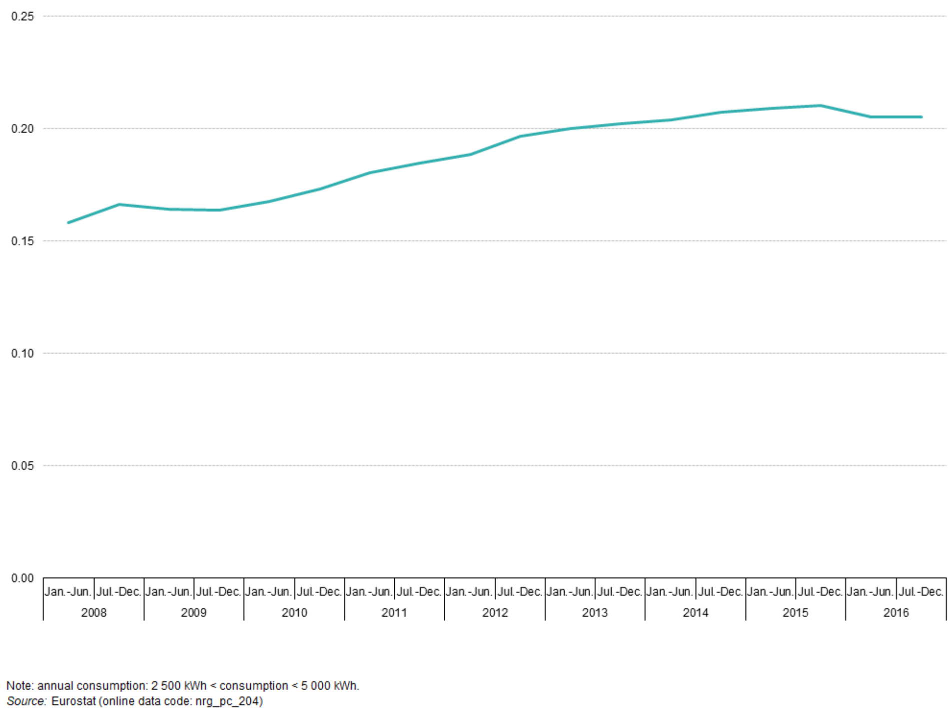

Figure 2.1 - Electricity cost (€/kWh) for the final user wrt. Time

2.1.2. Sizing examples

Ex.1

Let's consider a user which requires 3'000 kWh of electrical energy per year. As will be explained better in the next chapter, the formula for the evaluation of the required PV power P_{PV} is:

$$P_{PV} = \frac{E_{AC}}{PR \cdot h_{eq}} \quad (2.1)$$

E_{AC} is the user's energy need, while PR is a parameter standing for system efficiency. h_{eq} is the number of equivalent solar hours per reference time, strongly influenced by meteorological data of the location considered; usually, for northern Italy latitudes, the value of the multiplication at the denominator can be approximated to 1'000 h/year.

Therefore, the PV plant size can be roughly determined as:

$$P_{PV} = \frac{3'000}{1'000} = 3.00\ kW$$

Of the energy produced, a certain amount is expected to be contextual to the user's request; if this share is assumed equal to 33.3 %, this means that, in a year, 1'000 kWh of electrical energy produced by the plant are used to feed directly the user, with 0 costs. The other 2'000 kWh produced are injected into the grid, and, thanks to SSP mechanism, are re-bought from the grid at a lower price; if the national price of electrical energy, for the final user, is averagely 200 €/MWh, with this mechanism the price of the 2'000 MWh will be reduced to 60 €/MWh, producing a net saving of 140 €/MWh. The eventual extra energy consumption is satisfied buying energy from the grid at full price.

The PBT of such an investment can be determined roughly as:

$$PBT = \frac{Cost_{PV}\ [€]}{Savings_{year}\ \left[\frac{€}{y}\right]}\ [y] \quad (2.2)$$

, having assumed negligible O&M costs.

For roof-mounted plants, the cost per installed kW could be estimated equal to 1’300 €/kW_p[15]; for the considered example, it follows that:

$$PBT = \frac{1'300 \cdot 3}{140 \cdot 2 + 200 \cdot 1} = 8\ years$$

For the project of PV plants, it is crucial the estimation of the energy consumption that the PV generator has to cover. In general, it is difficult to have at disposal load diagrams, which represent the power absorbed by the loads on an average day of the month; it is more common to have electric bills in which, for every month, the energy consumed by the user is given, and subdivided into energy bands. PV production should equalize, every time, load’s consumption; since this is not possible, the equilibrium between production and consumption is achieved at monthly/yearly scale.

[15] This value is strongly influenced on the size of the plant considered; bigger plants have normally lower values per kW installed.

Ex.2

Let’s consider another example whose data are taken from an existing problem treated at Entec. The goal is the sizing of the plant starting from the monthly request of energy of the user, given divided in bands in the electrical bill, so as to minimize the pay-back time of the investment. The user under analysis is a medium-scale factory.

Usually, the energy consumption of the final user can be divided into three bands, depending on the time of day it is present. These three bands are named F1, F2 and F3.

Ore del giorno	0	1	2	3	4	5	6	7	8	9	10	11	12	13	14	15	16	17	18	19	20	21	22	23	24
lunedì	F3	F3	F3	F3	F3	F3	F3	F2	F1	F1	F1	F1	F1	F1	F1	F1	F1	F1	F1	F2	F2	F2	F2	F3	
martedì	F3	F3	F3	F3	F3	F3	F3	F2	F1	F1	F1	F1	F1	F1	F1	F1	F1	F1	F1	F2	F2	F2	F2	F3	
mercoledì	F3	F3	F3	F3	F3	F3	F3	F2	F1	F1	F1	F1	F1	F1	F1	F1	F1	F1	F1	F2	F2	F2	F2	F3	
giovedì	F3	F3	F3	F3	F3	F3	F3	F2	F1	F1	F1	F1	F1	F1	F1	F1	F1	F1	F1	F2	F2	F2	F2	F3	
venerdì	F3	F3	F3	F3	F3	F3	F3	F2	F1	F1	F1	F1	F1	F1	F1	F1	F1	F1	F1	F2	F2	F2	F2	F3	
sabato	F3	F3	F3	F3	F3	F3	F3	F2	F2	F2	F2	F2	F2	F2	F2	F2	F2	F2	F2	F2	F2	F2	F2	F3	
domenica	F3	F3	F3	F3	F3	F3	F3	F3	F3	F3	F3	F3	F3	F3	F3	F3	F3	F3	F3	F3	F3	F3	F3	F3	

Figure 2.2 - Energy hourly bands

Current consumption (kWh) of the user is now reported:

	Gen	Feb	Mar	Apr	May	Jun	Jul	Ago	Sep	Oct	Nov	Dec	Tot
F1	5’248	4’272	3’555	2’374	2’553	1’316	1’338	1’227	2’401	3’853	5’091	5’090	38’318
F2	1’278	1’188	1’535	834	1’002	714	728	587	1’109	1’440	1’372	1’257	13’044
F3	401	471	516	130	148	357	291	263	172	588	552	605	4’494
Tot	6’927	5’931	5’606	3’338	3’703	2’387	2’357	2’077	3’682	5’881	7’015	6’952	**55’856**

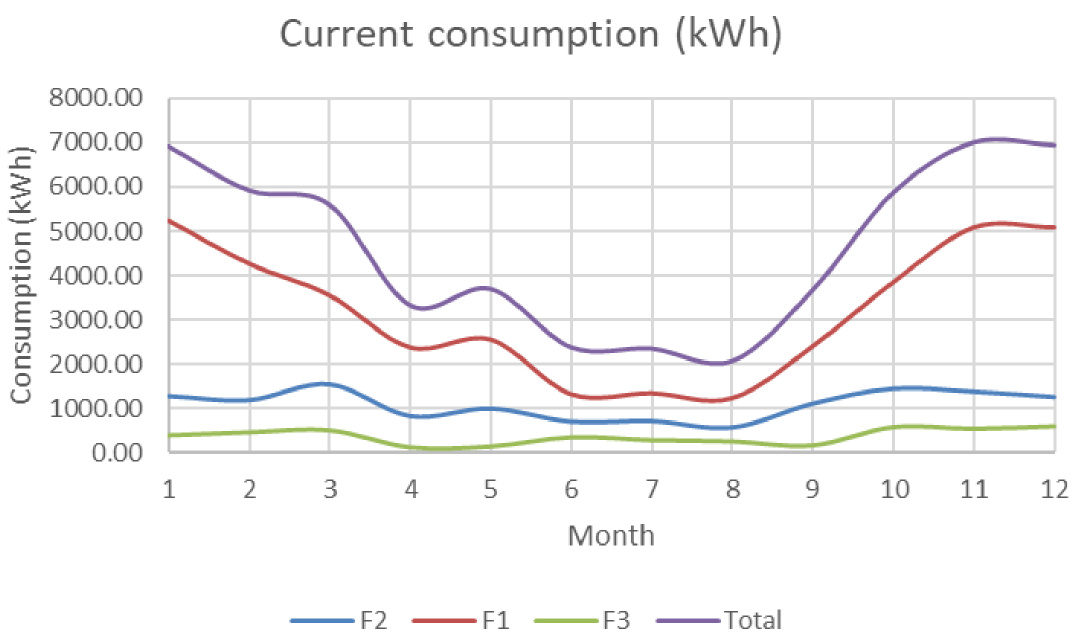

As it can be easily seen, most of the consumption is present in band F1, which accounts for the central hours of the day during weekdays.

Modules chosen present a nominal power of 275 W_p. Consequently, varying the number of installed modules (i.e. plant's size), it has been carried out an optimization analysis aimed at reducing the PBT of the investment.

The complete sizing analysis will be explained considering 200 modules (plant's size: 55 kW_p); a final optimization procedure on the PBT will be carried out afterwards, varying, as said before, the number of panels.

According to Entec experience in PV sector, monthly subdivision of production, expressed as a percentage of the yearly production, have been determined using several real data from installed plants in different locations of northern Italy. Averagely:

Month	Productivity (%/year)
January	3.6
February	3.7
March	8.2
April	10.3
May	12.8
June	13.5
July	13.7
August	12.7
September	9.0
October	5.7
November	3.5
December	3.1
Total	100

Table 2.1 - Monthly energy productivity (%/year), averaged for different real plants

If the plant's final yield, i.e. the ratio between the plant's real production (considering all disgraceful effects) and the plant's nominal power, is assumed equal to 1'015 kWh/kW_p, then, for each month, plant's productivity can be easily estimated. In detail:

Month	Productivity (kWh)
January	2’943
February	3’022
March	6’636
April	8’349
May	10’391
June	10’907
July	11’130
August	10’279
September	7’255
October	4’644
November	2’854
December	2’537

Table 2.2 - Monthly energy productivity (kWh), averaged for different plants

Plant’s production can be then subdivided into the three energy bands, by using information of fig.2.2.:

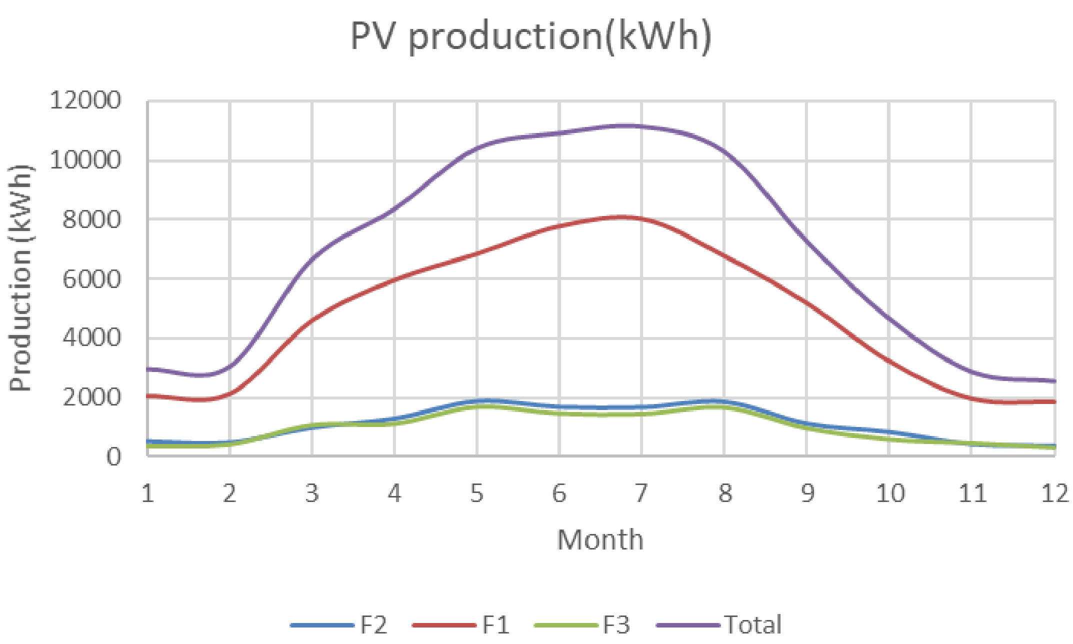

The contextual energy consumption, i.e. the energy consumption which is contemporary with PV plant's production, can be roughly estimated as:

- Equal to PV production, if the energy demand is higher than the energy production in that specific band;
- Equal to energy demand, if the PV production is higher than the energy demand in that specific band.

Adopting the previous mentioned hypothesis:

	Gen	Feb	Mar	Apr	May	Jun	Jul	Ago	Sep	Oct	Nov	Dec	Tot
F1	2'028	2'096	3'555	2'374	2'553	1'316	1'338	1'227	2'401	3'200	1'939	1'828	25'854
F2	535	495	993	834	1'002	714	728	587	1'109	845	439	382	8'663
F3	380	432	516	130	148	357	291	263	172	588	476	327	4'079
Tot	2'943	3'022	5'064	3'338	3'703	2'387	2'357	2'077	3'682	4'633	2'854	2'537	**38'597**

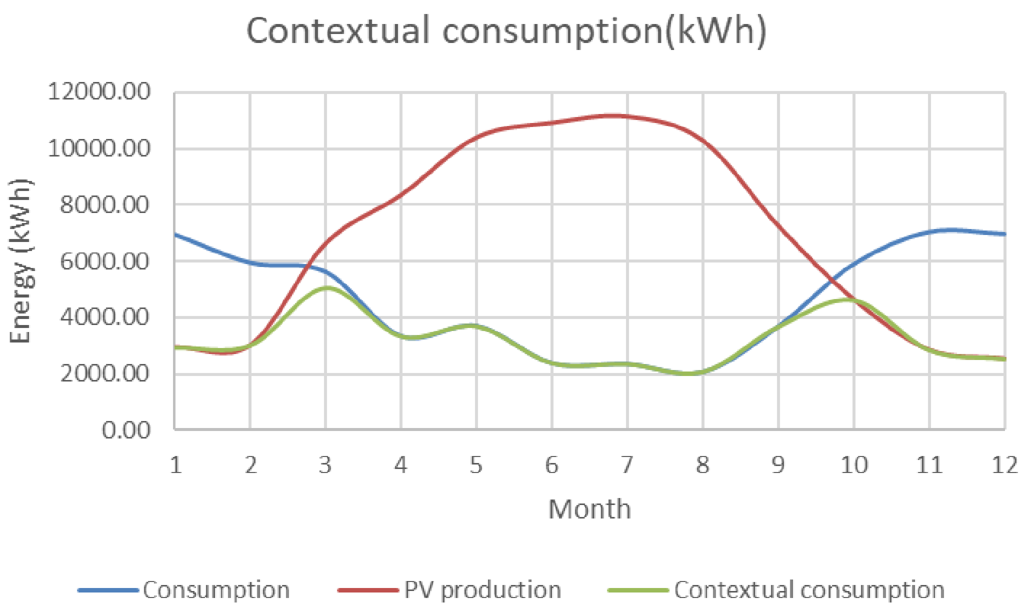

There are many factors for which, also during the day, demand and production are not contemporary; for instance, thunderstorm can cause a dramatic decrease of PV daily production, while energy demand is almost independent on this factor. Conversely, a temporary interruption of the normal activities can lead to a decrease of the demand, which can result in a not complete exploitation of the PV power.

The average value of contextuality can be estimated as the ratio between the contextual consumption and the energy demand. In this example:

$$C = \frac{38597}{55856} = 69\% \quad (2.3)$$

Consequently, the eventual excess energy (kWh) sold to the grid (SSP mechanism) is evaluated from the difference between the PV production and the energy demand; if the difference is negative, then the parameter takes value 0.

	Gen	Feb	Mar	Apr	May	Jun	Jul	Ago	Sep	Oct	Nov	Dec	Tot
F1	0	0	1’017	3’570	4’281	6’450	6’679	5’534	2’764	0	0	0	
F2	0	0	0	457	879	973	949	1’274	13	0	0	0	
F3	0	0	554	983	1’528	1’097	1’145	1’395	795	11	0	0	
Tot	0	0	1’572	5’011	6’688	8’520	8’773	8’202	3’573	11	0	0	**42’349**

Similarly, the eventual energy levied (kWh) from the grid can be determined as the difference between the energy demand and the PV production; if the difference is negative, then the parameter takes value 0.

	Gen	Feb	Mar	Apr	May	Jun	Jul	Ago	Sep	Oct	Nov	Dec	Tot
F1	3’220	2’177	0	0	0	0	0	0	0	653	3’152	3’262	
F2	743	693	542	0	0	0	0	0	0	595	933	875	
F3	21	39	0	0	0	0	0	0	0	0	76	278	
Tot	3’984	2’909	542	0	0	0	0	0	0	1’248	4’161	4’415	**17’259**

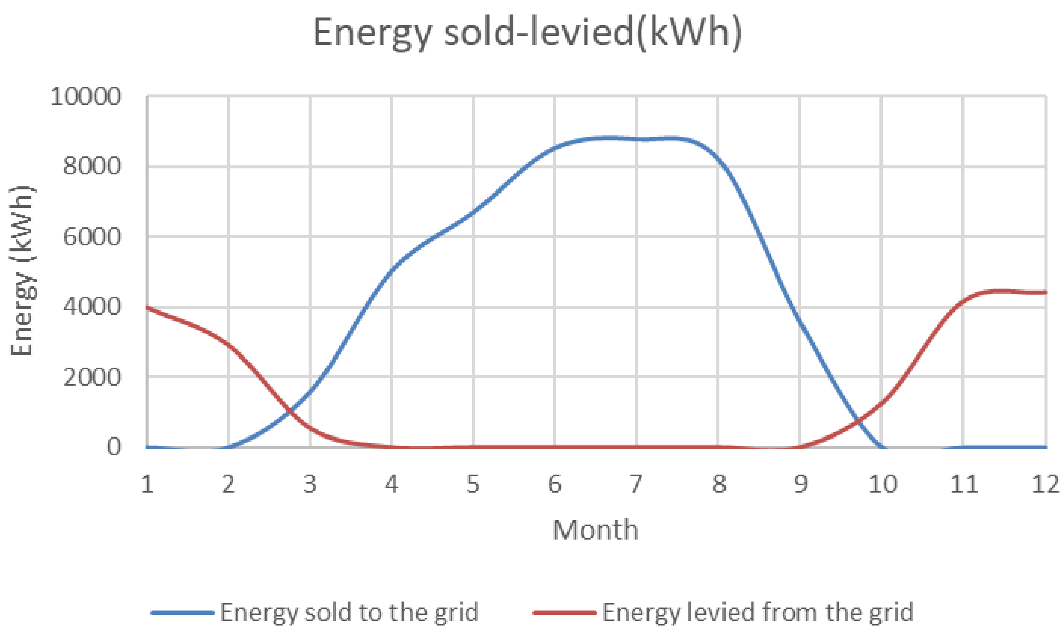

Through this parameter, a short economic analysis can be performed; the following hypothesis will be made:

Electricity cost (€/kWh)	0.166
Electricity cost SSP (€/kWh)[16]	0.050
Electricity sold (€/kWh)	0.050

Therefore, cash flow ante and post PV installation can be compared:

- Ante:

Yearly electricity need (kWh)	55'856
Annual cash flow (€) - C_{ante}	=-55'856*0.166=-9272

- Post:

Yearly electricity need (kWh)	55'856
Yearly PV productivity (kWh)	80'946
Yearly self-consumed electricity (kWh)	38'597
Yearly electricity TO the grid (kWh)	=80'946-38'597=42'349
Yearly electricity FROM the grid (kWh)	=55'856-38'597=17'259
Yearly electricity TO the grid, net of SSP (kWh)	=42'349-17'259=25'090
Cost of self-consumed electricity (€)	$=0\,\frac{€}{kWh}$*38'597=0
Cost of electricity in SSP (€)[17]	$=0.05\,\frac{€}{kWh}$*17'259=-862.95
Gain from extra electricity sold (€)	$=0.05\,\frac{€}{kWh}$*25'090=1'254.50
Annual cash flow (€) - C_{post}	=1'254.50-862.95=391.55

[16] With SSP mechanism, the energy in excess injected into the grid can be recovered afterwards at the 30% of the normal price. In practice, the 70% of the cost of electricity is refunded to the owner of the PV plant, given that the amount of energy levied from the grid is lower than the one injected. In this case, it can be assumed that the cost of energy levied in SSP is exactly equal to the 30% of the standard one (0.30*0.166=0.05 €/kWh). Taxes are not refunded.
[17] Since the electricity levied from the grid is lower than the electricity injected into the grid from the PV plant, all the energy levied from the grid is subjected to SSP tariff.

All considered, the annual savings are equal to:

$$Savings = C_{post} - C_{ante} = 391.55 - (-9272) = 9'664\ €/year \quad (2.4)$$

According to Entec databases, the behavior of a PV plant cost can be approximated through a piece-wise function:

$$Investment = 1'200 \cdot P_n + \begin{cases} 6'000, & if\ P_n < 20\ kWp \\ 8'000, & if\ P_n > 20\ kWp \end{cases} \quad (2.5)$$

The PBT of the investment can be then easily determined as the ratio of initial investment and savings:

$$PBT = \frac{Investment}{Savings} \quad [year] \quad (2.6)$$

The procedure presented has been repeated for different values of number of installed modules, varying consequently investment costs and annual cash flow, as a function of the installed power. Results are reported both numerically and graphically.

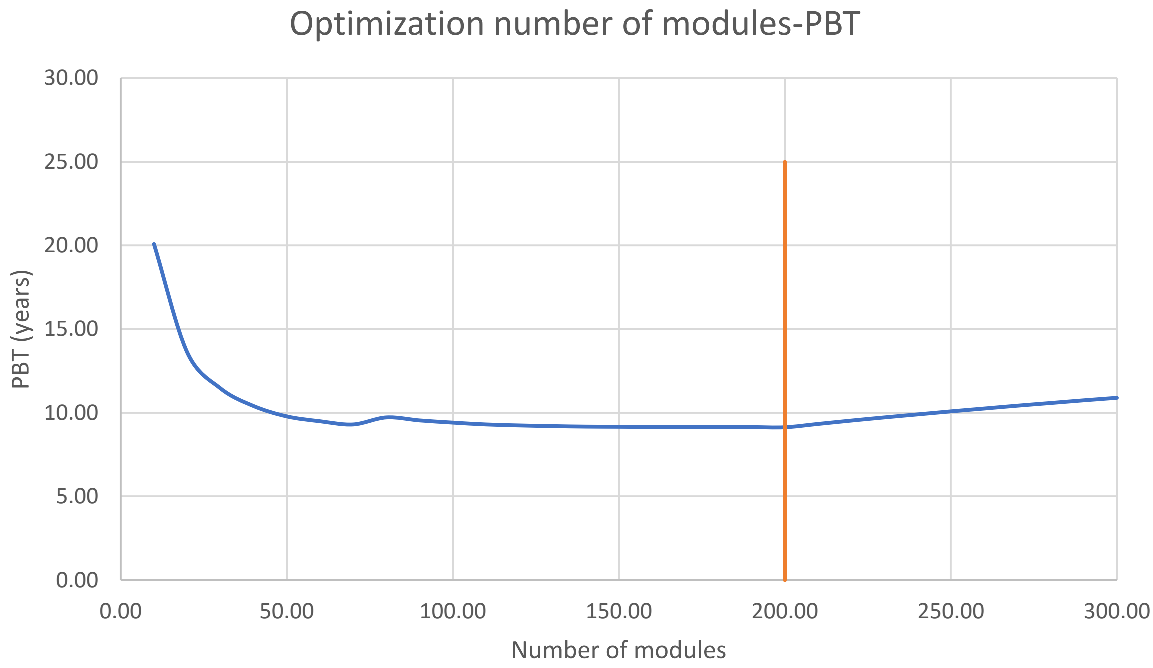

Figure 2.3 - Optimization results

The graph shows two minima; the relative minimum is in correspondence of the change of slope of the curve, due to the approximation made in the estimation of the installation costs. The absolute minimum, exactly for 200 modules, corresponds to a PBT of around 9 years.

Design parameters considered can be different for distributed and centralized PV plants; the last ones are not associated to a user and inject all the energy produced into the grid. In general, the adopted design parameter is the available area, which should be optimally covered with the largest amount possible of modules, so as to maximize the energy produced.

Especially in the past years, when the Italian energy landscape included a flourishing amount of incentives, the superior limit of the installable power was determined not only by the available area, but also through pre-established power limits, clearly expressed within the regulations of reference, which implied substantial variations in the incentive rates if exceeded; as a rule, these economic variations, the more the power grew, were pejorative. Therefore, it is quite common to see big PV plants whose upper power has been limited to 999 kW, for example, so as not to lose possible economic benefits in the case of the overcoming of the 1 MW threshold.

With the end of the incentives in 2013, the diffusion of these types of plant has been dramatically reduced. As a matter of fact, the presence of very large incentives was the key of making such a kind of investment favourable.

With the “Conto Energia” scheme, the electrical energy sold to the grid was averagely evaluated 250 €/MWh plus the market price. Today, a hypothetical centralized plant, configured in total input, would see an evaluation of the energy produced equal to the value of the Italian uniform purchase price (PUN[18]), now around 45 €/MWh.

Carrying out a brief analysis, based on the data extrapolated from the historical databases of the GME[19], it can be noticed how the value of the PUN is decreasing with time.

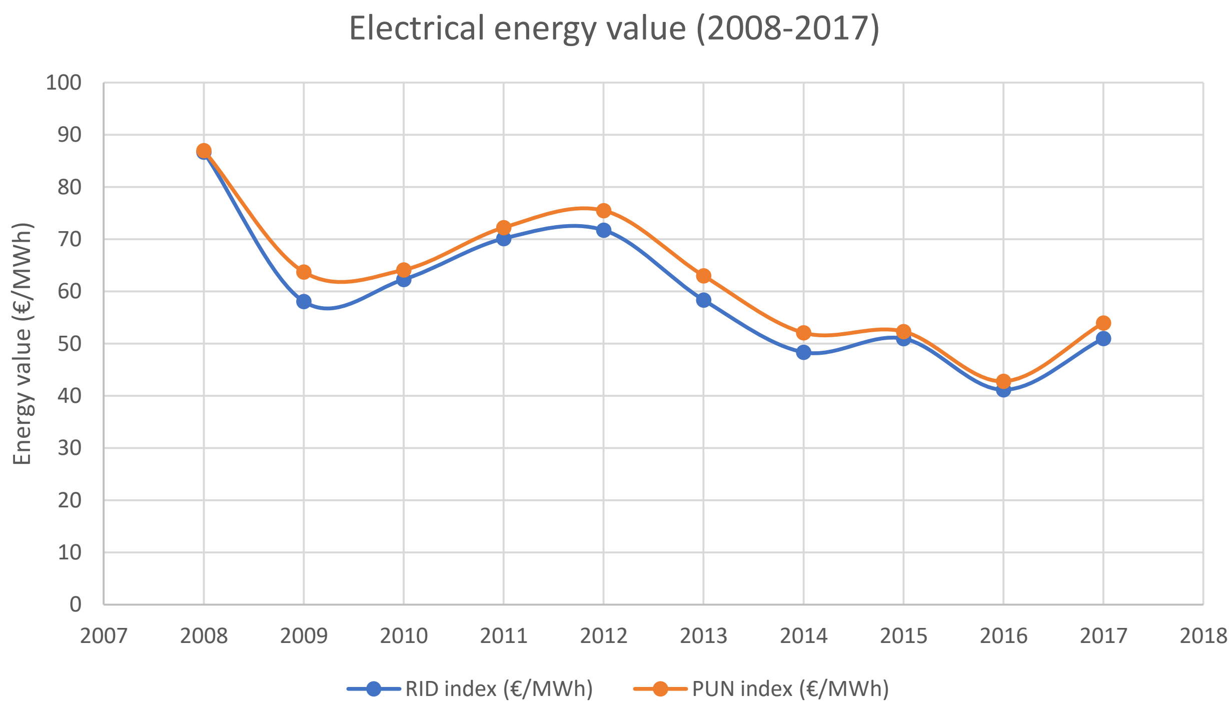

Figure 2.4 - Electrical energy value (2008-2017) - €/MWh, for the producer. This trend should not be confused with the one highlighted in figure 2.1, since that one was referred to the cost of electricity for final users buying energy from the grid, while this last represent the average price at which energy could be sold to the grid without specific incentives.

The value of PUN has been graphed together with the RID[20] index. For each month, data were given divided per bands. Graphed results are the average of 12 months; each month is evaluated as the average of the three energy bands.

---

[18] PUN = “Prezzo Unico Nazionale”.

[19] GME = “Gestore dei Mercati Elettrici” – Italian public company that manages, among other things, the electricity markets in Italy.

[20] RID = “Ritiro Dedicato” – sales scheme in which the sole interlocutor is the GSE.

An evident rate of de-growth over time should suggest that, without proper support scheme, these kinds of plants are not economically sustainable nowadays; the price of electricity in €/MWh is too low to compensate the investment costs.

It is therefore crucial, as it will be highlighted subsequently, for centralized PV plant built under “Conto Energia” scheme, not to lose the access to incentives, in case of modifications (e.g. revamping).

2.1.3. Installation

Having introduced the design parameters characteristics of the preliminary steps of the project, the attention should be now posed to the technical aspects of the intervention. A professional PV generator study must necessarily pass for the evaluation of the installation site; a first site inspection is crucial in order to understand what the physical boundaries of the intervention are, especially for roof-mounted plants.

The main aspects which should emerge are the available area dimensions and orientation, its exact location (latitude, longitude and altitude, in order to adopt proper meteorological data), the location of all the possible sources of shadowing and eventual administrative restrictions which can determine a substantial reduction of the intervention's area, as well as a consequent decrease of the plant's installed power or economic convenience.

According to the criterion adopted (maximum area exploitation or customer's energy request), a first general layout of the plant, after the choice of a proper type of module and plant's mechanical structure, can be introduced.

The first step for the evaluation the installation site is the determination of the solar South. A solar photovoltaic system facing south is reached by the greatest amount of solar energy because the sun is higher and the path of its rays within the atmosphere is shorter. Azimuth is defined as the angular displacement from the South of the projection of a Sun ray on the horizon plane (positive toward West); in other words, it describes sun position on an horizontal plane from east to west.

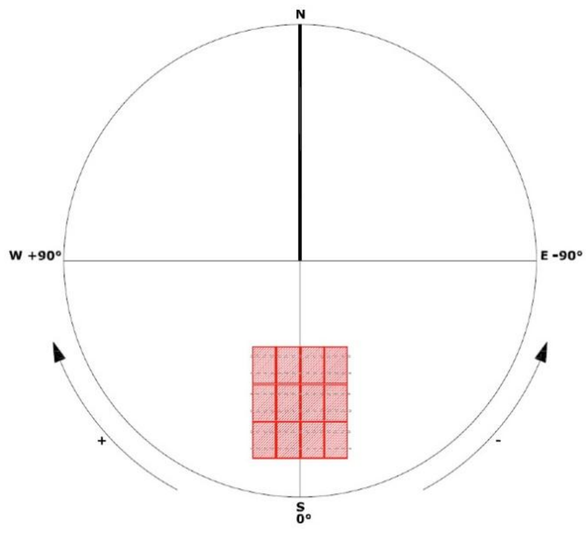

Figure 2.5 - Azimuth angle

The optimal value, as said before, is South, i.e. 0° azimuth. However, there are cases in which this could not be the best choice; for instance, when the horizon plane is limited due to the presence of imponent obstacles, such as mountains or buildings, which reduces the equivalent sun hours at the beginning or at the end of the day. Changing the azimuth in the opposite direction could allow to reduce shading losses due to the horizon profile.

Another crucial parameter is the tilt angle, i.e. the inclination of the available area with respect the horizontal plane.

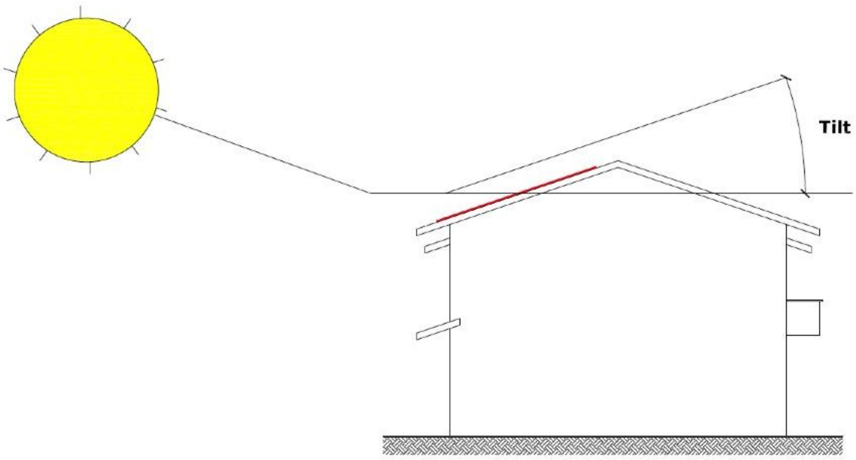

Figure 2.6 - Tilt angle

Optimal values are determined according to the sun height over the horizon; the higher is the Sun, the lower would be the optimal tilt angle, and vice versa.

In Italy, optimal design parameters are usually considered 30° for the tilt angle and 0° (South direction) for the azimuth angle. These values are the ones which allow the maximization of the energy productivity during the whole year.

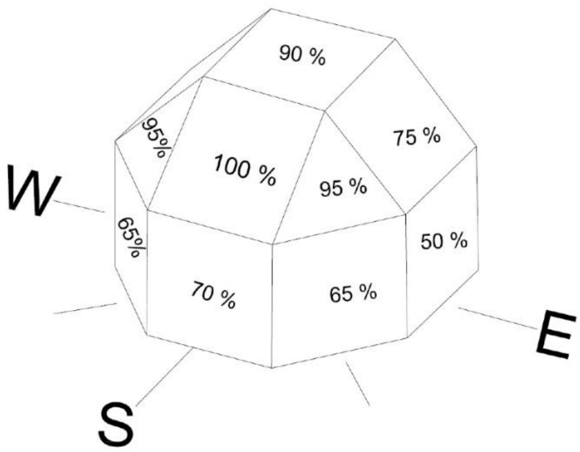

Figure 2.7 - Optimal tilt and azimuth angles

In the case of roof-mounted plants, in general, these two parameters are fixed and equal to the ones of the roof in which the plant would be installed. As a consequence, most of the case different from the optimal ones.

Figure 2.8 - Roof-mounted PV plant

For horizontal roofs, these two parameters can be chosen freely, since modules, in general, are positioned through adjustable structures. Attention should be posed in order to avoid reciprocal shading between different rows of modules. In general, it can be said that horizontal roofs present a better productivity with respect inclined roofs, but have a worst area occupation; indeed, for inclined roofs, it is not necessary a spacing between different rows of modules, since no reciprocal shading could be present, therefore a higher number of panels can be installed.

In the case of ground-mounted plants, the situation is quite similar to the one of horizontal roofs. In general, these plants are distributed on different rows; consequently, also row distance becomes a design parameter. Therefore, according also to the location, optimal azimuth and tilt angle are strongly affected by the row distance, due to the mutual shading between different rows.

Figure 2.9 - Ground-mounted PV plant

The second step for PV installation is the analysis of the location, in terms of latitude and longitude.

Latitude is defined as the angle between observer-Earth centre line and equator plane (positive towards North); longitude is the angle between the local meridian plane and Greenwich meridian (positive towards West).

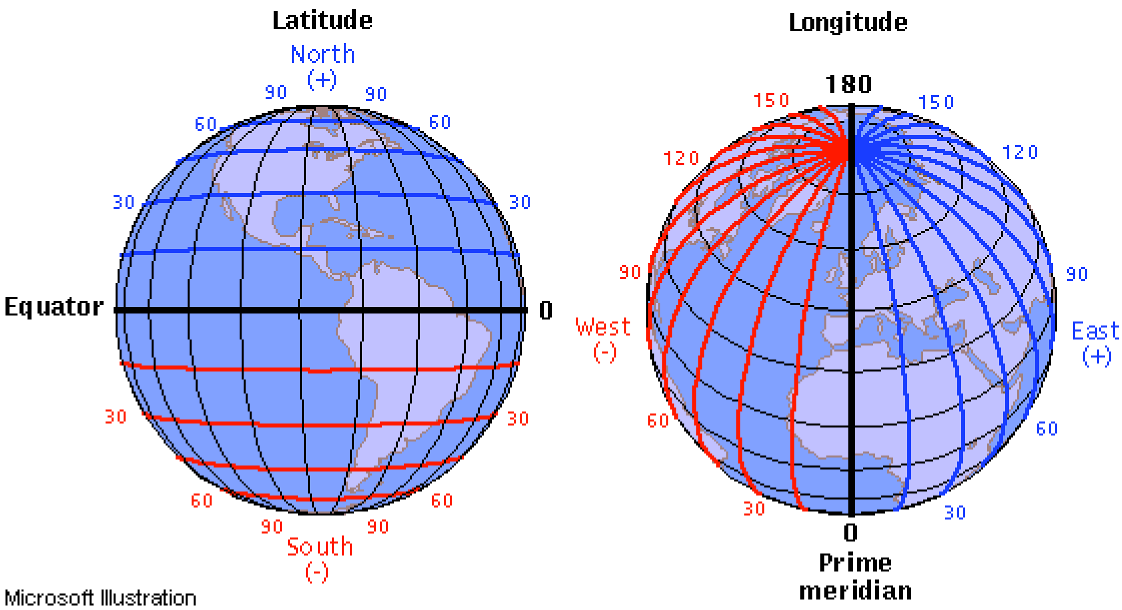

Figure 2.10 - Latitude and longitude concepts

The exact location allows the determination of the Sun path, through the Solar chart, and of the amount of incident radiation. Solar plots are a 2D representation of the Sun paths over the sky vault. Each solar plot is drawn for a specific location (that is, for a certain latitude, ϕ) and allows to assess the Sun position for every hour of the day and for every day of the year, by means of the solar altitude angle and of the solar azimuth. In order to retrieve the correct chart, online tools or software programs which are able to generate the plot for the specific location under analysis can be adopted.

With these data, also the global in-plane radiation can be estimated. This value affects directly the amount of energy which can be produced by the system. The value of solar radiation varies both with the hour of the day and with the day of the year. As a direct consequence, the productivity of the PV plant changes in the same way.

For a given location, equivalent sun hours can be defined as the sum of virtual hours at the maximum of solar irradiance in a year, usually considering $G=G_{STC}$. They can be estimated as the ratio between the daily radiation Hg (kWh/m^2) and the reference STC irradiance (kW/m^2); the number represents also the daily hours of functioning of the system at nominal power. It is a purely theoretical number, since it does not include system's losses, contained in the term PR (performance ratio, see ch.3.1). Generally, this value is around 1'500 h/y near Turin; yearly final yield of the plants, in terms of kWh/kW$_p$ would be necessary lower, since given by the product of the equivalent hours and the performance ratio.

The third step includes shadow analysis. Given that shadows on PV surface cause very important productivity reductions, it is necessary, during the installation phase and once the location has been defined, the individuation of all possible sources of shadowing, such as trees, buildings etc. Through the solar chart, it is possible to understand what the most critical periods are, in which shadows have the major influence, i.e. during which obstacles project the greater shadow above the generator.

Figure 2.11 - Example of a wrong installation due to persistent shadowing

As seen in chapter 1, the effect of shadow can cause mismatch problems, and therefore, strong limitations on the power. Even very small shadows can cause dramatic reductions of the productivity of the module, and consequently on the whole plant, through a sort of bottleneck effect, for the other series connected cells, which can be only partially resolved through the before mentioned bypass diodes. A correct design of strings can limit the problem. In general, when the percentage of shading is high, it is better, if possible, to concentrate the shading on a single string, in order to fix the maximum voltage power to the one in absence of shading.

General solutions to shadowing problems are:

- *Correct string subdivision*, so as to concentrate all the shading on the most limited numbers of strings;
- *Elimination of the sources of shadowing*, when possible. They are essentially of two types: temporary (such as clouds, birds etc.) and persistent (trees, chimneys); only the last one could be eliminated, due to the random nature of the firsts;
- Compensation of the lower production by *enlarging the generator*;
- *Bypass diodes* insertion;
- *Multiple MPPT's inverters*, in order to limit the negative effects of shadowing on a single string.[21]

Worst situation is in winter, when Sun is lower above the horizon, causing longer shadows.

[21] The newcomer technology into this field is represented by the power Optimizers technology. A power optimizer, which acts as a MPPT, is connected to a small set of PV modules; it is presence is recommended only in case of strong shadowing, and permits a very precise optimization of performances, compared to the one assured by a traditional MPPT.

2.1.4. Electrical project

The electrical project is the fundamental part for the assembly of the PV plant, considering its principal components, i.e. modules and inverter, which must be sized in order to be compatible. In the second part of the chapter, an example of the required calculations for the inverter-module configuration will be proposed, using as example the plant under analysis.

INVERTER

If the choice of the module is dictated mostly by economic reasons, for the inverter other selection parameters are considered.

First of all, an inverter could be mono-phase or three-phase; in general, it is preferable, for high power (> 5 kW), the usage of a three-phase inverter, since it allows to reduce the number of transistors. Furthermore, the three-phase permits a greater voltage on DC side, allowing a reduction of cable's section.

On the contrary, the usage of three mono-phase inverters consents to have a greater availability of the whole system, since, during maintenance activities, only a part of the plant is forced to be shut down; furthermore, the effect of shadowing is less evident with respect the case of a single three-phase inverter.

If the mono-phase inverter presents a greater voltage range for MPPT's operation, the three-phase has lower THD ("Total harmonic distortion", see ch.1.6) and ripple on DC side, i.e. it has an higher conversion efficiency (from DC to AC).

ELECTRICAL SYSTEM

The electrical system of a PV plant should include other components, such as switches and transformers, like the ones presented in ch.1.6.

In general, on DC side, it is appropriate to consider a disconnector ("Sezionatore") for each string, in order to easily disconnect in case of maintenance.

On AC side, it is mandatory the insertion of a magnetermic switch in order to close the circuit for its maintenance, appropriate switches for PV disconnection in case of grid problems, possible transformers for the voltage level elevation, and necessary energy counters.

The final electrical scheme is reported in the "Single-wire diagram", which symbolically represents the plant and all its components.

2.1.5. Testing

After its mechanical installation, the project of the plant can be concluded by testing its performances. In general, procedures in order to overcome the test are reported through certificated guidelines; they require the evaluation of certain global parameters characterizing the plant as a whole, through experimental measures.

As an example, following the last variant of CEI[22] 82-15, in order to guarantee the plant to be performant, the value of the PR ("Performance Ratio") evaluated through a simplified formula, neglecting the effect of temperature (i.e. independent on the season on which the test is made), should be greater than a certain pre-established value.

These tests involve the usage of certificated instrumentation for the irradiance detection (solarimeter), modules temperature (IR thermo-camera) and energy production (energy counters with display, installed in place, can be used for this purpose).

[22] CEI = "Comitato Elettrotecnico Italiano"

2.2. Case study: 1 MW PV plant

The plant under analysis (case study plant) is ground-mounted grid connected, located in North Italy, on an agricultural terrain. In its original configuration the nominal power is 901.6 kW; it is composed of 3’920 modules of 230 W_p each. The configuration of the inverters is centralized; all the three inverters, of 330 kW each, are located into a special cabin. To each inverter, equipped with 6 MPPT, are connected around 60 strings of modules, of 20 modules in series each. Main features of the PV plant are schematically reported:

Year of installation	2011
Plant’s location	Fraction Canapile - Racconigi (CN)
Latitude	44° 44' 20'' N
Longitude	7° 41’ 35’’ E
Altitude above sea level	270 m
Ground type	Agricultural
Plant’s type	Ground-mounted grid-connected
Grid voltage level	3F 15 kV (MV)
Nominal power	901.6 kW_p
Module’s model and technology	LDK 230P polycrystalline silicon
Number of installed panels	3920
Module’s peak power (STC)	230 W_p/mod
Inverter’s model and type	Aurora Power One, PVI Central model 330 TL-IT – CENTRALIZED
Number of installed inverters	3
Inverter’s AC power output	330 kW, 6 modules of 55 kW each
Inverter operational configuration	Multi-master
Modules’ tilt	30°
Modules’ azimuth	0° (South)
Row distance	6.5 m
Albedo	10 %

Table 2.3 - Case study plant features

2.2.1. Location

The photovoltaic park is located south of the town of Racconigi, south-west of the Canapile fraction, located east of the State Road 20 which connects Cavallermaggiore to Carmagnola.

Figure 2.12 - Area of installation of the plant, before the intervention

In order to correctly proceed with the project of a plant of this size, it was necessary to verify that the subject area, identified by a land registry number, was not subject to any kind of constraints. Through the municipality of reference, having identified the lot of useful land, it was demonstrated that, in this case, there were no hydro geological and landscape constraints, but an archaeological constraint; therefore, in order to proceed with the excavations, it was necessary to obtain a specific authorization.

Figure 2.13 - Lot of ground under analysis

Furthermore, a portion of the land where the photovoltaic park is currently installed is subject to a constraint due to the presence on the west side of the ground of a canal. Due to municipal regulation, being a dammed channel, it was necessary to maintain a minimum distance of 25 m from the latter.

The horizon results free from obstacles, potentially causing shading.

2.2.2. Modules

Modules adopted, produced by the company LDK Solar, present a power of 230 W_p; they consist of 60 polycrystalline silicon cells of square shape (156x156 mm). Main features from the datasheet are reported.

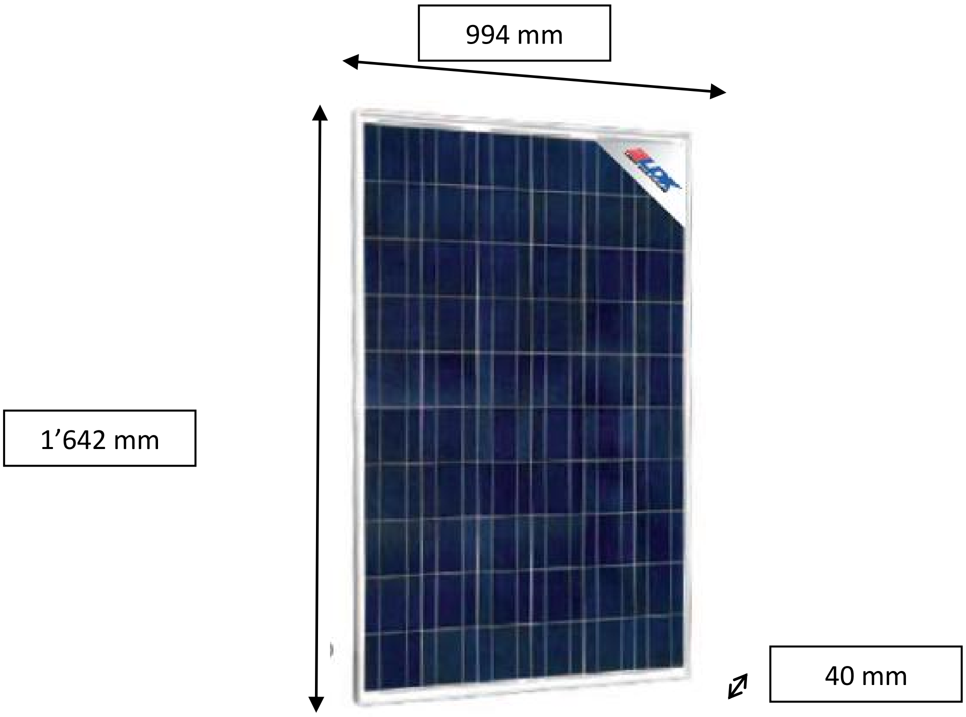

Brand	LDK Solar
Model	230P-20
Dimensions	994x1642x40 mm
Nominal power P_n (W_p)	230 W_p
Module's efficiency	14.09 %
Weight	19 kg
MPP voltage (U_{MPP})	29.3 V
MPP current (I_{MPP})	7.88 A
Open Circuit Voltage (U_{OC})	36.9 V
Short Circuit Current (I_{SC})	8.43 A
Thermal coefficient of P_{MPP}	-0,45 %/°C
Thermal coefficient of I_{SC}	0,060 %/°C
Thermal coefficient of V_{OC}	-0,33 %/°C
Fill Factor FF	73,9%
Power/weight ratio	12,1 W/kg

Table 2.4 - PV module's specifications

In the figure below, the characteristic curve I-V of the solar cell, at different solar irradiance values, is reported.

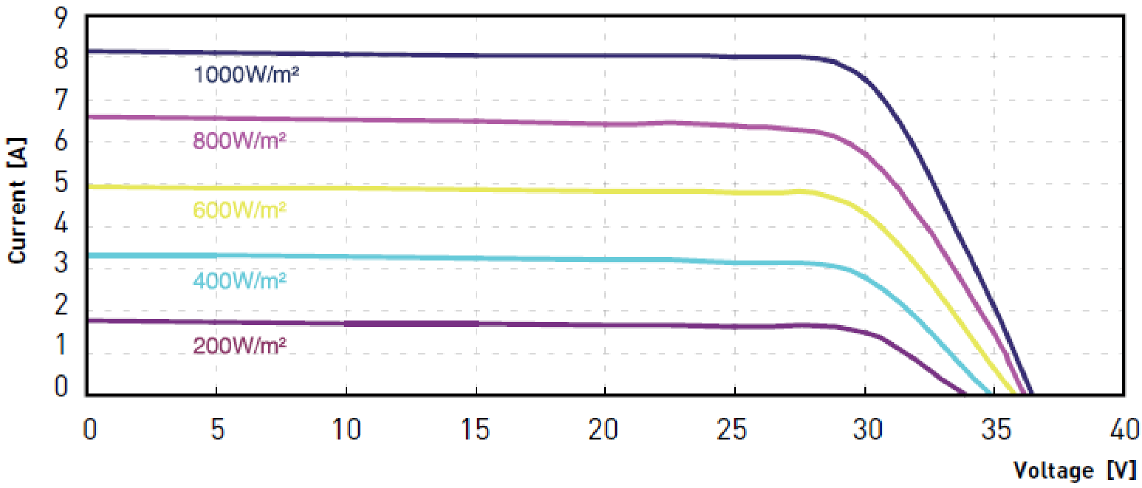

Figure 2.14 – I-V curves at different irradiance values, LDK modules

2.2.3. Inverters

There are three centralized inverters, of 330 kW each; each of them divided into 6 modules, of 55 kW each.

Each module operates as MPPT ("Maximum Power Point Tracker"), in a Multi-Master configuration, that is, every module operates like a master. In other words, all of them are switched on contemporary.

Brand	Power-One (ABB)
Model	PVI-330.0-TL-IT
Maximum efficiency	98 %
DC input	
Nominal power P_{DC}	338.4 kW
Maximum power $P_{DC,max}$	354.0 kW
MPPT DC voltage range U_{DC}	485 - 850 V
Maximum DC voltage ($U_{DC,max}$)	1'000 V
Maximum DC current ($I_{DC,max}$)	738 A
AC output	
Nominal power P_{AC}	330.0 kW
Nominal AC current ($I_{AC,nom}$)	606 A
Nominal AC voltage ($V_{AC,nom}$)	320 V
Nominal power factor (cosϕ)	1

Table 2.5 - Inverters' specifications

Inverters are then connected to an external transformer for the energy input, at medium voltage level (15000 V) into the external grid.

The conversion efficiency as a function of the DC voltage and P_{AC}/P_{DC} ratio is reported.

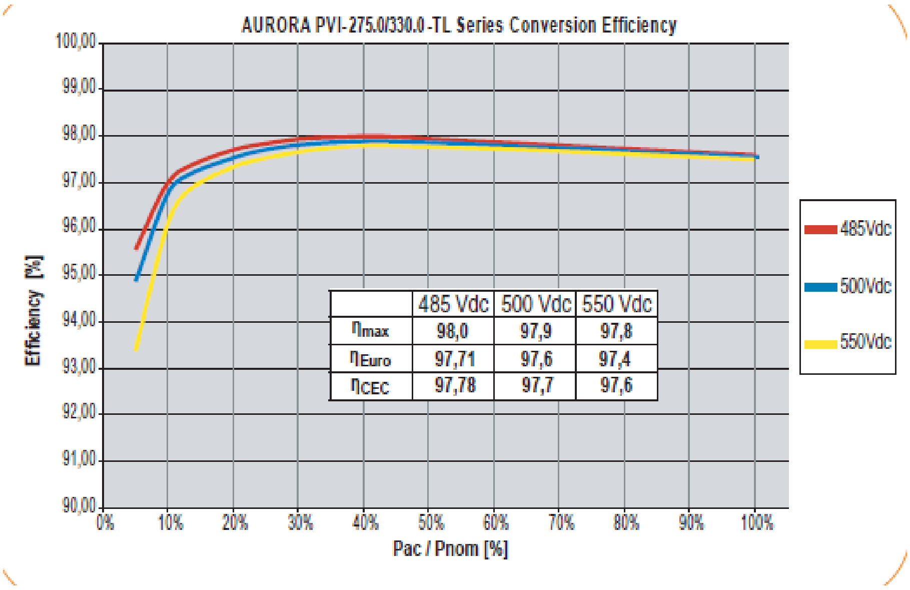

Figure 2.15 - Inverter's conversion efficiency as a function of power rating

Figure 2.16 - Inverters positioned in their current location

2.2.4. Support structure

Panels positioned at an angle of 30° with respect the horizontal and vertically side by side two by two, reach a maximum height of 2.80 meters. To prevent the rows of panels from shading each other in the hours of the day and in the periods of the year when the sun is lower on the horizon, a distance of 6.50 m was kept between one row and another.

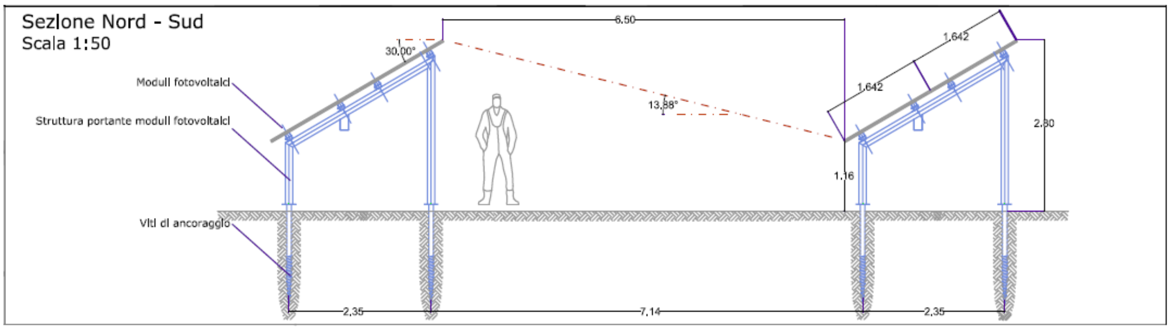

Figure 2.17 – Schematic design of the support structure with main dimensions and angles

Panels are anchored to the ground by means of screw foundations, i.e. galvanized steel poles which have a thread on the final part that allows a real screwing of the pile into the ground.

Figure 2.18 - Effective support structure

Since there are no relevant obstacles nearby the area, as stated before, the horizon profile can be considered as free. Therefore, the only source of shading is the mutual shading between parallel rows.

When PV modules are arranged in rows, the second row may be partially shaded by the first, the third by the second, and so on. For the case in which modules' rows are long enough in extent, the border effects (at the ends of the rows) are negligible, and the profile angle, i.e. the angle between two different rows of modules, provides a useful mean of determining shading.

The limit profile angle is the one under which mutual shading is present; in other words, it is the minimum sun height which is not causing mutual shading between different rows.

Reducing the value of the limit profile angle, mutual shading is minimized also for relatively low sun heights but, consequently, the area occupied increases (more spacing between rows) and the installable power decreases; vice versa, if higher angles are considered, the area occupied decreases, i.e. the installable power increases, but, as a consequence, shading effects are more relevant, and cause a greater loss of production.

2.2.5. Plant's layout

The plant consists of 16 rows of fixed photovoltaic panels installed on metallic structures anchored to the ground, oriented towards south and with an inclination with respect the ground of 30°. Each row consists of two strips of panels placed alongside the short side, while horizontally they are flanked by a minimum of 60 modules to a maximum of 240 modules.

Panels are connected to each other on 196 strings of 20 modules each combined in series, connected, in turn, to three inverters able to convert the direct current produced by the photovoltaic modules into alternating current; a transformer then proceeds to raise the voltage for feeding into the medium voltage grid.

Some pictures of the existent configuration will be inserted, as well as the original planimetry of the project (Tav.I).

Figure 2.19 & 2.20 - Panoramic pictures of the area

Figure 2.21 – Satellite image – OLD configuration

Main features of plant's configuration are reported.

Number of modules per string N_S	20
Number of strings per Inv.1	64
Number of strings per Inv.2	66
Number of strings per Inv.3	66
Average N° of strings per AC/DC module (55 kW) N_{ave}	11
Total nominal power P_N	901.6 kW_p
Total surface covered	6'397 m^2

Table 2.6 - Main features of the plant

Through easy calculations, voltage and currents of the strings can be determined:

- *Nominal string voltage*:

$$V_{Ns} = U_{MPP} \cdot N_s = 29.3 \cdot 20 = 586\, V \tag{2.7}$$

- *Nominal open circuit string voltage*:

$$U_{NsOC} = U_{OC} \cdot N_s = 36.9 \cdot 20 = 738\, V \tag{2.8}$$

- *Minimum nominal string voltage (75 °C)*:

As a reasonable assumption, the thermal coefficient of voltage at open circuit will be assumed equal to the thermal coefficient of voltage at maximum (nominal) power, i.e.:

$$\beta = \frac{dU_{MPP}}{dT} = \frac{dU_{OC}}{dT} \left[\frac{V}{°C}\right] \tag{2.9}$$

Since the thermal coefficient is given in (%/°C) for the open circuit voltage, it is value ,in V/°C, is given by:

$$\beta = \frac{-0.33}{100} \cdot U_{OC} = \frac{-0.33}{100} \cdot 36.9 = -0.12177 \frac{V}{°C}$$

It follows that:

$$V_{NsMIN} = V_{NS} + \beta \cdot (T - T_{STC}) \cdot N_s = 586 - 0.12177 \cdot (75 - 25) \cdot 20 = 465\, V \tag{2.10}$$

- *Maximum nominal string voltage (-10 °C)*:

As before, the thermal coefficient of voltage at open circuit will be assumed equal to the thermal coefficient of voltage at maximum (nominal) power, i.e.:

$$\beta = \frac{-0.33}{100} \cdot U_{OC} = \frac{-0.33}{100} \cdot 36.9 = -0.12177 \frac{V}{°C}$$

It follows that:

$$V_{NsMAX} = V_{NS} + \beta \cdot (T - T_{STC}) \cdot N_s = 586 - 0.12177 \cdot (-10 - 25) \cdot 20 = 672\ V \qquad (2.11)$$

- *Maximum open-circuit string voltage (-10 °C)*:

As before, the thermal coefficient of voltage at open circuit will be assumed equal to the thermal coefficient of voltage at maximum (nominal) power, i.e.:

$$\beta = \frac{-0.33}{100} \cdot U_{OC} = \frac{-0.33}{100} \cdot 36.9 = -0.12177 \frac{V}{°C}$$

It follows that:

$$U_{NsOCMAX} = U_{NsOC} + \beta \cdot (T - T_{STC}) \cdot N_s = 738 - 0.12177 \cdot (-10 - 25) \cdot 20 = 823\ V \qquad (2.12)$$

- *Maximum nominal current (75 °C)*:

The thermal coefficient of current at short circuit will be assumed equal to the thermal coefficient of current at maximum (nominal) power, i.e.:

$$\alpha = \frac{0.060}{100} \cdot I_{SC} = \frac{0.060}{100} \cdot 8.43 = 5.06 \cdot\ 10^{-3} \frac{A}{°C}$$

It follows that:

$$I_{DCMAX} = I_{DC} + \alpha \cdot (T - T_{STC}) = 7.88 + 5.06 \cdot 10^{-3} \cdot (75 - 25) = 8.13\ A \qquad (2.13)$$

Considering a single inverter module, the total maximum DC current flowing is:

$$I_{DCMod} = I_{DCMAX} \cdot N_{ave} = 8.13 \cdot 11 = 89.43\ A \qquad (2.14)$$

For an inverter, then, it follows:

$$I_{DCInv} = I_{DCMod} \cdot N_{inv} = 89.43 \cdot 6 = 536.58\ A \qquad (2.15)$$

Since:

- Maximum and minimum nominal sting voltages are belonging to the MPPT tracking range;
- Maximum open circuit voltage is below maximum DC voltage;
- Maximum current is below the nominal value;

, the configuration is acceptable and correct.

2.2.6. Electrical project

The electrical single-wire diagram of the plant is reported.

Starting from the top, the following items are represented:

- PV modules;
- DC field switchboards (not represented): allow the parallel connection of different strings, which should arrive in the same inverter's module;
- DC/AC converters;
- AC field switchboard (parallel switchboard), in LT, for the parallel of the plant with the grid. It contains the mono-directional production counter and the interface device (DDI);
- Branch towards auxiliary circuits for the plant;
- Grounding system against overvoltage;
- AC field switchboard, in MT. It contains the transformer and the general device (DG);
- Exchange bi-directional counter: it is located at the point of connection to the electricity grid and measures the electricity input and withdrawn.

The plant is connected to the medium-voltage grid; it receives state incentives (IV Conto Energia), and therefore it sells all the electricity produced into the grid (total exchange mechanism).

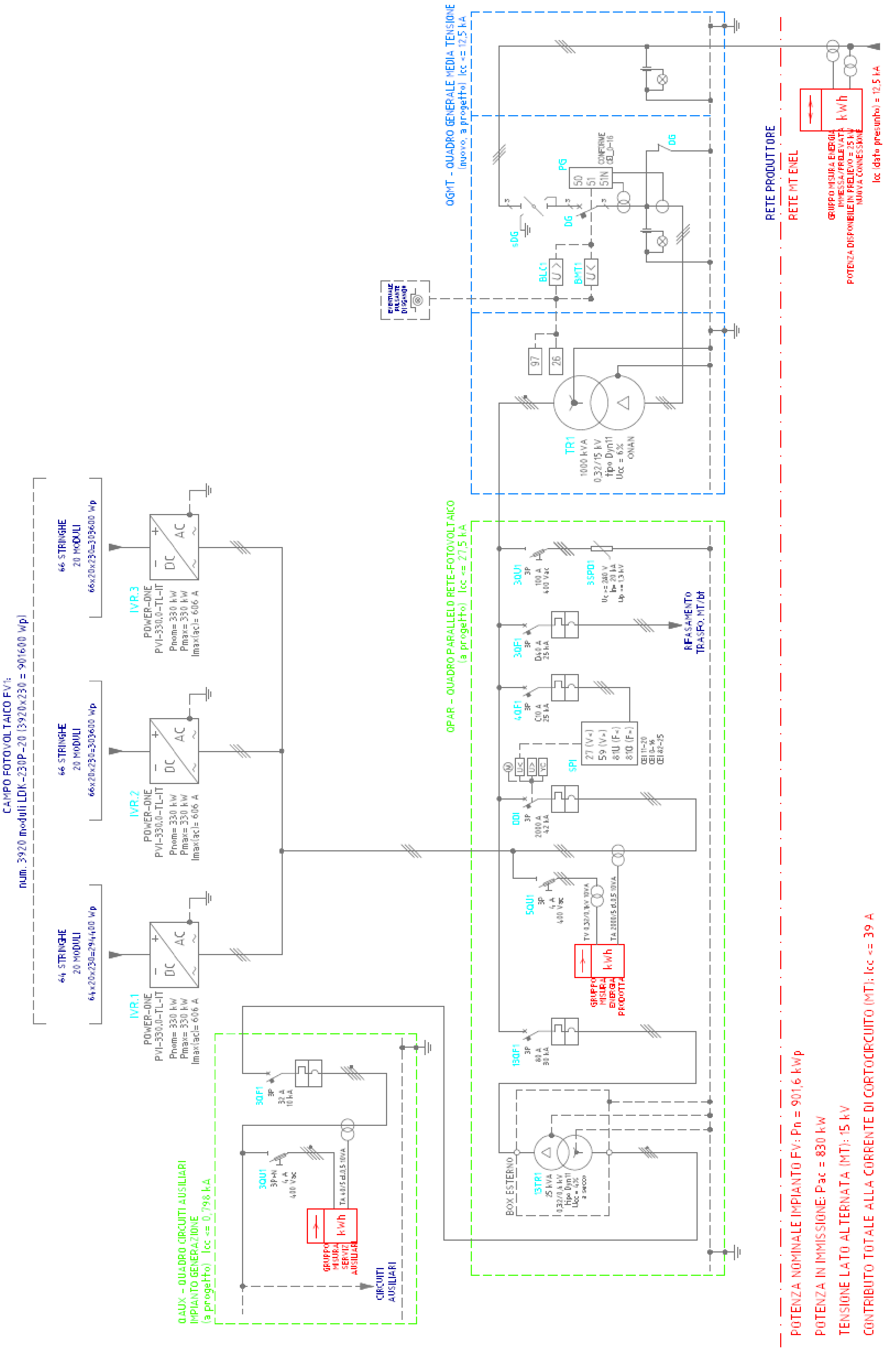

Figure 2.22 – Single wire diagram – OLD configuration

3. Energy assessment: PV plant

The estimation of the energy producibility is a crucial aspect in the design of a PV plant, since it influences strongly the convenience or not of the whole investment. Indeed, the energy produced by the plant is directly connected to the economic gain. The designer should try to estimate the producibility of the system before the effective installation, in order to decide possible improvements or variations in the design, according to the results obtained.

In this chapter, attention will be posed to the concept of plant's energy producibility, and on the ways to estimate its value. This concept will be applied to the plant under analysis, in its original configuration described in chapter 2. Results obtained through estimations by literature formulas and specific programs will be counterchecked with real data coming from the monitoring activity of the plant and of similar PV plants, owned by the same company.

In chapter 5, also the new configuration of the plant (after revamping) will be simulated, and its energy productivity assessed; this result will be the basis for the final economic assessment.

3.1. Basic definitions

The energy producibility of a PV system is the amount of energy which can be produced by the system in a defined period of time. It is strongly influenced by the system size, global irradiance in the site of installation, and by the system efficiency and losses.

The conventional calculation of the parameter is the following:

$$E_{AC} = H_g \cdot S_{PV} \cdot \eta_{STC} \cdot PR \tag{3.1}$$

where:

- H_g is the global in-plane irradiation (kWh/m^2) at the time of reference;
- S_{PV} is the total PV generator's area;
- η_{STC} is the rated efficiency of PV modules at STC;
- PR is the performance ratio.

Multiplying and dividing eq. 3.1 by G_{STC} (STC irradiance), it follows:

$$E_{AC} = \frac{H_G}{G_{STC}} \cdot S_{PV} \cdot \eta_{STC} \cdot G_{STC} \cdot PR = h_{eq} \cdot P_N \cdot PR = Y_R \cdot P_N \cdot PR = Y_F \cdot P_N \tag{3.1a}$$

where:

- h_{eq} are the equivalent solar hours (or reference yield Y_R), expressed in $\frac{kWh}{m^2}/(1\frac{kW}{m^2})$;
- Y_F is the final yield, numerically equal to E_{AC}/P_N, and expressed in kWh/kW_p.

Inside the PR different losses (or rarely gains) are included; the main ones are:

1. tolerance with respect to STC data and intrinsic mismatch of modules current-voltage characteristics (η_{mis});
2. dirt and reflection of the frontal glass (η_{dr});
3. different solar spectrum compared to the reference solar spectrum (AM = 1.5) (η_{spec});
4. wiring, blocking diodes, fuses and breakers (η_{wir});
5. over-temperature (or under-temperature) compared to 25°C (η_{temp});
6. non-uniform illumination on all modules (shading effect) (η_{shad});
7. MPP tracker and DC-AC conversion of the inverter (η_{PCU}).

Definitely, PR can be determined as:

$$PR = \eta_{mis} \cdot \eta_{dr} \cdot \eta_{spec} \cdot \eta_{wir} \cdot \eta_{temp} \cdot \eta_{shad} \cdot \eta_{PCU} \tag{3.2}$$

Each parameter of the equation 3.2 is representative for one item (from 1 to 7).

Given the external ambient temperature, the real irradiance and the NOCT conditions, it is then possible to estimate the cell's temperature:

$$T_c(°C) = T_a(°C) + \frac{NOCT(°C) - 20°C}{800\frac{W}{m^2}} \cdot G\left(\frac{W}{m^2}\right) \tag{3.3}$$

where:

- T_a is the ambient temperature;
- NOCT is the Nominal Operating Cell Temperature, function of the specific module considered. It is defined as the temperature which can be reached by cells in short circuit, with an ambient temperature of 20°C, an in-plane irradiance of 800 W/m^2 and a wind speed of 1 m/s;
- G is the in-plane solar irradiance.

3.2. Estimation of energy production – Case study plant

Productivity of the case study plant in its original (OLD) configuration will be assessed, considering real data coming from the monitoring of the exchange counter installed. Since the plant does not perform correctly due to panel's defectiveness (ch.4.3), an estimation on the potential benefit in substituting the whole plant's modules will be given in terms of expected energy production rise for a possible revamped configuration (NEW configuration).

The series of data starting from the year in which the plant first entered into operation till 2017 will be reported in terms of yearly average.

Year	Energy produced (kWh)	Energy to the network (kWh)	Final yield (kWh/kW$_p$)
2012	1'242'052	1'219'213	1'378
2013	1'183'389	1'161'167	1'313
2014	1'142'968	1'121'388	1'268
2015	1'167'014	1'144'656	1'294
2016	1'147'365	1'124'244	1'273
2017	1'195'665	1'171'933	1'326

Table 3.1 - Energy production from exchange counter – Case study plant (OLD configuration)

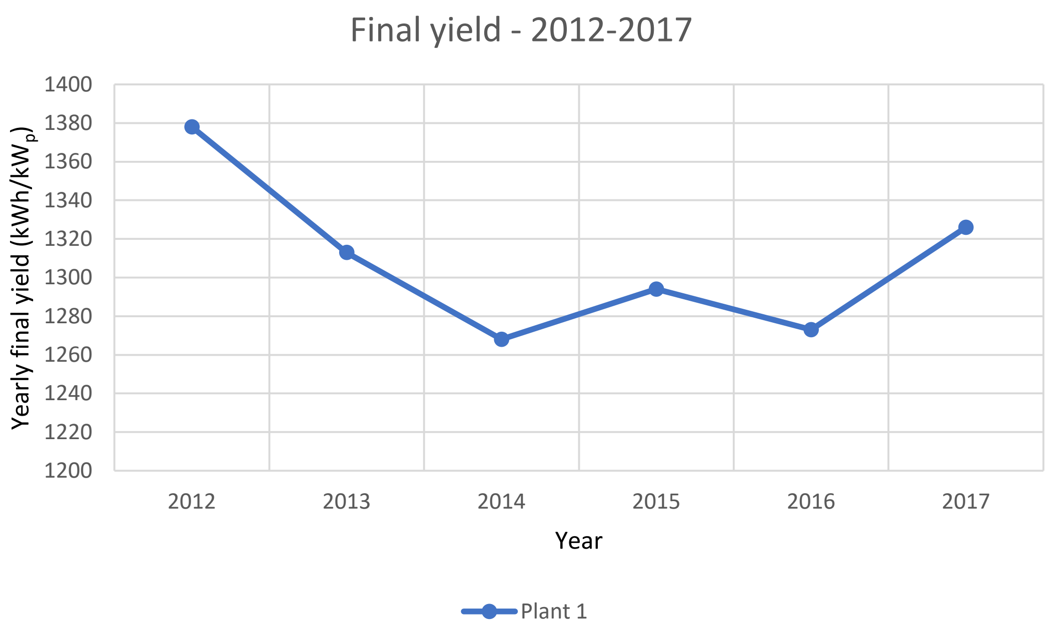

Figure 3.1 - Case study plant - OLD configuration

The average final yield is equal to **1’308 kWh/kW$_p$**.

Due to modules technical problems, which will be examined in detail successively, the energy production of the plant is lower with respect the energy production of similar plants in the same area.

The result just obtained is also partially influenced by the fact that every year a certain number of modules (averagely 100 per year) are substituted because heavily compromised and damaged. Therefore, without this activity, the expected final yield would be even lower.

As a consequence, the energy productivity of the PV plant under study cannot be considered satisfying, especially if put in comparison with other plants, owned by the same company, of almost the same size and design, installed in the same area, as will be explained in next paragraph.

3.3. Final yield estimation: NEW configuration

The aim of this part is the estimation of the possible benefits deriving from the plant's revamping (ch.5.1.) in terms of final yield, compared to the value presented by the case study plant in its OLD configuration. Three different methods will be used for the estimation.

3.3.1. Comparison with near similar plants

Entec has projected and installed other 2 ground-mounted grid-connected PV plants (plant 2 and plant 3) in the neighborhood of the plant under analysis (plant 1). In particular:

	Plant 1	**Plant 2**	**Plant 3**
Power (kW_p)	901.60	510.40	999.70
Location	Racconigi (CN)	Scarnafigi (CN)	Cervere (CN)
Modules' model	LDK 230W-20p	Hyundai HiS-M200-SF	Trina TSM-235-PC05 Schott POLY TM 230
Number of installed modules	3'920	2'552	2'140 (Trina) 2'160 (Schott)
Tilt angle (°)	30	30	30
Azimuth (°)	0	0	0
Row distance (m)	6.5	6.5	6.5
Average final yield (kWh/kW_p)	1'308.0	1'436.5	1'446.0

Table 3.2 - Overview of the main features of the three plants considered

The three plants have the same type of inverter and electrical structure; furthermore, they are quite near as the crow flies. The only difference is the modules' type: the last two plants have no evident problems in modules defectiveness like the first one, therefore they have quite bigger performances in terms of energy yield.

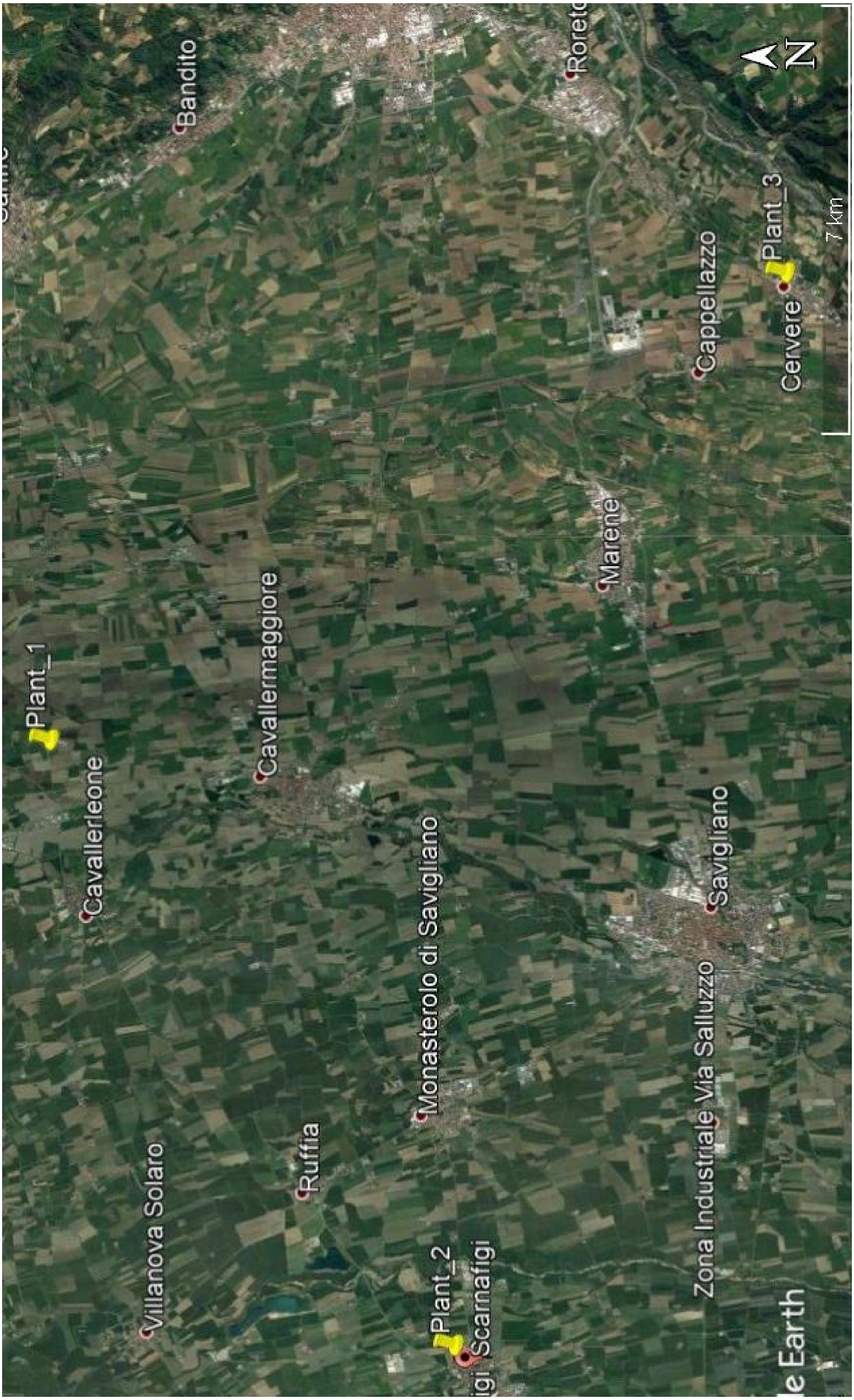

Figure 3.2: Plant's location (satellite image) – Google Earth

Same yearly analysis made for the first plant will be carried out for the other two:

Year	Energy produced (MWh)	Final yield (kWh/kW$_p$)
2012	765.1	1’499
2013	732.4	1’434
2014	716.2	1’403
2015	735.0	1’440
2016	723.4	1’417
2017	727.7	1’426

Table 3.3 - Energy production from counter - Plant 2

Year	Energy produced (MWh)	Final yield (kWh/kW$_p$)
2012	1’485	1’486
2013	1’414	1’414
2014	1’383	1’377
2015	1’455	1’455
2016	1’430	1’431
2017	1’514	1’515

Table 3.4 - Energy production from counter - Plant 3

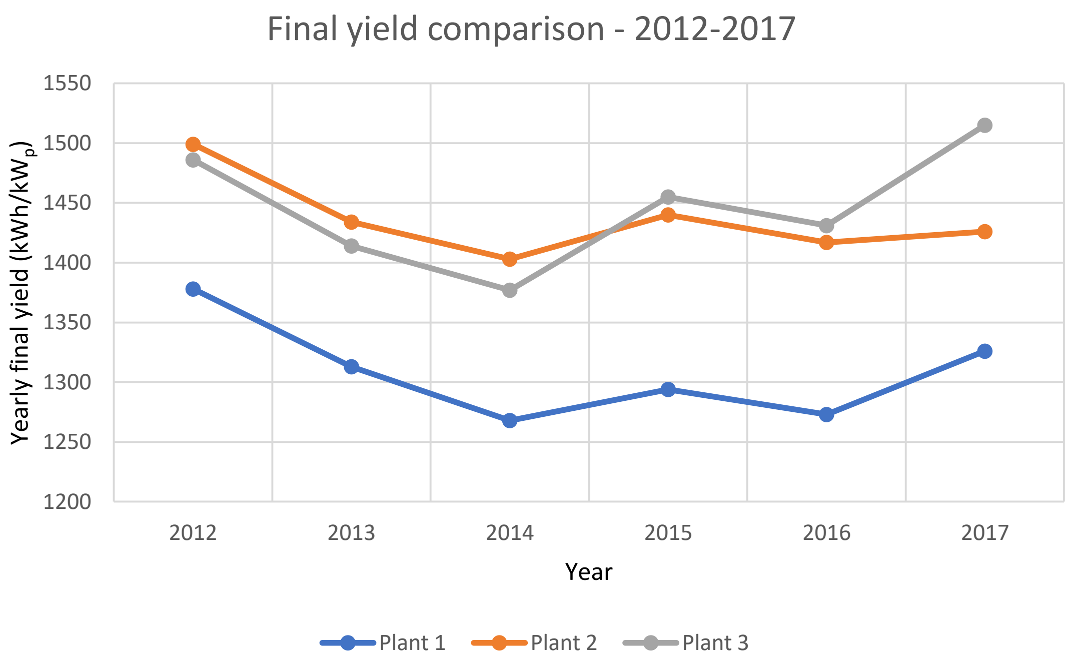

Figure 3.3 - Comparison between yearly yields of different PV plants

As it is clearly evident, the final yield of the plant under analysis is lowest; the average discard between the values of the 3 plants is around **10 %** (factor k_1). That is, it can be expected, averagely, an improvement of 10% in the final yield, after the revamping process, since the renewed plant is expected to perform like nearby plants.

The estimation is conservative since it neglects the inevitable decadence of performances caused by time for the other two plants chosen as meter of comparison; indeed, a more accurate estimation should have been considered the decay rate of production of the other two plants and evaluated the expected yield of the case study plant after the intervention taking into account also this factor. Nevertheless, an estimation of yearly losses in productivity will be now proposed.

From the previous analysis, the yearly decay rate of the final yield of the three plants with time can be identified. Linearly interpolating the data, following results can be obtained:

	Plant 1	**Plant 2**	**Plant 3**
Decay rate (%/y) of final yield (kWh/kW$_p$)	-0.77	-0.75	+0.54

Table 3.5 - Determined decay rate

Due to the limited amount of statistical data, results obtained are not so relevant; furthermore, they are influenced by the global irradiance of the considered year. Therefore, in order to eliminate this dependency, the same final yield will be normalized to the average yearly total radiation on the horizontal plane.

Monthly radiation data will be extrapolated from the ARPA databank, considering two meteorological stations of Fossano (CN) and of Villanova Solaro (CN), near to the whole three plants.

Station 1 - Fossano

Monthly total radiation will be reported in kWh/m^2. Considering the period 2012-2017:

Year	Jan.	Feb.	Mar.	Apr.	May	June	July	Aug.	Sept.	Oct.	Nov.	Dec.	Tot
2012	61.1	68.6	124	119	154	205	206	170	122	85.8	48.3	52.2	**1’414**
2013	55.0	78.3	116	108	154	205	210	178	121	60.0	48.3	43.3	**1’376**
2014	55.0	68.6	116	134	174	188	196	169	118	60.0	48.3	43.2	**1’369**
2015	61.7	68.6	116	134	186	198	208	170	125	74.7	61.1	45.6	**1’449**
2016	48.3	57.8	123	152	170	195	204	189	139	77.5	48.4	46.1	**1’449**
2017	47.5	59.7	126	166	201	212	214	185	132	93.6	50.0	48.1	**1’535**

Table 3.6 - Total monthly irradiation on the horizontal plane (kWh/m^2) – Fossano (ARPA)

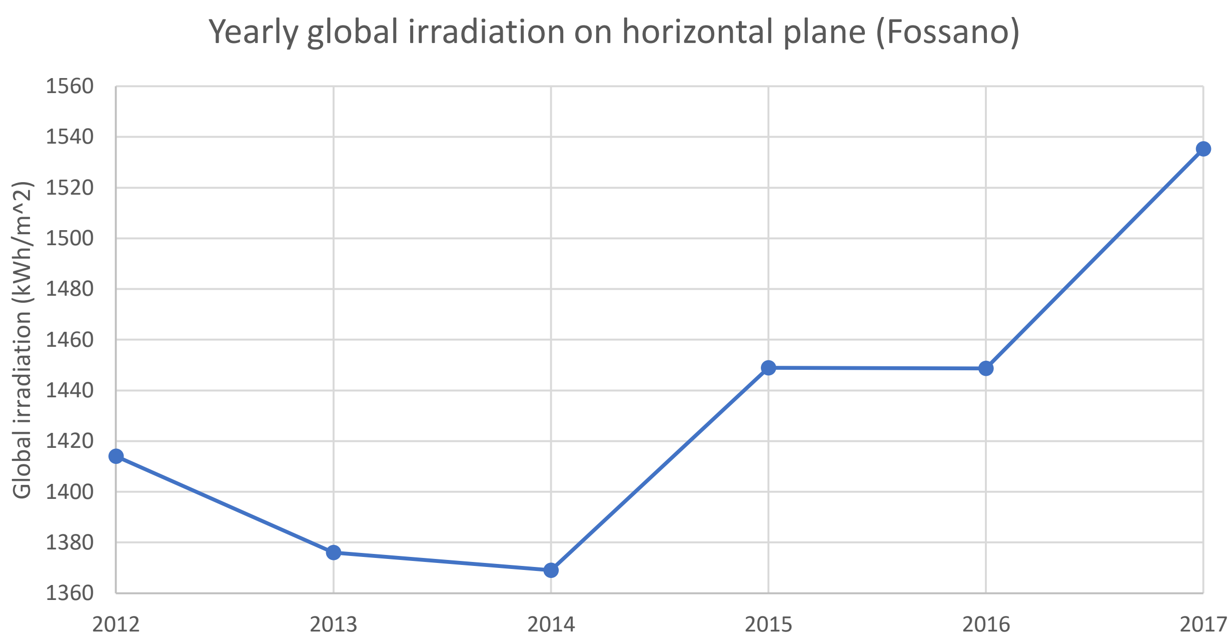

Figure 3.4 - Yearly global irradiation (2012-2017 – Fossano - ARPA)

This value coincides numerically with the reference yield Y_r on the horizontal plane, since it can be obtained by dividing the irradiation with the STC irradiance of 1 kW/m^2.

The final yield (Y_f) divided by the reference yield on the horizontal plane (Y_r) will be reported with time.[23]

Year	Reference yield (Y_R)	Final yield normalized with respect reference yield (Y_F/Y_R)		
		Plant_1	Plant_2	Plant_3
	kWh/kW	/	/	/
2012	1’414	0.98	1.07	1.05
2013	1’376	0.96	1.06	1.03
2014	1’369	0.93	1.03	1.01
2015	1’449	0.90	1.00	1.00
2016	1’449	0.88	0.99	0.99
2017	1’535	0.87	0.94	0.99
Average	1'431	0.92	1.01	1.01

Table 3.7 - Normalized final yields with respect reference yield on horizontal plane - Plant 1-3 - (2012-2017)

[23] The value is dimensionless. Since radiation data available from ARPA databases are not present for the in-plane radiation of modules, the parameter obtained is different from the PR (“Performance Ratio”) of the plant.

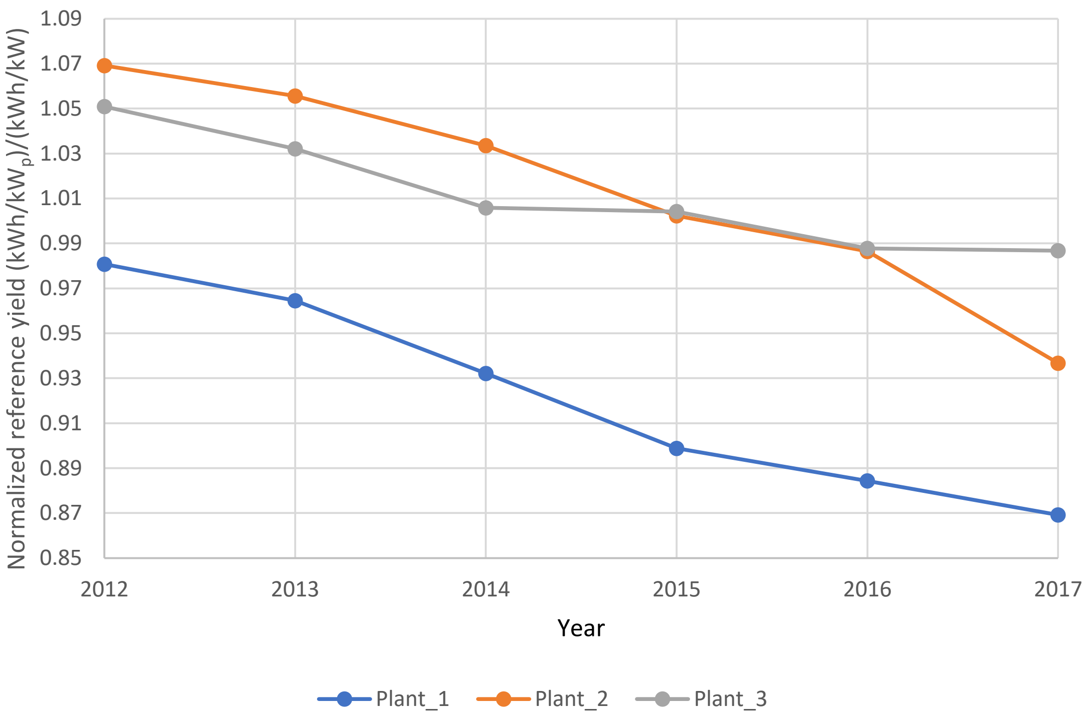

Figure 3.5 - Comparison between normalized final yield of different PV plants

	Plant 1	Plant 2	Plant 3
Decay rate (%/y)	-0.9	-0.9	-0.3

Table 3.8 - Yearly decay rate of normalized final yield with respect reference yield on the horizontal plane

Station 2 – Villanova Solaro

The same analysis and considerations will be repeated considering data from a second station (Villanova Solaro).

Year	Jan.	Feb.	Mar.	Apr.	May	June	July	Aug.	Sept.	Oct.	Nov.	Dec.	Tot
2012	47.8	82.8	126	127	189	196	216	176	109	71.4	56.9	43.1	**1’441**
2013	46.7	65.6	90.6	118	187	210	205	189	131	58.6	56.9	41.9	**1’400**
2014	41.1	56.7	119	138	189	190	188	168	124	74.4	56.9	41.9	**1’388**
2015	50.8	65.0	108	159	179	209	225	192	119	75.3	56.9	39.7	**1’480**
2016	46.9	55.8	126	150	177	199	206	190	132	77.5	56.9	43.1	**1’460**
2017	47.8	54.7	130	172	197	229	205	190	132	92.8	50.0	49.7	**1’550**

Table 3.9 - Total monthly irradiation on the horizontal plane (kWh/m^2) – Villanova (ARPA)

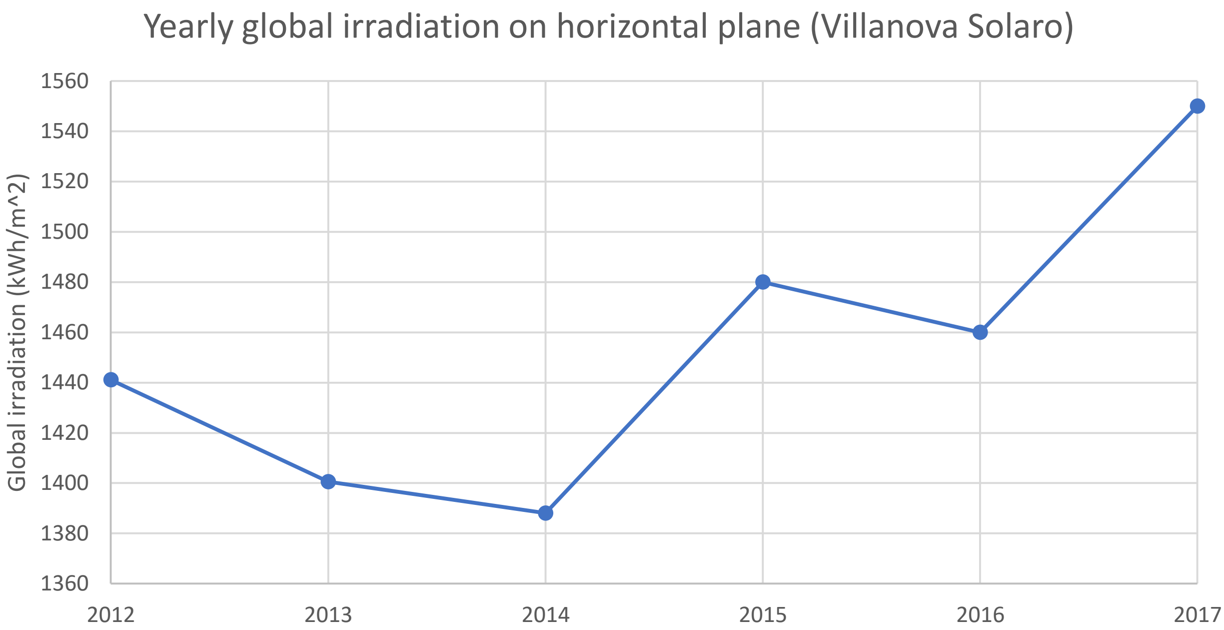

Figure 3.6 - Yearly global irradiation (2012-2017 – Villanova - ARPA)

This value coincides numerically with the reference yield Y_r on the horizontal plane, since it can be obtained by dividing the irradiation with the STC irradiance of 1 kW/m^2.

The final yield (Y_f) divided by the reference yield on the horizontal plane (Y_r) will be reported with time.[24]

Year	Reference yield (Y_R)	Final yield normalized with respect reference yield (Y_F/Y_R)		
		Plant_1	Plant_2	Plant_3
	kWh/kW	/	/	/
2012	1’441	0.95	1.04	1.02
2013	1’400	0.94	1.02	1.00
2014	1’388	0.91	1.01	0.98
2015	1’480	0.87	0.97	0.97
2016	1’460	0.87	0.97	0.97
2017	1’550	0.85	0.92	0.97

Table 3.10 - Normalized final yields with respect solar irradiance - Plant 1-3 - (2012-2017)

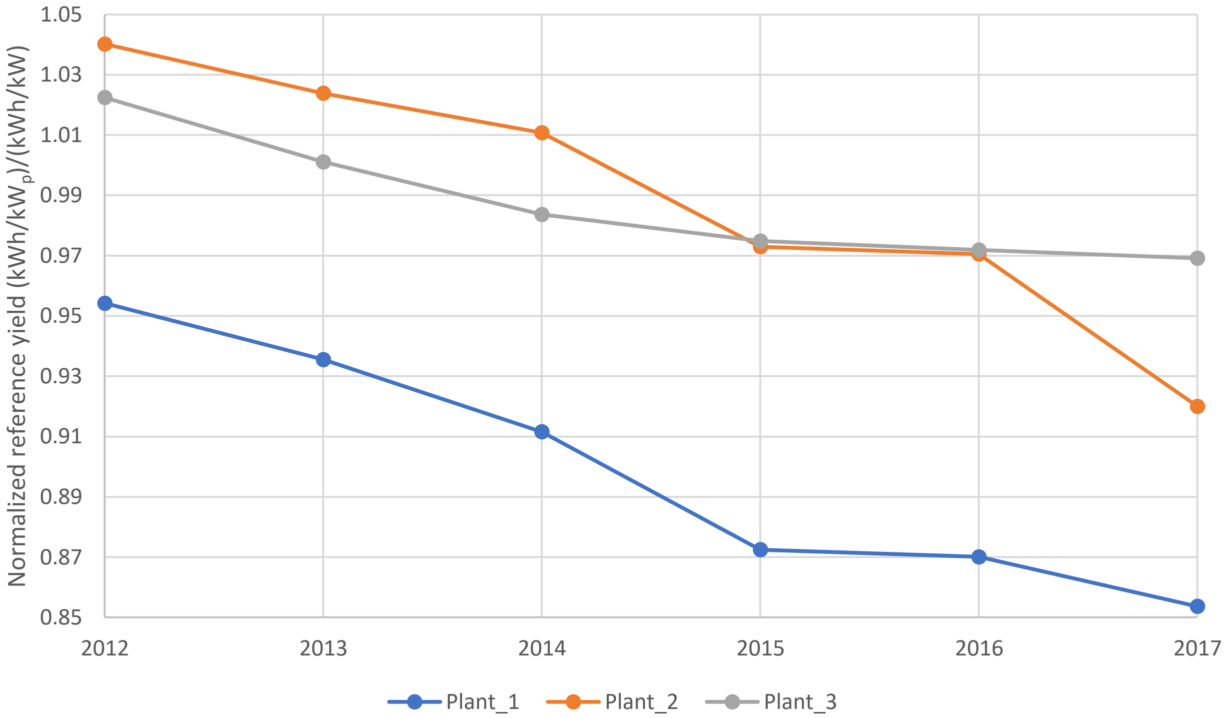

Figure 3.7 - Comparison between normalized final yield of different PV plants (normalized wrt. Villanova irradiation)

[24] The value is dimensionless. Since radiation data available from ARPA databases are not present for the in-plane radiation of modules, the parameter obtained is not equal to the PR (“Performance Ratio”) of the plant.

	Plant 1	Plant 2	Plant 3
Decay rate (%/y)	-1.3	-1.3	-0.5

Table 3.11 - Yearly decay rate of normalized final yield with respect reference yield on the horizontal plane

Due to the very few amounts of data at our disposal, results obtained show irregular behaviors.

In order to choose a common appropriate decay rate of production, which will be useful subsequently for the economic assessment of the intervention, module's datasheet can be considered. The yearly decay rate typically suggested is around 0.8 % per year. This value can be assumed as decay rate for all the three plants studied.

The same value will be considered valid also for plant 1, both before and after the intervention. Indeed, considering the ante operam status, it can be considered reasonable under the hypothesis of yearly substitution of a certain number of defective modules (as said before, around 100), able to keep the decay rate of the whole generator to the standard value. The following hypothesis will have some repercussions on the economic analysis, since it implies the presence of higher annual operating costs for the OLD configuration.

3.3.2. Computational simulation

In order to furnish another estimation of the expected gain in final yield after the revamping operation, the commercial software PV*SOL premium 2018, from Valentine Software, will be used.

PV*SOL is a program for the simulation of photovoltaic systems. With the 3D visualization, complex shading situations can be easily modeled and its effects on the yield can be precisely calculated for each module at any time.

The program has inside a rich database about commercial PV modules and inverters; therefore, simulations are carried on with the proper models chosen at design stage.

By specifying the module temperature and the irradiance to the tilted surface of the PV generator, the power output of the PV module is determined. Each irradiance and temperature value, determined according to the location and time, results in a random number of working points from which the PV module can be operated. These working points describe the electrical characteristic curve of the module (APPENDIX A).

For the analysis, five plants have been modeled: plant 2, plant 3 and other two plants, number 4 and 5, which are also managed by Entec, in addition to the case study plant.

The step by step procedure of modeling will be presented only for plant 2, being equal in all the cases.

Results obtained with the program are then compared to real data obtained through the production counter installed in place. The inevitable difference between those numbers is used in order to determine a correction factor for the simulation results, useful to estimate the production of the plant under analysis after the revamping process (in absence of monitoring data).

Modeling plant 2

Firstly, main general data of the project must be inserted. Most important options to include are:

- Type of system: it must be highlighted whether the system is grid-connected or stand-alone, and what is the type of utility to which it is enslaved (total input into the grid, grid-connected with electrical appliances etc.). The correct option for our purposes is grid-connected PV system; that is, the plant enters the grid the totality of the energy produced;

- System Location: very important to set the exact location of the plant in order to consider proper meteorological data. If the location is present in program database, climatic data considered are the one from the UNI 10349[25]; otherwise meteorological data are generated with MeteoSyn[26].

Successively, the plant is modeled in 3D. In particular, the terrain inclination and azimuth are defined, as well as the horizon profile. For whole the plants studied, terrain is flat and oriented towards South, while horizon is free from main obstacles; main sources of shadowing are the module's rows, causing therefore reciprocal shading problems.

[25] Italian norm called "Dati climatici".
[26] The MeteoSyn climatic database contains around 450 data sets from the German Weather Service for Germany with the averaging period 1981-2010, as well as over 8000 global data sets, with the averaging period 1986-2005.

The following pictures report the rendering of the plant inside the program 3D environment.

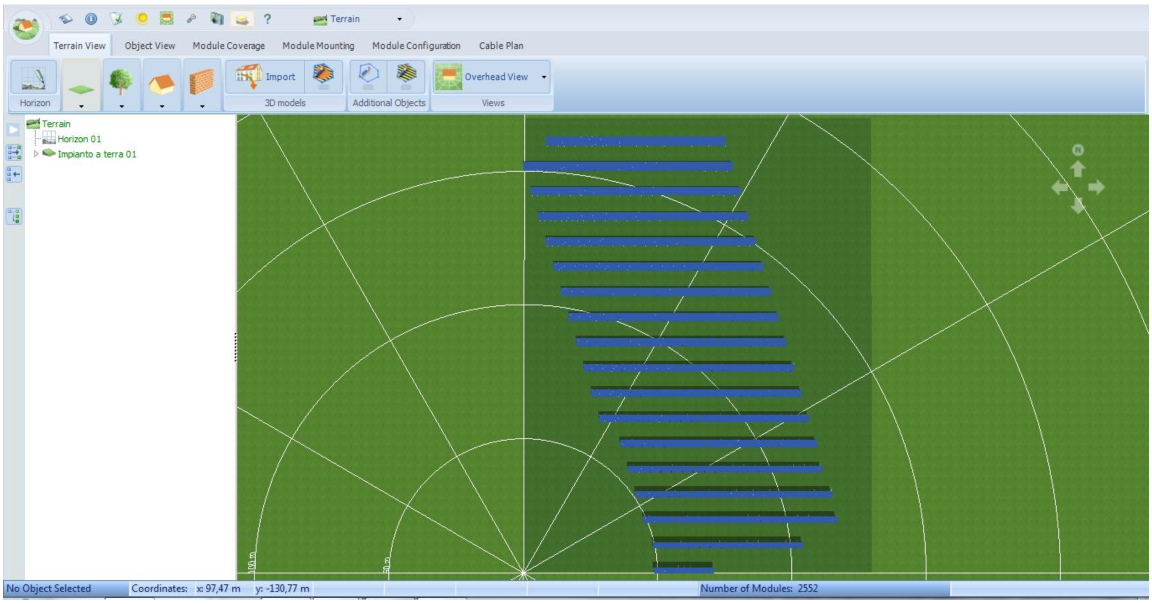

Figure 3.8 – Plant 2 (PV*SOL rendering)

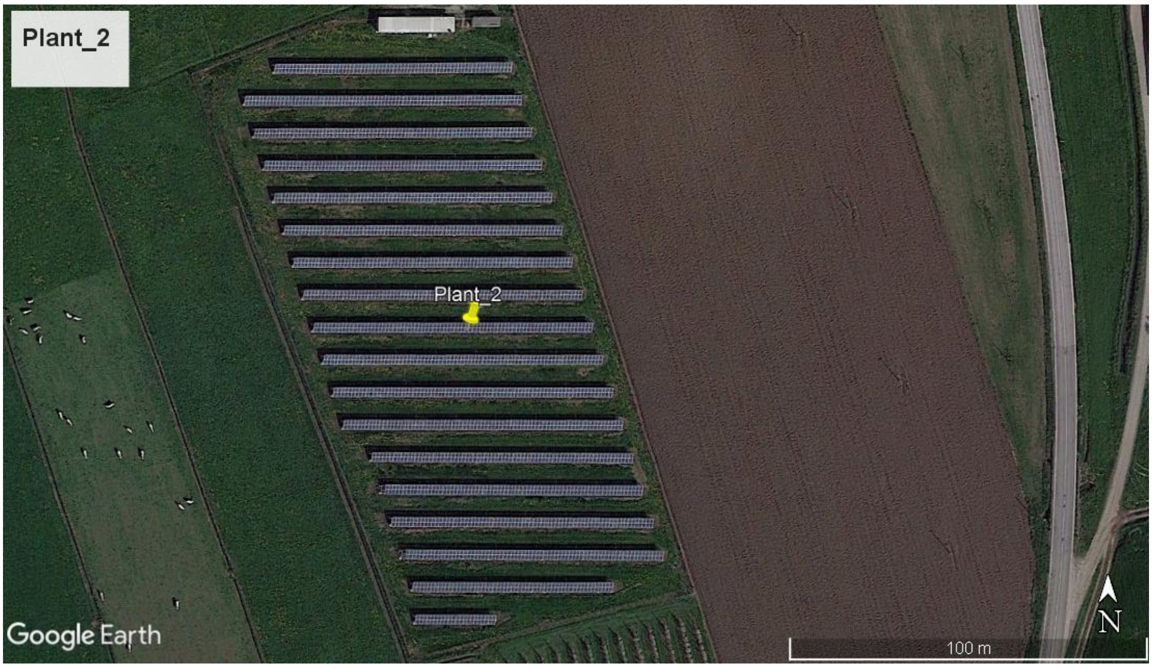

Figure 3.9 - Plant 2 (satellite image)

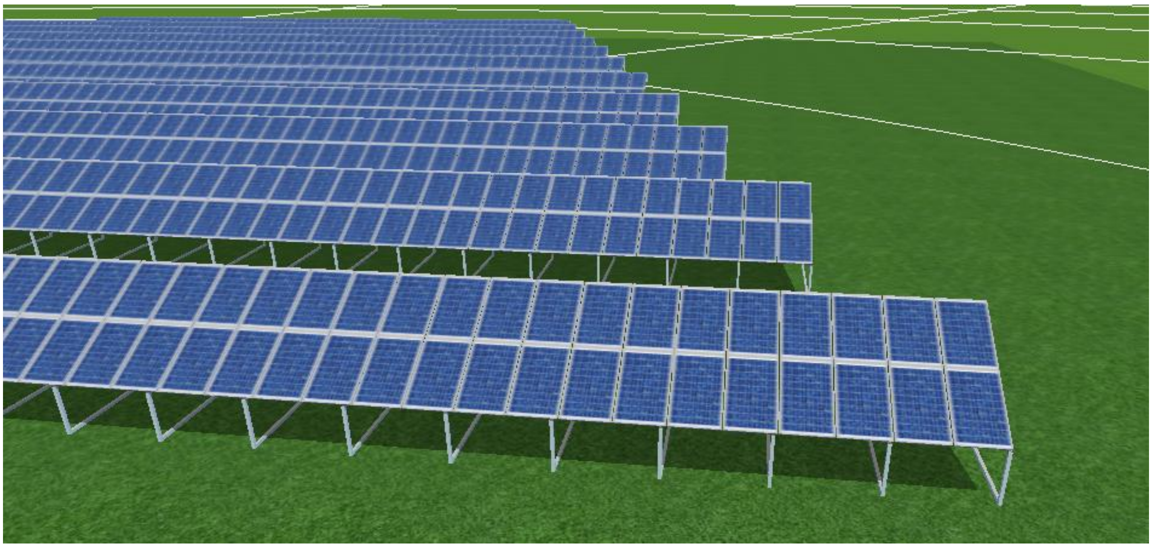

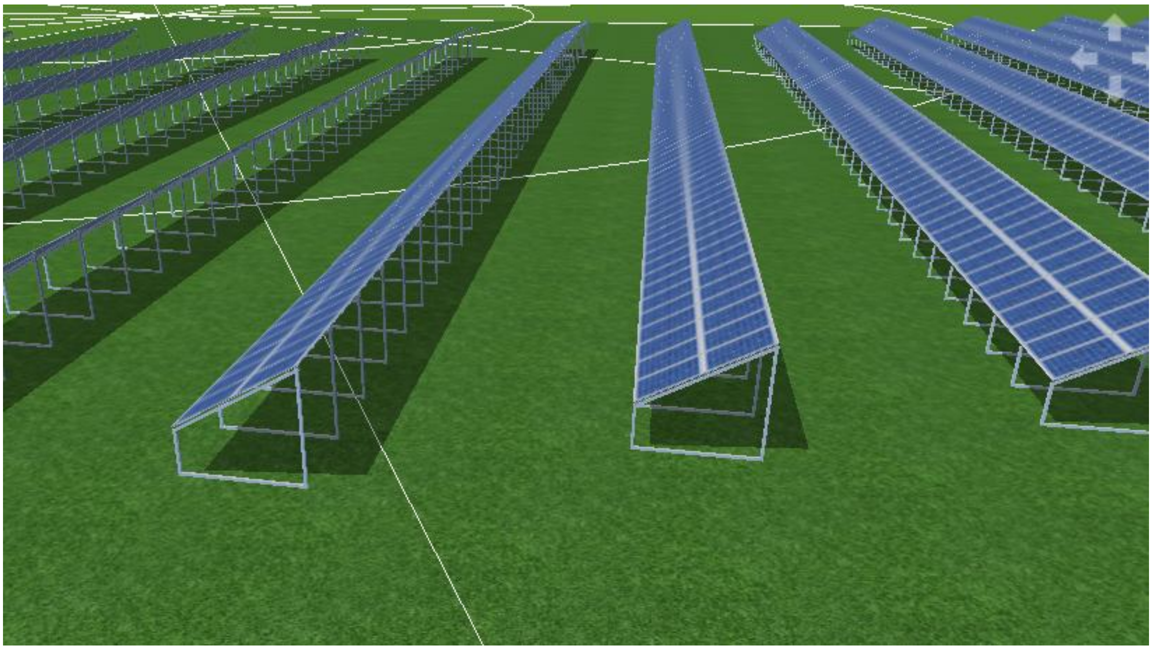

Figure 3.10 – PV*SOL -Rendering of rows and support structures (Plant 2)

The next step consists in the inverter definition and string configuration. The choice of the inverter is strictly connected to the string subdivision process, since it determines the maximum allowable number of series connected modules per string, as well as the maximum number of string in parallel for inverter (or MPPT, if the inverter has more than one). The program allows to define inverter's type, number of modules per string and string per MPPT (if any). The string subdivision is performed by the program according to predefined patterns.

Having set up the plant, before the estimation of energy productivity, losses should be defined. As a hypothesis, these parameters are kept equal to default parameters given by PV*SOL, except for shadowing losses, which are simulated daily by the program, according to data present in its internal databases.

As result screen, the program gives values of annual energy production and of final yield, as well as the repartition of the energy produced among all the months. Economic data should be neglected because no hypothesis was formulated about financial analysis.

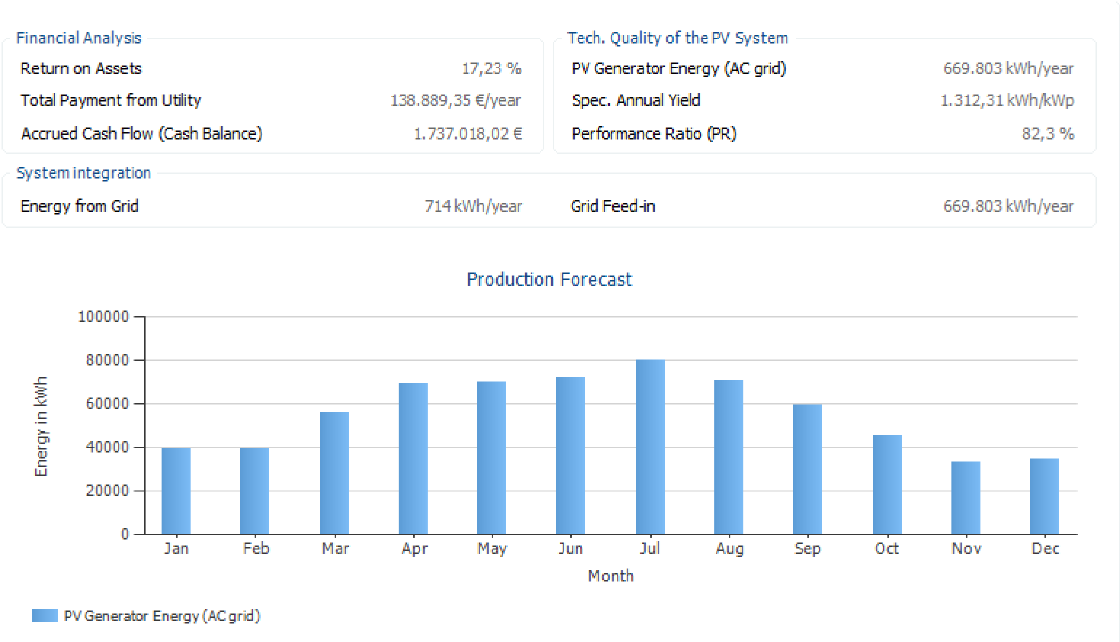

Figure 3.11 – PV*SOL - Outcome

The following procedure has been followed for all the four plants analyzed. All the four simulations were set identically, in terms of additional parameters taking into account specific losses, since no further information were available. Final results can be shortly resumed:

Plant	Effective (monitoring) final yield (kWh/kW_p)	Simulated final yield (kWh/kW_p)	Percentage difference (%)
Plant 2 (Scarnafigi)	1'436.5	1'312.3	9.46
Plant 3 (Cervere)	1'446.3	1'326.8	9.01
Plant 4 (Barge)	1'388.3	1'313.3	5.71
Plant 5 (Barge)	1'374.0	1'280.1	7.33

Table 3.12 - Simulation results

The program underestimates the final yield; the **average difference** (correction factor k_2) is **8.1%.** This value will be adopted in the last chapter (ch.5.3.2.) for the estimation of the final yield of the revamped plant and its increment with respect the original configuration.

3.3.3. Literature formulas

A further estimation can be obtained through literature formulas, adopting PVGIS values for solar irradiance and ambient temperature (APPENDIX B – PVGIS values for irradiance and ambient temperature– time resolution: 15 min). These values are furnished for a location close to all plants under study (plant 1,2 and 3); therefore, as an assumption, data will be taken as constant for the three cases.

Through these data, it is possible to apply formulas for productivity estimation presented in ch.3.1. In particular, using equation 3.3, cell's temperature can be determined.

It is then possible to determine the output AC power P_{AC} of the plant using the following equation, which derives from eq. 3.1:

$$P_{AC} = P_N \cdot \frac{G}{1000} \cdot (1 + \gamma \cdot \Delta T) \cdot \eta_{PCU} \cdot k \tag{3.4}$$

with clear meaning of the symbols.

In this form, it is possible to highlight the contributions to PR which are easily determinable with a simple calculation - over-temperature $(1 + \gamma \cdot \Delta T)$ and Power Conditioning Unit efficiency (η_{PCU}) - i.e. items 5 and 7. (Ch.3.1); all the other losses are included in parameter k, whose suggested value is equal to 0.92.

By the comparison of calculated data of yearly final yield (kwh/kW$_p$) using eq.3.4 and real production data from monitoring activity (ch.3.3.1), being the two results theoretically equal, it has been possible to determine a parameter k to satisfy the equality ; then, the resulting k obtained has been compared to the value suggested by literature, in order to understand whether or not the plant under analysis is performing correctly, and what is the average discard from the expected value.

Data of power temperature coefficients of modules and inverter's efficiency have been taken from respective datasheets for all the plants considered.

Briefly:

	Plant 1 (OLD)	**Plant 2**	**Plant 3**
Module's power coefficient (%/°C)	*-0.45*	*-0.43*	*-0.46*

PCU efficiency	*0.98*	*0.974*	*0.97*
NOCT (°C)	*44*	*44*	*47*
Plant's nominal power P_N (kW)	*901.6*	*510.4*	*999.7*
Average final yield (kWh/kW_p)	*1'308.0*	*1'436.5*	*1'446.3*

Table 3.13 - Input parameters

Performing the described calculation adopting a time-step of a quarter of an hour, it has been possible to determine, for each time interval, the output AC power; the energy produced is simply given by the product of the AC power, assumed constant in the time interval, and the time-step adopted. The procedure has been repeated for all months of the year; each day of the month has been considered equal in terms of irradiance and ambient temperature, according to data extrapolated from PVGIS. Yearly productivity is then simply given by the sum of daily energy, in turn given by the sum of energy on the specific time interval adopted.

The value of the final yield has been calculated as a function of parameter k; assuming as final yield the real value measured (reported in the table 3.13), it has been estimated the value of the parameter k which fits better the final expected result. Values of k for the three plants, obtained as explained, are now reported:

	Plant 1 (OLD)	**Plant 2**	**Plant 3**
k (estimated)	*0.80*	*0.88*	*0.92*

Table 3.14 - k parameter estimation

Being 0.92 the expected value, it can be seen how plant 1 is in enormous deficit with respect both the theoretical value and the other two plants, which instead present a value of k very close to the optimal.

Adopting the theoretical value of k, it is possible to furnish an estimation of the final yield for plant 1 after the revamping process (NEW configuration); as a hypothesis, the plant is expected to perform optimally (k=0.92). Performing exactly the same procedure exposed before, with the aim, this time, of determining a value of final yield with a pre-established value of k, the resulting final yield is **1'517 kWh/kW_p**, with an expected increment with respect OLD configuration of **16%** (ch.5.3.3).

3.3.4. Main results

Resuming the main results obtained in this chapter:

Estimation type	Main result	Notes
Comparison with real plants of the same area	Expected final yield increase versus OLD configuration :**10%**	The increment has to be applied to the final yield of the OLD configuration (factor k_1 = 1.10)
Computational simulation using PV*SOL software	Corrective coefficient for simulated final yield: **8.1%**	The increment has to be applied to the final yield of the SIMULATED NEW configuration (factor k_2 = 1.08)
Literature formulas	Expected final yield increase versus OLD configuration :**16 %**	The increment has to be applied to the final yield of the OLD configuration (factor k_3 = 1.16)

Table 3.15 - Productivity estimation results

The decay rate of final yield of the plant in the NEW configuration will be assumed equal to **-0.8 %/year**.

3.4. Case study – OLD configuration – Daily profiles

Using results obtained with literature formulas, it is then possible to estimate the daily production profile for the case study plant in its OLD configuration. In order to fit the calculated yearly production value with the real one, analysis is performed adopting a value of k of 0.80 (Tab.3.14). In ch.5.3, the same results will be presented also for the NEW configuration, highlighting the main differences between the two cases.

The analysis will be carried on for four days, representative for the month, respectively in winter, spring, summer and autumn, in order to highlight the differences in performance for different seasons.

3.4.1. Daily analysis

The behavior of cell's temperature (T_C), ambient temperature (T_a), solar irradiance (G) and AC power output (P_{AC}) will be represented for a typical day of January.

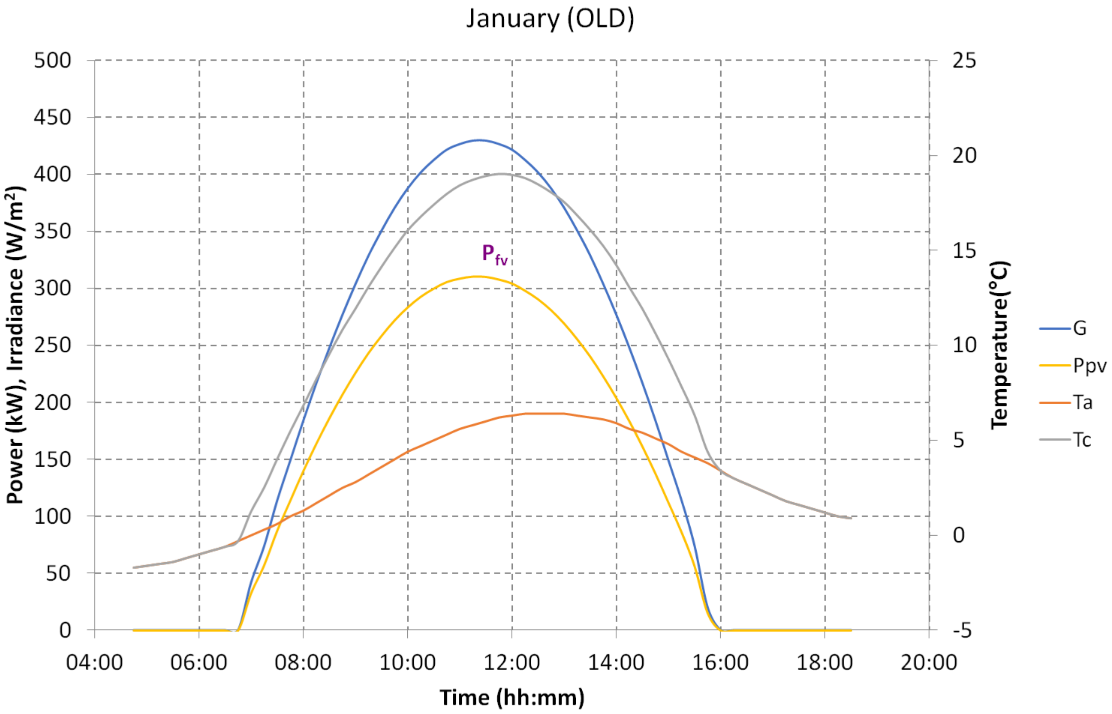

Figure 3.12 - Global irradiance, ambient temperature, cell's temperature and PV power output (January)

Due to the very low daily irradiance, which, in the plane of the modules, reaches at maximum a value around 440 W/m^2 at noon, the PV power output is far from the nominal, being only the 33 % of the installed power.

When ambient temperature is very low, module's efficiency grows, since the effect of temperature, if below 25°C, is beneficial for the module. Generally, a PV module works less but better in winter, due to low temperatures and irradiances.

When irradiance is zero, cell's temperature is equal to ambient temperature. As the Sun rises, ambient temperature rises, reaching a maximum briefly after noon. Cell's temperature, which is always greater-equal than ambient temperature, has a profile which is strongly influenced by the solar irradiance, having exactly the same behavior.

In terms of current and voltage at MPP, for simplicity considering the ones of a single module, a time dependent behavior can be observed, since both of them are related respectively to irradiance and temperature. In detail:

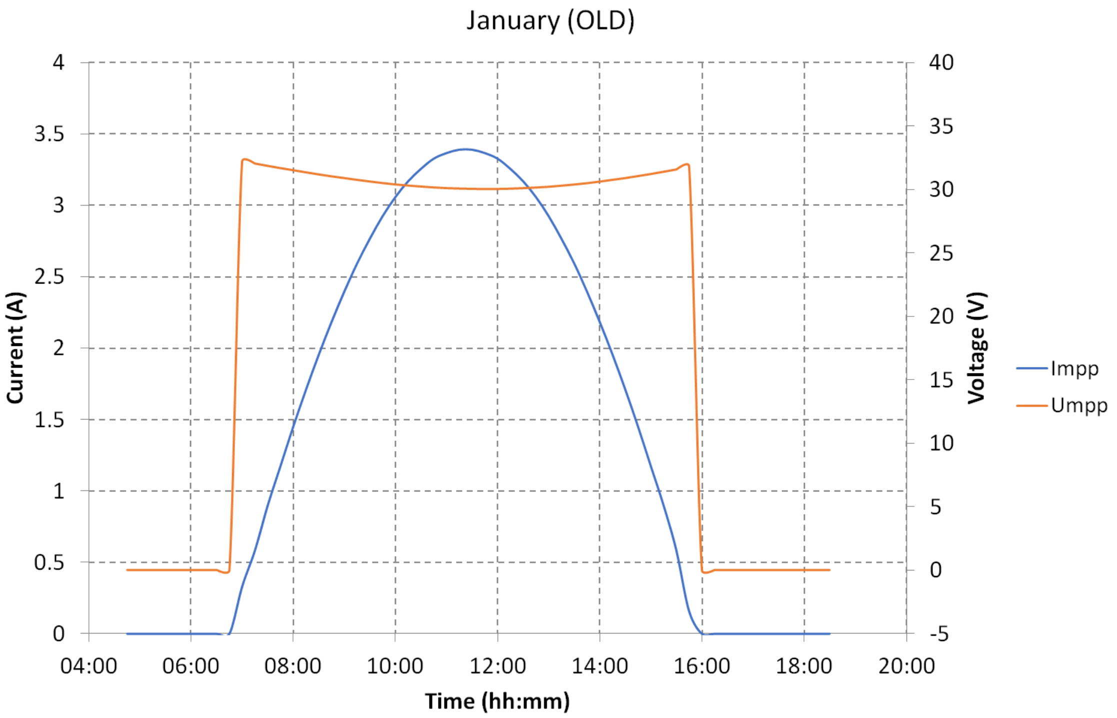

Figure 3.13 – MPP current and voltage (January)

For what concerns the MPP current, its behavior is strictly connected to the one of the solar irradiance, since, as seen in chapter 1, the two parameters are directly proportional (photo-generated current). Therefore, it shows a maximum when the irradiance is higher, i.e. at noon. For its calculation, it has been neglected the dependence on temperature, due to the very low thermal coefficient of current.

Oppositely, the voltage at maximum power point is calculated only with the contribution of temperature. Solar irradiance has no influence except when it takes zero value (night); in that case, voltage drops down to zero almost immediately. Since its behavior is strongly influenced by temperature, the curve shows two maxima, in correspondence of the lowest external temperatures, and therefore lowest cell's temperatures, respectively at sunrise and sunset. The value assumed at sunrise it is a bit higher, due to the even colder temperatures.

In terms of daily energy produced, it is interesting to report the cumulative profile.

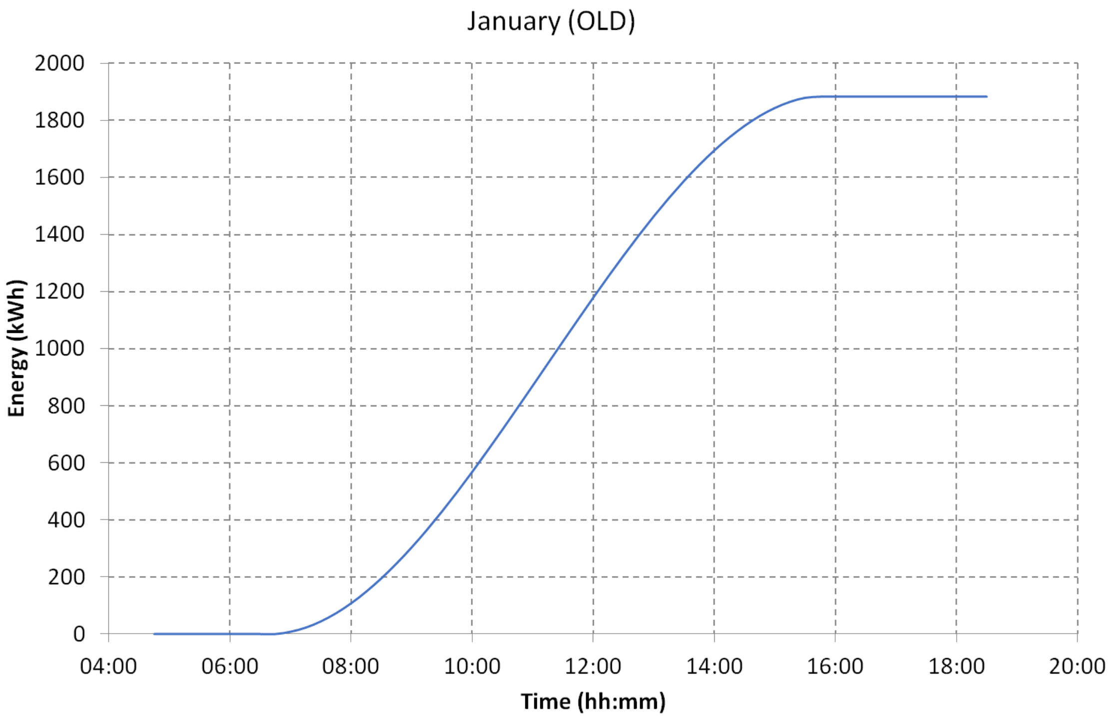

Figure 3.14 – Daily cumulated energy behaviour with time

The slope of the curve resembles the instantaneous power produced; in the central hours of the day, the slope, i.e. the power produced, is greater. The flex corresponds almost to noon time, i.e. with Sun culmination.

3.4.2. Monthly analysis

Analyzing comparatively these parameters in four different seasons, further comments can be proposed.

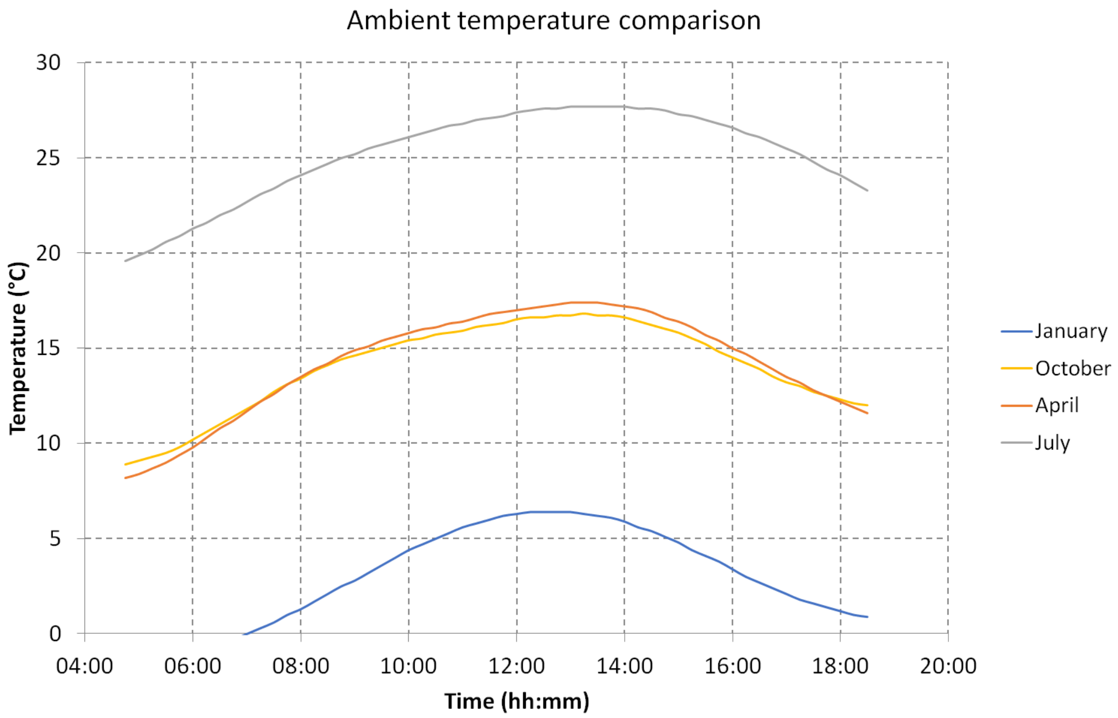

Figure 3.15 - Ambient temperature for different seasons

As expected, behavior of ambient temperature, for different seasons, is the same in terms of shape (higher in the central hours of the day), but with different values, strongly influencing cell's temperature.

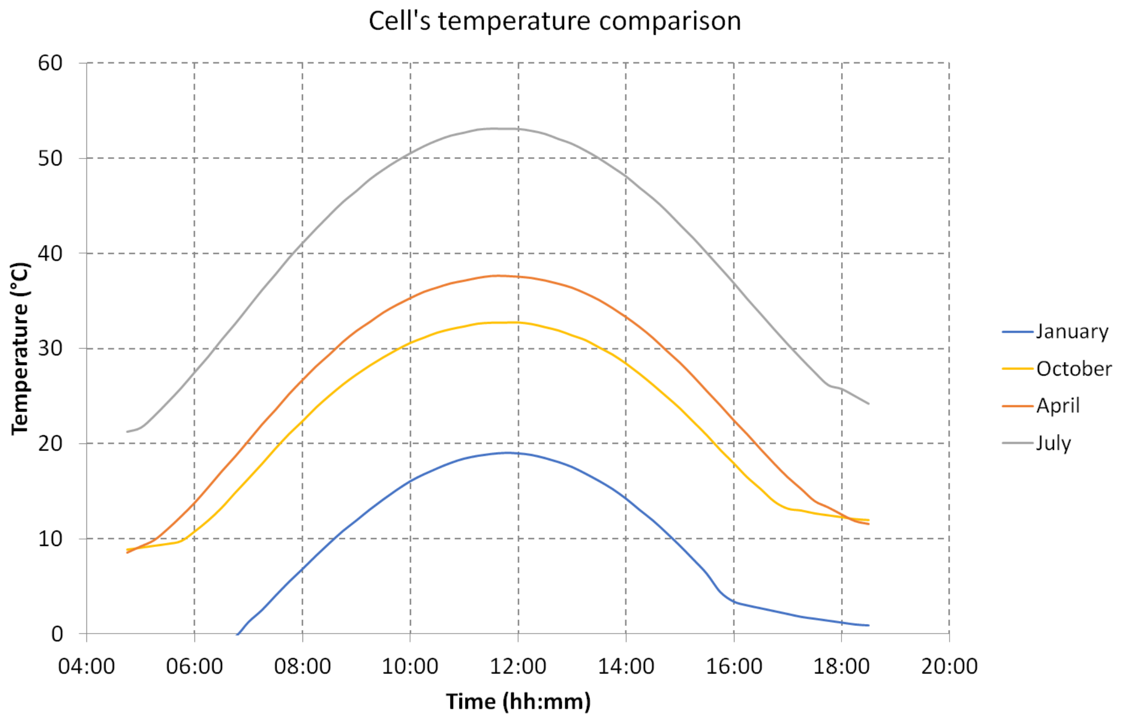

Figure 3.16 - Cell's temperature for different seasons

Peak temperatures are reached in summer, when cell's temperature can overcome 50 °C; in these conditions, losses due to over-temperatures with respect STC are more relevant. As a preliminary calculation, the amount of losses with respect STC, for a module at 55°C, can be roughly evaluated as:

$$Loss_{overtemperature}[\%] = \gamma \cdot (T - 25°C) = 0.45\% \cdot (55 - 25) = 13.5\% \; wrt \; P_{STC}$$

, where γ is the thermal coefficient of power, and T is the average cell's temperature.

This is the opposite situation with respect winter case: modules work worse, due to the high temperatures, but more time, since the light time is longer.

Autumn and spring present an intermediate situation, which can be considered as representative for the whole year, on average.

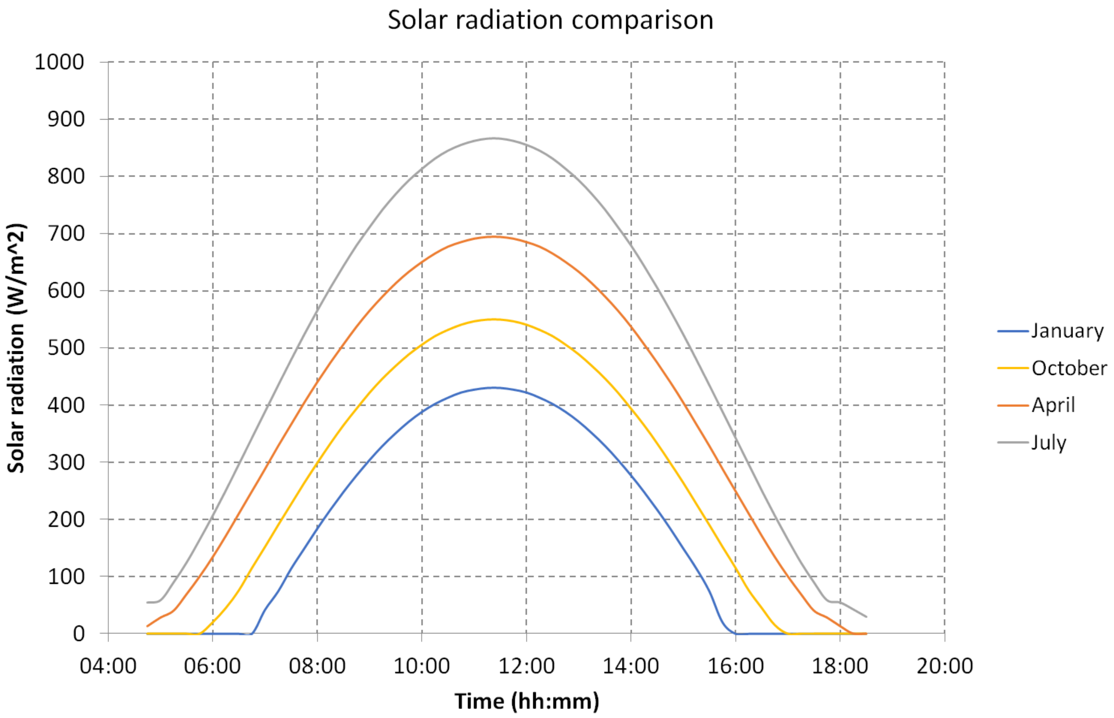

Figure 3.17 - Solar irradiance for different seasons

As expected, solar irradiance is higher for summer months. Furthermore, due to the more favorable climatic conditions, spring radiation is generally higher than the autumn one. It is clearly visible how, averagely, for the location and angles considered, the STC value of 1’000 W/m^2 is never reached; this means that there will always be an inevitable loss due to an irradiance deficit with respect standard conditions.

The consequent output power of the plant is strongly influenced by this limitation:

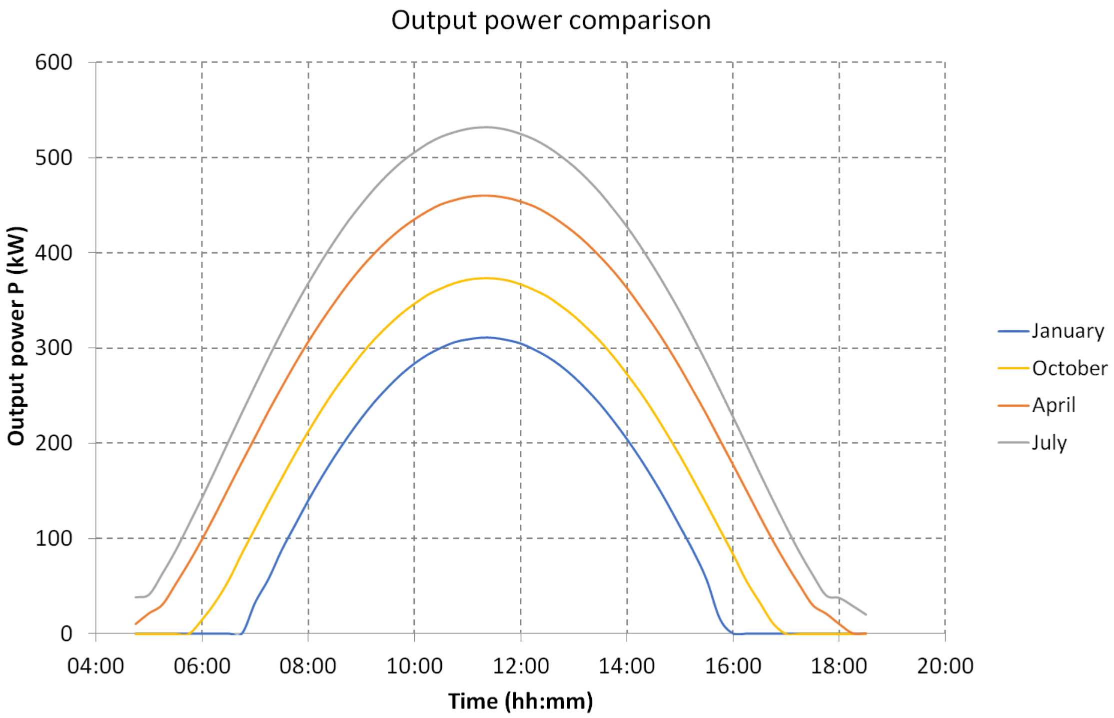

Figure 3.18 - Output power for different seasons

Maximum power, near 500 kW, is reached in summer. This value results a lot lower than the nominal power of 901.6 kW_p. In the following table, the average power for months chosen for the analysis is reported.

Month	Daily average (kW)
January	210
April	368
July	434
October	278

Table 3.16 - Daily average power for selected months – literature results

Finally, it is interesting to see how current and voltage profiles are affected by seasons:

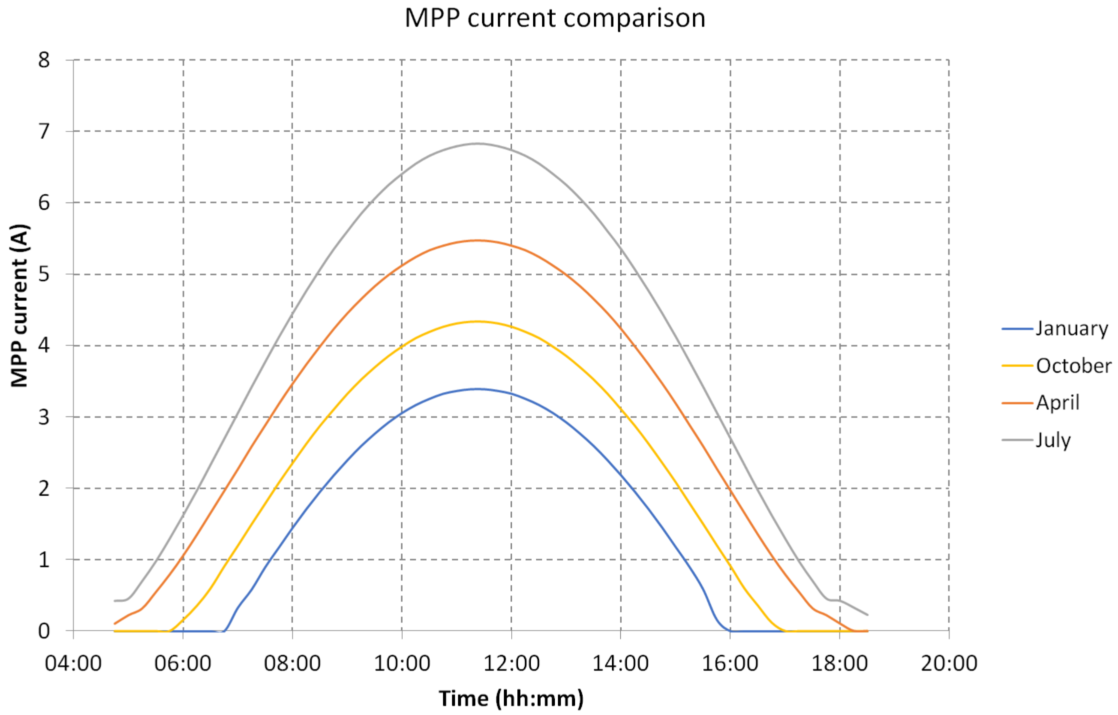

Figure 3.19 - MPP current for different seasons

As current is mainly affected by solar irradiance, the shape of the curve is strictly connected to the irradiance curve; that is, it reaches greater values during summer, and it presents also a greater time interval during which it is different from 0.

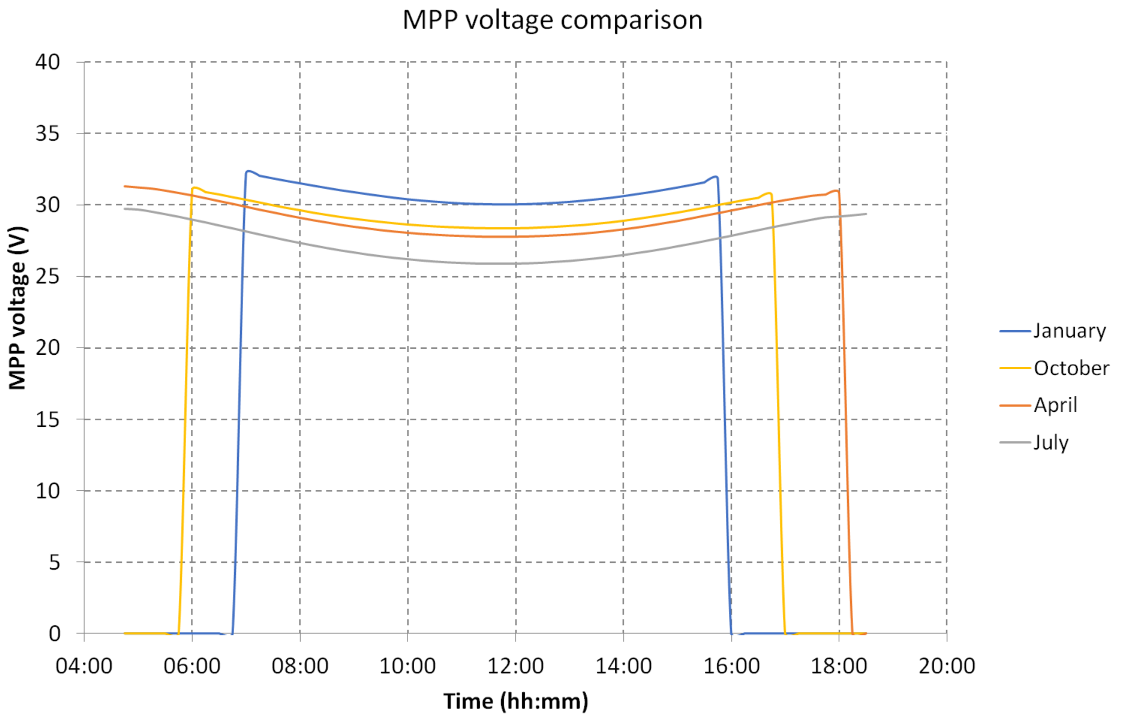

Figure 3.20 - MPP voltage for different seasons

Change in seasons affects voltage for two reasons:

- Temperature difference: voltage thermal coefficient is very relevant, therefore the absolute voltage's value in warmer months is lower with respect colder months;
- Solar irradiance: despite it does not influence voltages magnitude, it is relevant to determine when voltage can be detected. As said, when irradiance is zero, voltage falls to zero immediately. Therefore, for summer months, when days are longer, also voltage's value is different from zero for a longer period, as the consequent power production.

3.4.3. Validation

The formula adopted furnishes an estimation based on the annual productivity of the plant, measured by production counters, i.e. the adopted value of k is the one which matches the real yearly production with the yearly calculated production. However, daily profiles of power, given by monitoring activity, can be extremely different from the ones obtained above, due to the strong variability of meteorological conditions or and other situations which can affect plant's behavior.

Therefore, monitoring data coming from the data acquisition system (DATALOGGER), connected to the case study plant, will be reported for the four months considered before, in terms of AC power (kW).

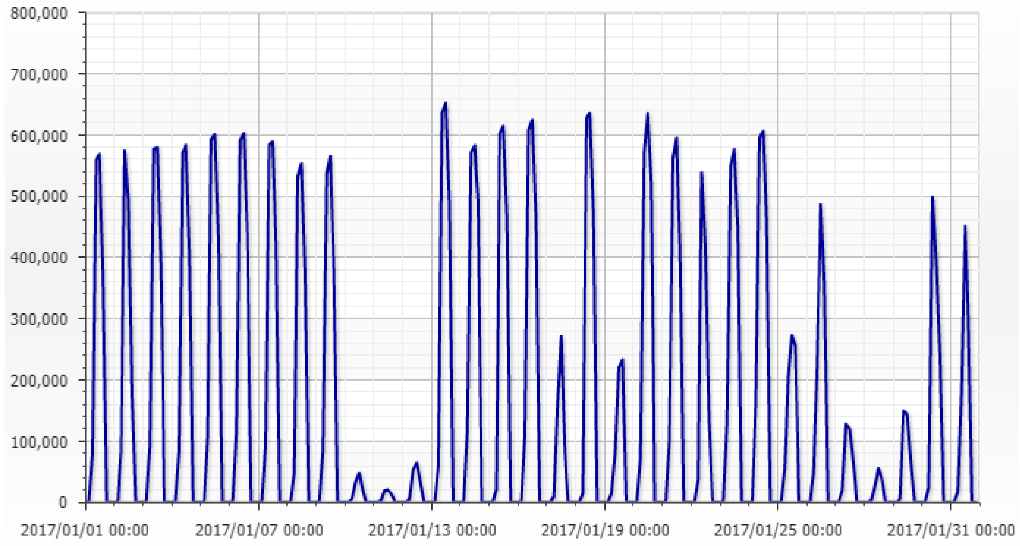

Figure 3.21 - Monthly profile from data logger (January)

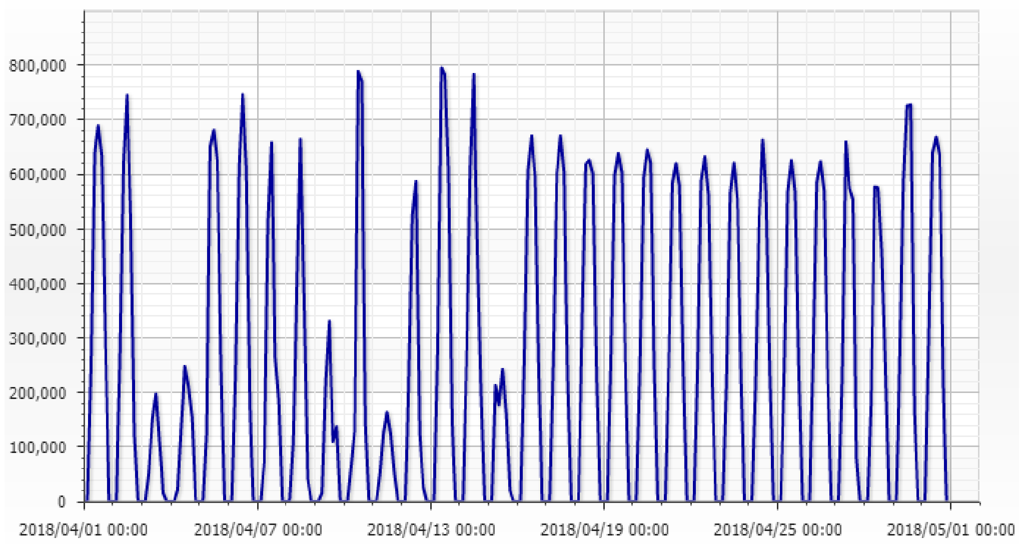

Figure 3.22 - Monthly profile from data logger (April)

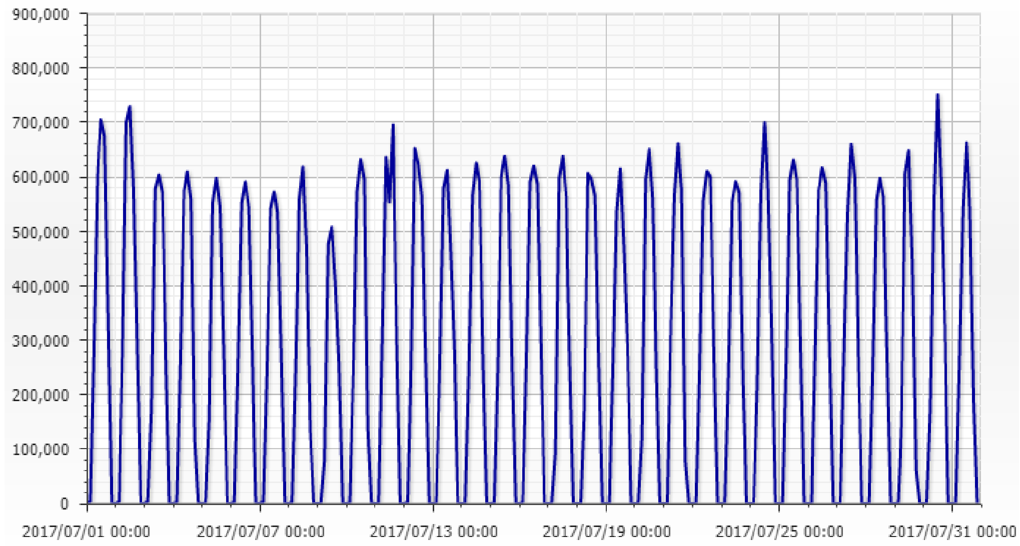

Figure 3.23 - Monthly profile from data logger (July)

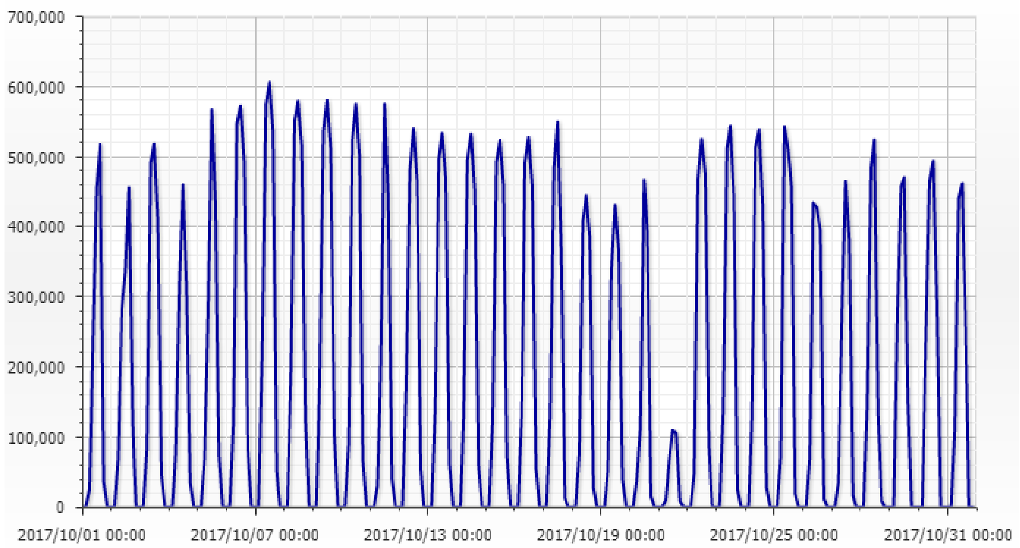

Figure 3.24 - Monthly profile from data logger (October)

In this representation, the behavior of the AC power output (kW) from the inverter is reported with time on monthly basis.

What can be suddenly noticed are the strong irregularities in the behavior of power with respect time, comparing different days of the month; indeed, monitoring concerns all the possible weather conditions as well as maintenance activities, which are not predictable using the simplified mathematical model adopted before.

Secondly, peak powers are higher than ones calculated; this is because the formula adopted was adjusted in order to fit the real annual production with the calculated one, therefore it represents averagely the behavior of the plant, and it is not able to detect local peaks or variations on a daily basis.

Finally, spring peak power seems to be greater than summer's one; this is because the effect of temperature is dominant with respect to the one of solar irradiance, and therefore measured power are higher in fresher climatic conditions.

In order to validate the model, the average daily profiles measured should be comparable with the one calculated.

Month	Monitoring daily average (kW)	Calculated daily average (kW)	Discard (%) with respect calculated value
January	283	210	+35 %
April	367	368	-
July	354	434	-18 %
October	300	278	+8 %

Table 3.17 - Daily average power for selected months – Monitoring data

At first sight, the averages obtained with literature formulas are close to the one determined through monitoring activity especially for temperate months, i.e. spring and autumn. Major differences can be found in winter, when the real value is greater than the one calculated, and summer, when the real value is lower.

This difference probably suggests that the influence of temperature (negative in summer, positive in winter) is more relevant than what considered through the adopted equation.

Nevertheless, since the yearly averages are very close (almost 323 kW for both), the result obtained with literature formulas can be reasonably accepted; at the end, what matters is the yearly final yield, which certainly matches for the two cases, thanks to the specific coefficient k chosen (ch.3.3.3).

4. Technical issues: PV modules

The goal of the chapter is the analysis of the main problems which can affect a single PV module, with particular emphasis to the hot-spot problem.

In the first part of the chapter, a general overview on major anomalies characterizing solar panels will be introduced. For each anomaly, the identification procedure, main causes and possible consequences on the whole panel will be presented.

The second part of the chapter will be devoted to the case study plant. Main problems affecting installed modules will be highlighted, also with experimental proofs; a literature research on the hot-spot problematic will be then introduced and a rough evaluation of loss of power with respect STC will be given, as a result of the experimental I-V curve determination and measuring procedure carried on the plant.

4.1. PV modules anomalies: an overview

Per definition, a PV module failure is an effect that degrades module power, which is not reversed by normal operation and creates a safety issue. Principal consequences of the glitches are performances reduction or panel failure.

For each anomaly, graphic visible and IR patterns are introduced, according to Entec databases.

4.1.1. Visible anomalies

Name	Visible pattern	IR pattern
Modules displacement	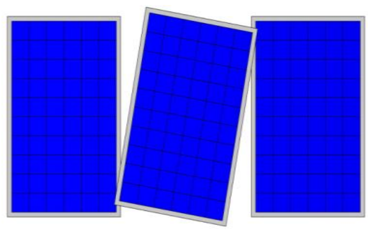	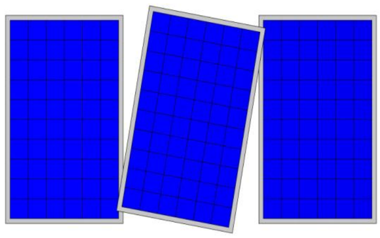
Glass Breakage	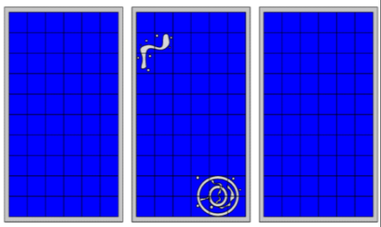	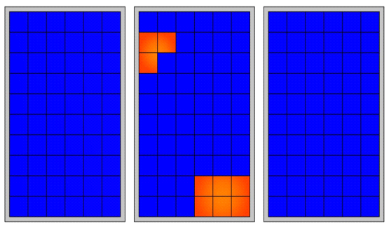
Soiling	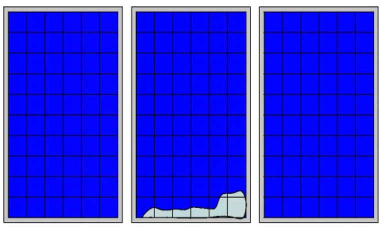	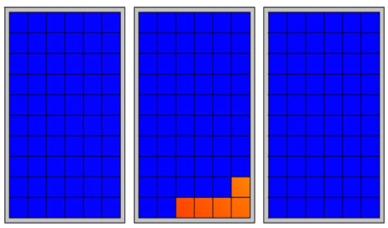
Frames deformation	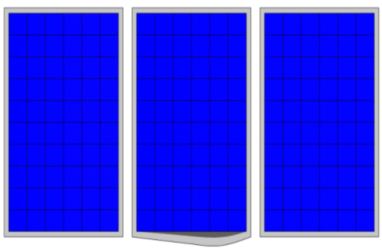	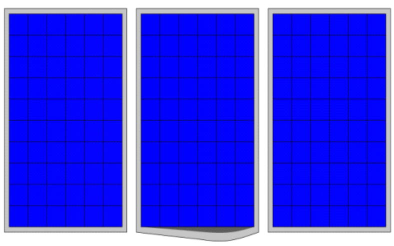

Figure 4.1 - PV modules anomalies (part 1) -Visible and IR patterns

- *Modules displacement*: PV modules out of their position. Main causes are an improper installation, or weak fixation system.

- *Glass breakage*: frontal glass of modules cracked. It can be due to an improper transport or handling, inappropriate clamping on structures, vandalism or maintenance inexperience. Usually, the problematic is limited to a well restricted area on the frontal glass, whose dimensions depend on the cause. It can be influenced by environmental conditions (normally, all modules are subjected to hail tests before being put on the market, therefore environmental influence can be evident in this sense only for extreme events). IR can highlight higher temperature levels in correspondence of breakages.

Figure 4.2 - PV module with broken glass

- *Soiling*: decrease in productivity due to the soiled surface. It can be caused by dust, pollen, sand, atmospheric pollutants, mould etc., which accumulate especially along the frame or in the corners; it is a very frequent problem, quite evidently affected by atmospheric conditions, both positively (rain falling can help washing modules) and negatively (strong wind can raise dust above module's surface). Different temperatures can be detected in correspondence of the accumulations.

Figure 4.3 - Dirty PV modules (soiled)

- *Frames deformation:* modules' frame damaged or deformed. Usually, the principal cause is the accumulation of a great amount of snow on the frame of PV modules (along the profile), which acts as a surface distributed charge. It is a quite rare event, strongly influenced by atmospheric conditions.

4.1.2. Infra-red anomalies

Most frequent faults cannot be detected by visual analyses, but a IR ("Infrared") inspection is required.

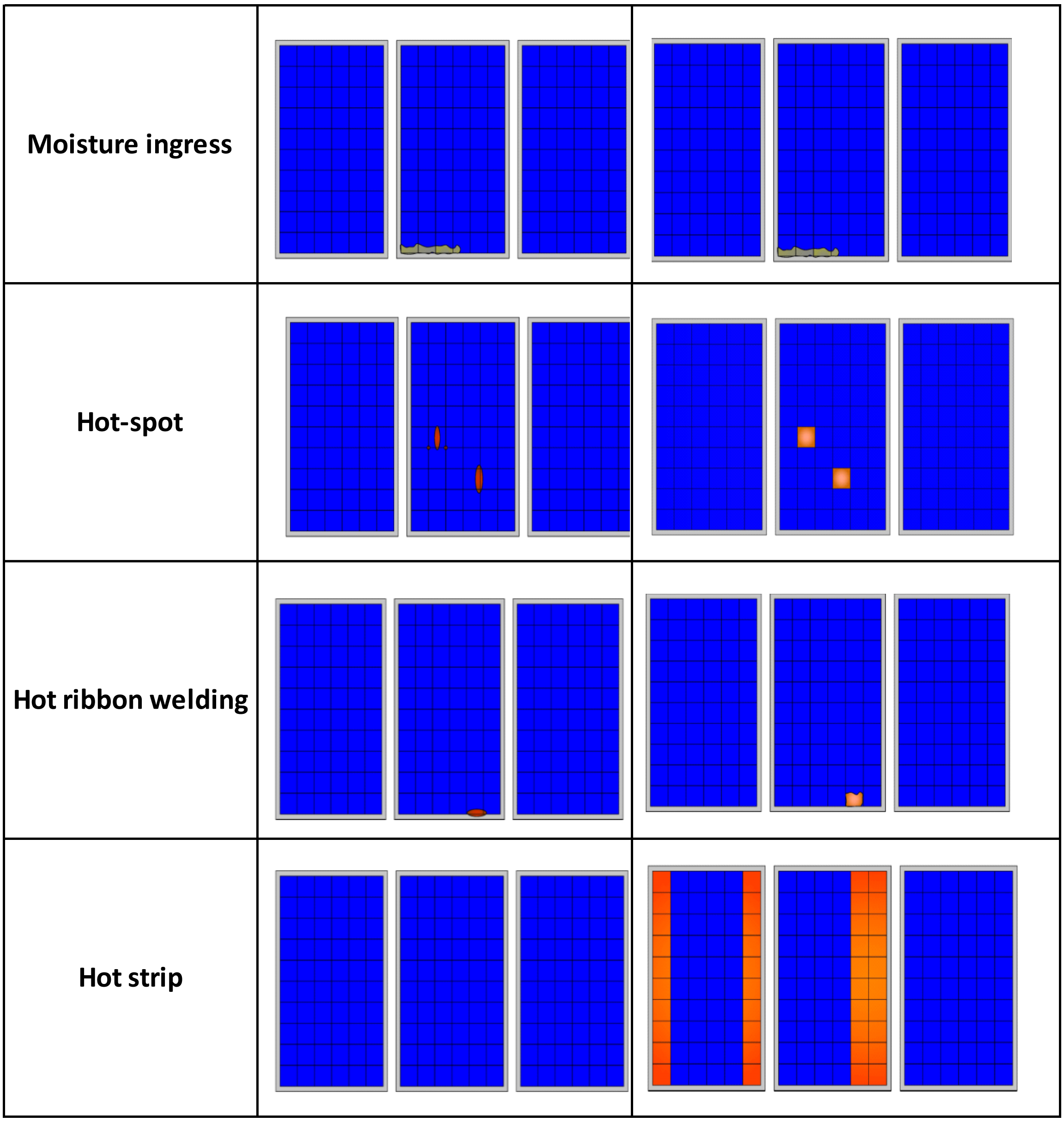

Figure 4.4 - PV modules anomalies (part 2) -Visible and IR patterns

- *Moisture ingress:* delamination of PV module's layers, reduction in glass transparency and corrosion of active parts. Principally, it is due to bad sealing and encapsulation of panels, more evident along the frames.
- *Cell's hot-spots:* single or multiple cells of a module clearly warmer than the other. Main causes can be overshadowing of a series of cells or modules, or internal cell's faults due intrinsic defects. In these conditions, cells affected by the problem start to behave like a load, and to absorb rather than produce power. It is a relatively frequent problem, whose detection is strongly influenced by external environment conditions, especially from the solar irradiance level. In general, it is possible to detect hot-spot presence only by IR analysis; however, for heavily damaged cells, evident burns can be noticed also with the naked eye. The argument will be deeper analyzed in the continuation of the discussion.

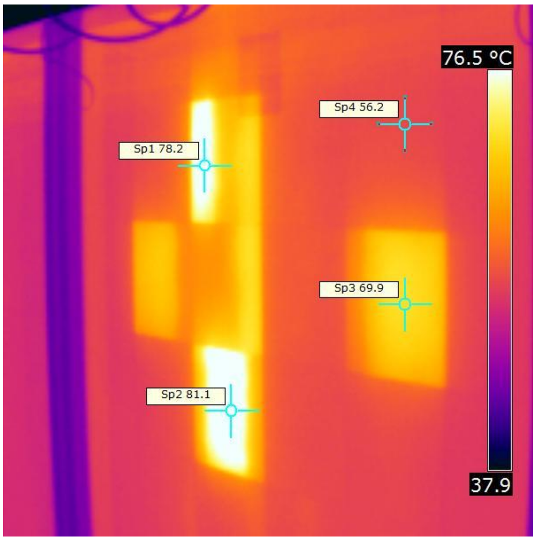

Figure 4.5 – Defective cell's (picture from plant 1)

Figure 4.6 – Visible burnings (picture from plant 1)

- *Hot ribbon welding:* PV rod connectors in over temperature, due to bad welding.

- *Hot strip:* series of PV cells over temperatures, caused by damaged or short-circuited bypass diodes, which can be extended for the whole panel's length. Similar to the hot-spot problem in terms of causes and frequency. A set of cells in series are completely bypassed, therefore start to heat up since not producing power.

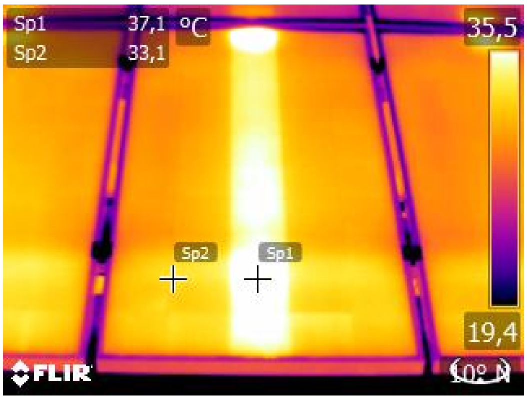

Figure 4.7 - Hot strip

Further anomalies detectable by IR analysis are reported:

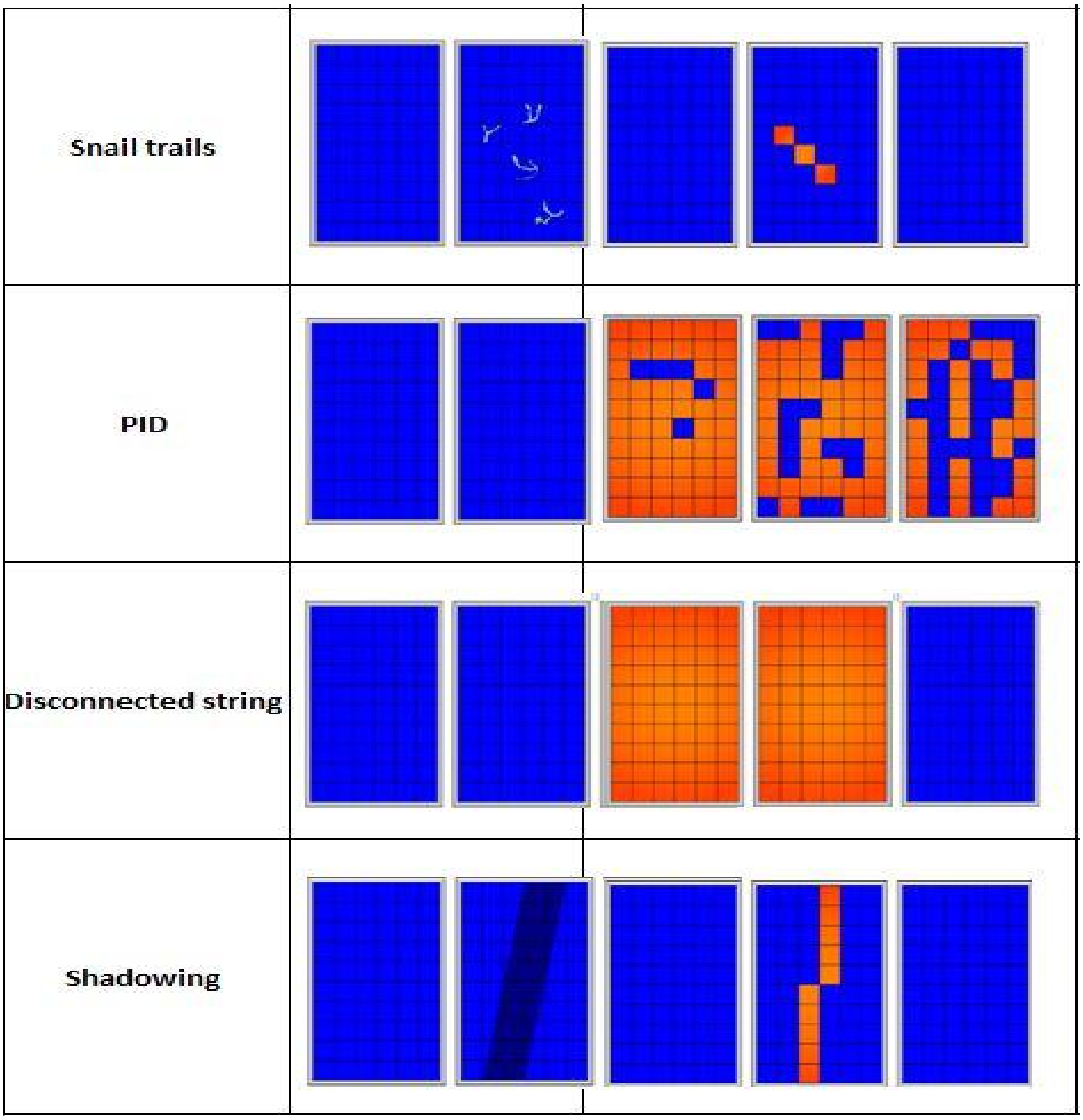

Figure 4.8 - PV modules anomalies (part 3) -Visible and IR patterns

Figure 4.9 - Snail trails on panel's surface

- *Snail trails:* optical effect (grey/black discolouration on the front of screen-printed solar cells) with typical aspect of snail trails, and subsequent thermal effect causing slight over temperatures of the interested cells. It can be due to construction processes with micro-cracking of cells and consecutive exposure to heat and UV. It is a relatively frequent phenomenon, which affects some cells of the panel.

- *PID:* leakage current created from the frame to the ground. Consequent decrease of PV production and overheating of cells. It is due to loss of insulation between the conductive part of the module and the earth potential or it is an effect of high voltage stresses;

- *Disconnected strings:* one string is warmer than the other. Due to open circuits, caused by wire's interruptions or burnt fuses. It can involve one or some strings;

- *Shadowing:* part of entire modules in shadow, due to the presence of near obstacles. The entity of the anomaly is strongly variable, depending on the obstacle considered. The shadowed part is warmer than the other, since part of the panel is not producing power.

4.2. HOT-SPOT

The analysis will be now focused on the hot-spot issue, being the most severe anomaly affecting modules of the case study plant.

According to Zhang et al.[27], an analysis on PV modules of almost 200 MW_p running in the United States for 1 to 3 years, has been carried out, listing main reasons for failure and degradation of the panels. Considering a sample of 115 defective modules, the 22% of them have shown a failure cause associated to hot-spot presence.

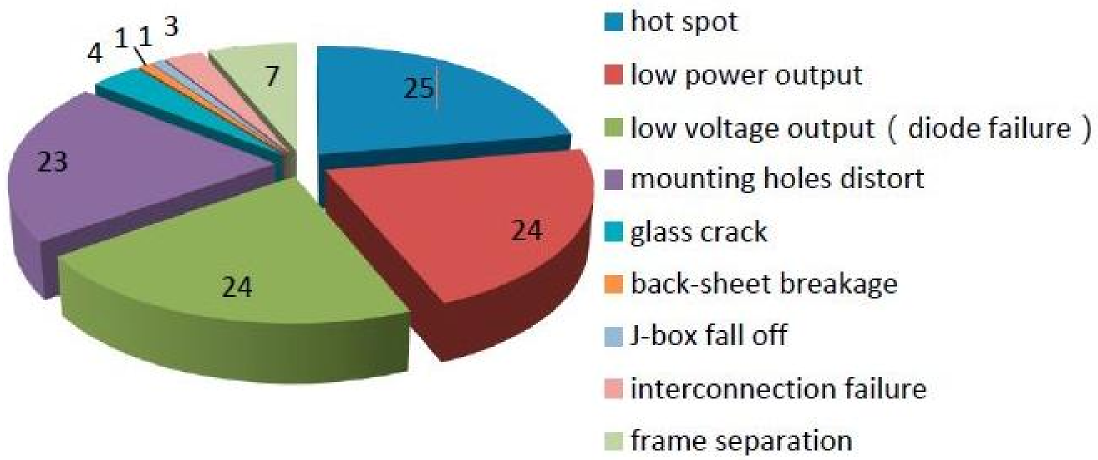

Figure 4.10 - Failure causes of PV modules (sample of 115 modules)

4.2.1. Causes and effects

Hot-spot problem regards cells or groups of cells which present a temperature higher than the average module's temperature.

The phenomenon arises when panel's operating current exceeds the short-circuit current of a low-current producing cell or group of cells. When such a condition occurs, the weak cell starts to operate like a load, i.e. acts in reverse bias (ch.1.3.2). All the power absorbed by the cell is dissipated in form of local overheating; as a result, cell's surface temperature increases considerably.

[27] Zhang Z, Wang L, et alia., "Study of bypass diode reliability under non-uniform irradiance distribution on PV module surface", Acta Energiae Solaris Sinica,2016.

The causes of the anomaly are still not clear; essentially, it can occur when solar cells are mismatched, i.e. when are shadowed or when they have some intrinsic defects (e.g. presence of impurities accumulated on the silicon wafer during junction diffusion) which cause a shunting behavior of the cell's PN junction.

Shunt resistance is the parameter introduced in ch.1.3.4 useful to measure the shunting phenomenon, i.e. the presence of superficial dispersion currents which reduces the amount of current effectively flowing into the junction of the solar cell, "weakening" the cell itself. Both a decrease or an increase of the shunt resistance can cause hot-spot formation, in different ways.

The so called "shunt paths", i.e. "*any position in a solar cell showing under forward or reverse-bias a dark-current contribution additional to the diffusion current*" [*Shifeng et al*], can be considered the main reason for shunt resistance lowering. They can have different origins; in general, nine typologies of shunt paths have been identified and classified according to the shape of the modules' I-V curve and their physical nature. They can be subdivided in two categories:

- **Process-induced shunt paths**: caused during the construction process of the cell. They are due to the presence of crack and holes, soldering defects, scratches and aluminum particles;
- **Material induced shunt paths:** due to recombination's sites near defects and precipitates of SiC (crystalline silicon) on grain boundaries. Usually, these precipitations are due to low-cost processes using low-grade materials.

When R_{sh} decreases, localized areas of the cell present a shunting behavior, i.e. the amount of current flowing strongly increases, and the consequent power to be dissipated. If the power dissipation overcomes cell's thermal limit (usually of 85 °C), it can lead to localized breakdown of the junction, and to hot-spot formation.

Also, the opposite condition (high R_{sh}) is not preferable; in reverse bias, the slope of the I-V curve gives the magnitude of the shunt resistance - the higher it is, the lower will be the leakage current. If the cell is shadowed/mismatched, it needs to dissipate a very high amount of power. Being R_{sh} so high, the bypass action possibly granted by the parameter (like a bypass diode, it can allow the presence of additional paths of current, which will help to dissipate power) is not present.

Standard value of shunt resistance is 10000 Ω; insulation tests performed on panels are aimed at determining the leakage current between modules frame and ground, and, indirectly, to assess the value of the shunt resistance, which must be exactly the same as the standard value.

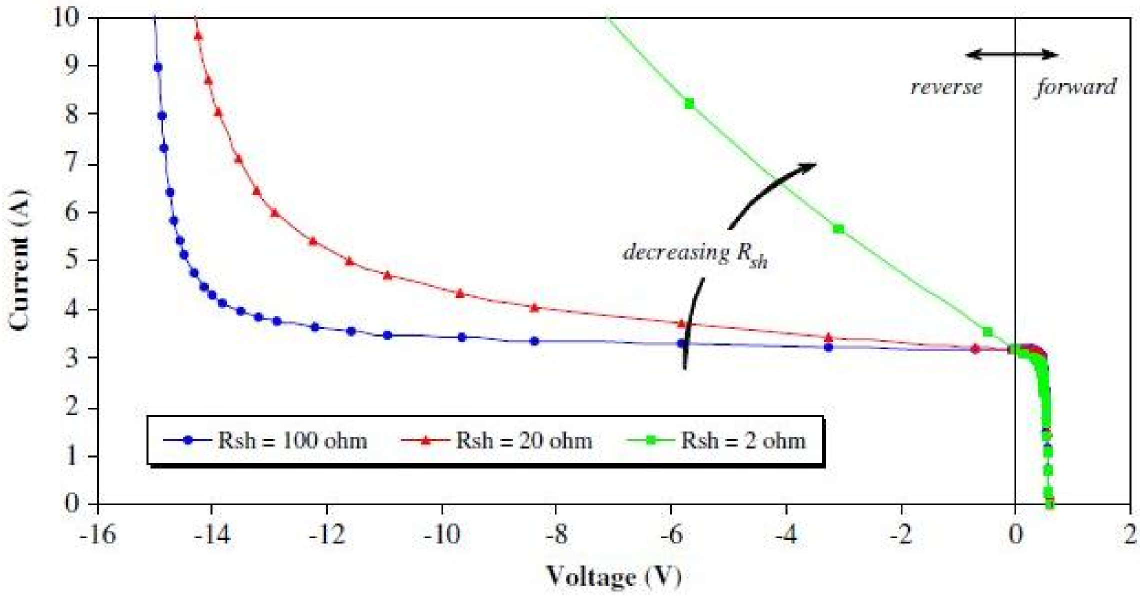

Figure 4.11 - I-V curve for reverse bias, considering different shunt resistances

It has been said that the complete I-V curve of a solar cell can be represented into four quadrants. The normal operating points are in the first quadrant, in which the cell operates like a generator. In the II and IV quadrants, respectively due to inverse voltage and inverse current, cell's behavior resembles a load behavior. The analysis of the curve can furnish a lot of information about hot-spot heating, since it allows to evaluate shunt resistance and mismatch behaviors . In fig.4.11, the behavior of the solar cell IV curve in the II° quadrant is highlighted. In particular, it can be seen how a shunt resistance reduction necessarily implies a higher dissipation of power, being the product of voltage and current.

The main effect of hot-spot heating is the performance reduction of the panel in which the phenomenon occurs and, indirectly, on all the other panels to which is connected in series (string), limiting the overall power production. Other secondary effects can be associated to physical deformations of the interested panels, in correspondence of problematic cells. The strong over-temperatures can bring to heavy damages for module's materials, and to deformations on the back sheet.

4.2.2. Hot-spot formation mechanism

The mechanism is the same seen in case of mismatch of series connected cells. The analysis will now be further investigated.

The worst condition, as highlighted in ch.1.3.7., is the short-circuit condition, i.e. when the current absorbed by the weak cell coincides with the current of the un-shadowed cells, and the voltage equals the sum of each voltage of good cells in series. In this condition, the heat to be dissipated is the maximum possible.

A basilar power balance can be made on the cell under this condition. The heat to be dissipated by the weak cell Q can be distinguished into three contributions:

$$P = P_{illu} + P_{ph} + P_{rev} \tag{4.1}$$

- P_{illu} is the solar power (irradiance) which cannot be converted into electricity by the weak cell and should be dissipated in form of heat. It can be determined as:

  $$P_{illu} = G \cdot \alpha \cdot A \tag{4.2}$$

  , where α is the absorption coefficient of PV panels;

- P_{ph} is the photo-generated power, due to the photo-generated current that flows in the weak cell. It can be found as:

  $$P_{ph} = I_{sc_{weak}} \cdot V_m \cdot (\#_{series} - 1) \tag{4.3}$$

  , where $I_{sc_{weak}}$ is the short-circuit current flowing in the series, which is limited to the one of the weak cell;

- P_{rev} is the power contributing to the hot-spot effect. It can be calculated as:

  $$P_{rev} = I_{rev} \cdot V_m \cdot (\#_{series} - 1) \tag{4.4}$$

, where I_{rev} is the reverse leakage current of the weak cell.

According to main results obtained by Zhang et al., which have made reference to specific mismatch models implemented in MATLAB, the heat dissipated by the cell has been graphed with the shading ratio[28] of the cell (i.e. assuming that the weakness' cause is shading, which is an easy-to-manage parameter, unlike the cell's defectiveness).

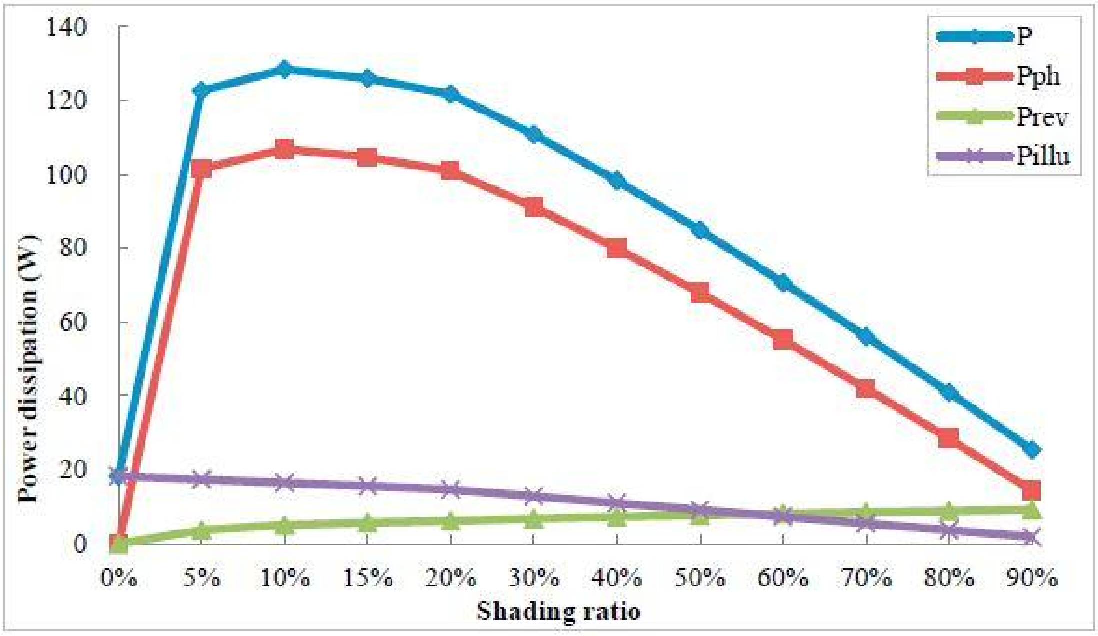

Figure 4.12 - Dissipated power with shading ratio

As expected, P_{illu} is linked to the available area for illumination, and decreases with increasing shading ratio.

P_{ph} behavior is related to the one of the un-shaded cells: after a first increase, limited to very low shading ratios, it decreases dramatically.

P_{rev}, which is the hot-spot effect contributing power, increases as the shading ratio increases, because the mismatch effect grows in the same direction.

[28] Ratio between shaded area and not-shaded area.

Further considerations have been made about the dependence of hot-spot temperature on defective area and module's output power.

The dependence on defect's area has been modeled through ANSYS. Results are reported in the next figure:

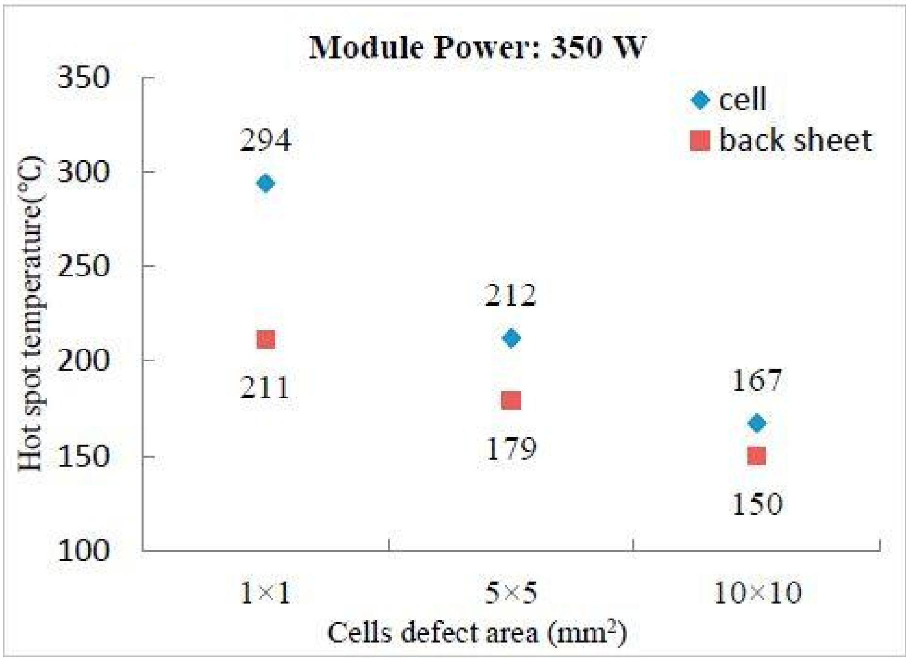

Figure 4.13 - Hot-spot temperature wrt. defective area

"The module hot spot temperature is negatively correlated with the defect area. The smaller the cell defect area, the greater the heat loss per unit area and the higher the hot spot temperature" – (*Zhang et al*.). Essentially, the fact could be explained considering that, if the dissipation ("exchange") area decreases, and the heat to dissipate is constant, the temperature of the interested area increases considerably, due to the very high specific heat flux [W/m^2].

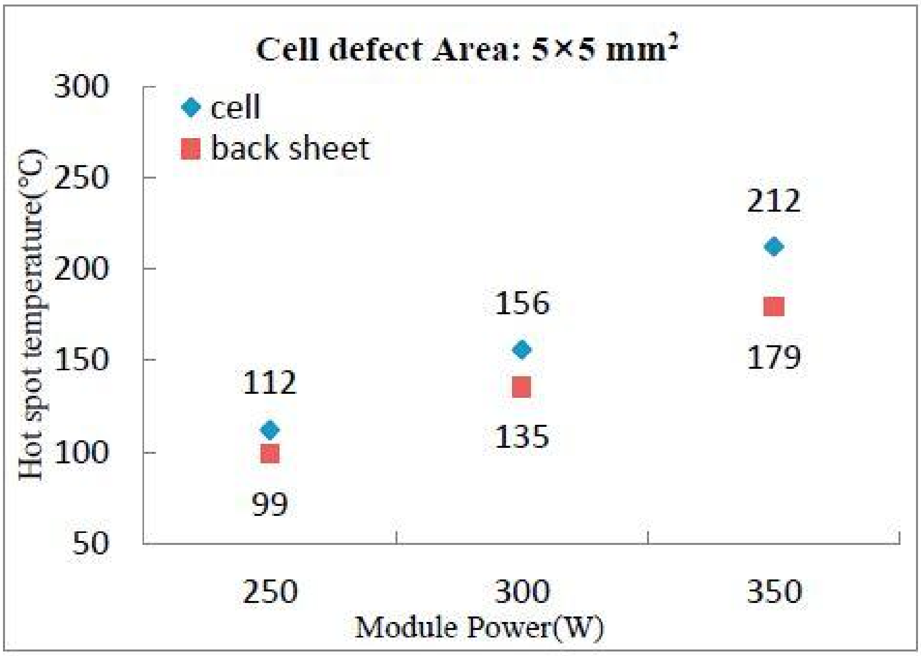

Figure 4.14 - Hot-spot temperature wrt. module's nominal power

A further analysis has also highlighted the positive dependence of hot-spot temperature with module’s output power. With increasing module power (simulated via an increasing value of the light source), the hot spot temperature increases per unit area, giving a higher hot spot temperature. As said previously, hot-spot phenomenon is strongly dependent on irradiance levels; if G value (and, consequently, the nominal power output of the module) is too low, hot-spot effect is less remarkable and evident.

4.3. Case study: thermo-graphic analysis and I-V curve simulation

The plant under analysis is affected mainly by hot spot problems. Consequently, module's equivalent I-V curve is strongly negatively involved, as the useful power guaranteed.

In the following part, thermographic analysis on the case study plant will be presented and, using a professional curve tracer, the I-V curve of installed modules will be defined, and put in comparison with the one given by the datasheet.

4.3.1. Thermographic analysis

In order to detect the exact location of these cells and what are the modules affected, thermo-graphic analysis has been carried on.

Different measurements campaigns have been conducted, which imply the presence of several operators, endowed of thermo-camera, useful to spot cells superficial temperature of the PV modules (see 4.5.3. for thermo-camera specifications).

IR inspections must be carried out under specific environmental conditions:

- Necessity of clear sky conditions, without clouds or other sources of shadowing;
- Sufficient solar irradiance (>600-700 W/m^2).

The effect of solar irradiance can be put into evidence monitoring the temperature's difference between cell and ambient temperature with varying level of solar irradiance. In order to highlight the following effect, a series of thermographic pictures in different times (i.e. at different irradiance levels) were taken for a problematic module, which presents four defective cells, affected by hot-spot.

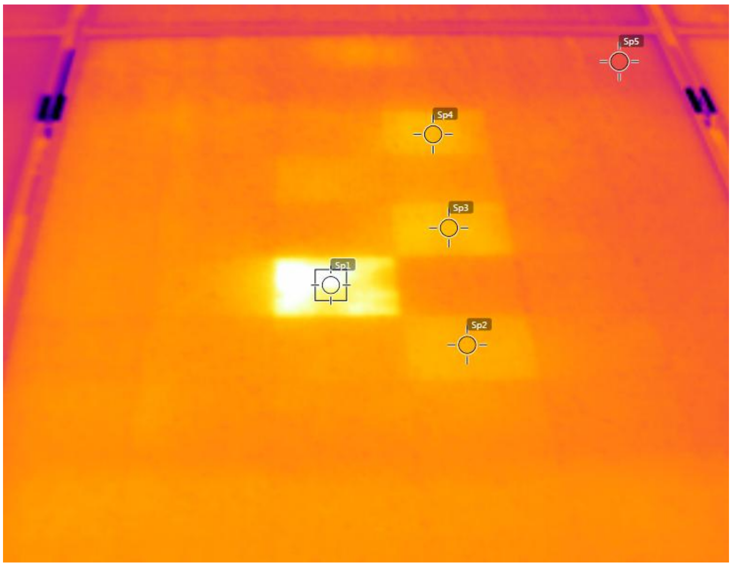

Figure 4.15 - Analysed defective panel – IR image

The temperature difference between defective cells and average surface temperature of the panel is an increasing function of the solar irradiance; it is easier to spot defective cells with high irradiance conditions, since this temperature difference is much higher in the latter case. Test results, carried on between 12:00 and 18:00 of a clear sky day, are reported and graphed. Acquisition angle[29] and distance are kept fixed and equal to 30 ° (modules' tilt) and 2 m.

		HOT SPOT 1			HOT SPOT 2			HOT SPOT 3			HOT SPOT 4		
G	Time	T_HS	T_ave	ΔT	T_HS	T_ave	ΔT	T_HS	T_ave	ΔT	T_HS	T_ave	ΔT
W/m^2	hh:mm	°C	°C	°C	°C	°C	°C	°C	°C	°C	°C	°C	°C
923	12.00	50.2	29.3	20.9	41.2	29.3	11.9	42.8	29.3	13.5	41.8	29.3	12.5
1034	12.30	52.3	30.5	21.8	44.0	30.5	13.5	45.4	30.5	14.9	43.6	30.5	13.1
940	13.00	50.2	33.0	17.2	44.6	33.0	11.6	45.6	33.0	12.6	43.2	33.0	10.2
1077	13.45	54.1	34.1	20.0	45.6	34.1	11.5	46.3	34.1	12.2	45.1	34.1	11.0
989	14.30	50.4	34.5	15.9	44.2	34.5	9.7	45.7	34.5	11.2	44.7	34.5	10.2
954	15.00	53.1	37.2	15.9	45.2	37.2	8.0	46.5	37.2	9.3	45.4	37.2	8.2
899	15.30	48.6	33.3	15.3	43.9	33.3	10.6	47.0	33.3	13.7	43.6	33.3	10.3
831	16.00	45.0	33.4	11.6	41.1	33.4	7.7	43.0	33.4	9.6	40.8	33.4	7.4
724	16.30	41.4	31.3	10.1	38.0	31.3	6.7	38.9	31.3	7.6	36.5	31.3	5.2
595	17.00	39.7	32.0	7.7	35.1	32.0	3.1	36.4	32.0	4.4	34.6	32.0	2.6
456	17.30	32.6	27.0	5.6	30.3	27.0	3.3	30.0	27.0	3.0	29.5	27.0	2.5
393	17.45	27.3	24.3	3.0	26.2	24.3	1.9	25.6	24.3	1.3	24.8	24.3	0.5
356	18.00	23.1	21.4	1.7	23.0	21.4	1.6	22.4	21.4	1.0	21.9	21.4	0.5

Table 4.1 - Influence of solar irradiance - Tabular results. T_HS is the hot-spot temperature, T_ave the average module's temperature, ΔT is the difference between the two.

[29] Angle between the perpendicular on the plane of the modules and the camera axis.

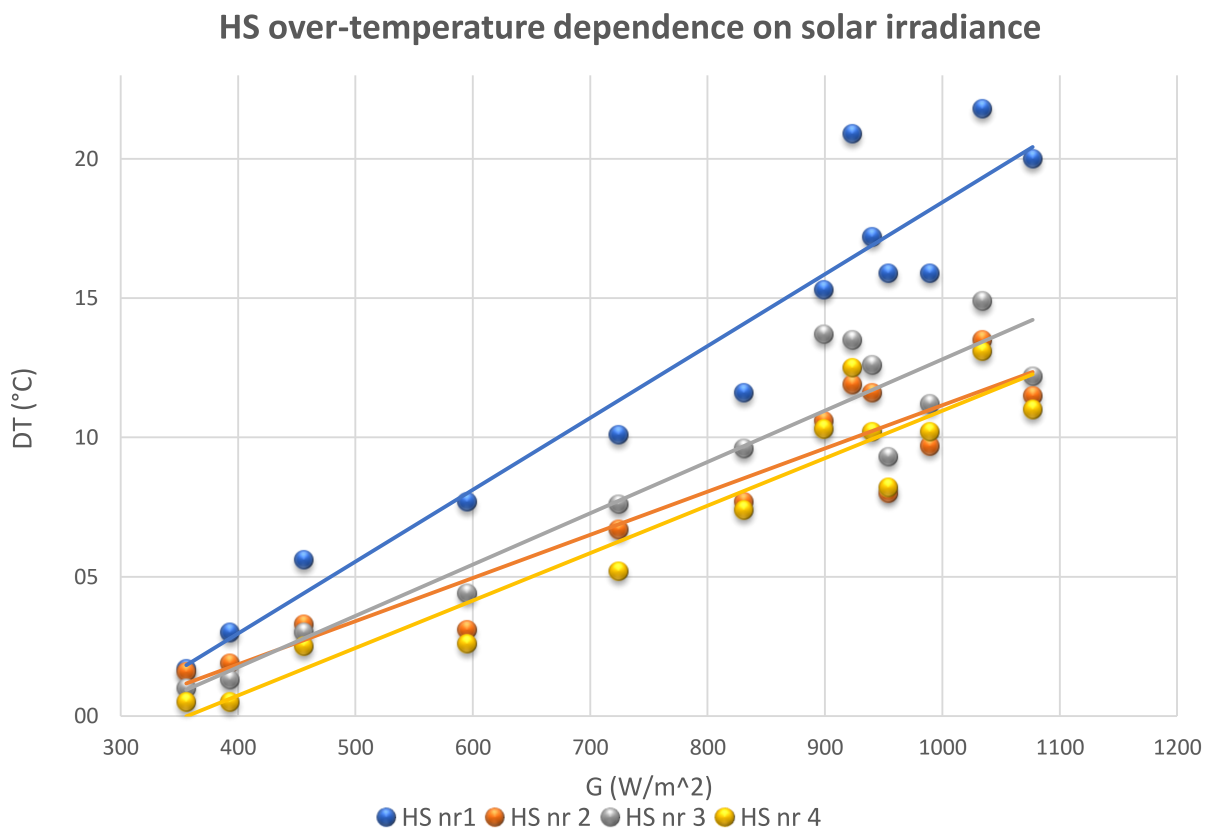

Figure 4.16 - Hot-spot temperature with different levels of solar irradiance

Through linear interpolation, it is evident how the hot-spot over-temperature almost depends linearly on the irradiance level; therefore, if the solar irradiance is too low (approximately below 600 W/m^2), hot-spot detection becomes far more difficult due to the reduced over-temperatures present in correspondence of the anomalies.

There are many other variables which can affect more or less significantly results of the analysis, and which are mainly related to the position of the thermo-camera with respect module's surface. In particular, the acquisition distance and the acquisition angle.

A set of tests were performed with different acquisition angle, considering a module without particular anomalies. The average surface's temperature, detected on a single representative point, assuming the whole module at the same temperature, has been determined for different values of acquisition angle. Results are graphed and interpolated with a second order polynomial. Measures were taken at a distance of 0.7 m from module's surface.

Angle	Time	T1
°	hh:mm	°C
0	15.20	53.1
36	15.20	52.4
55	15.20	51.2
71	15.20	44.9
77	15.20	40.5
80	15.20	35.9
82	15.20	33.9

Table 4.2 - Influence of the acquisition angle (T1 is the hot-spot temperature)

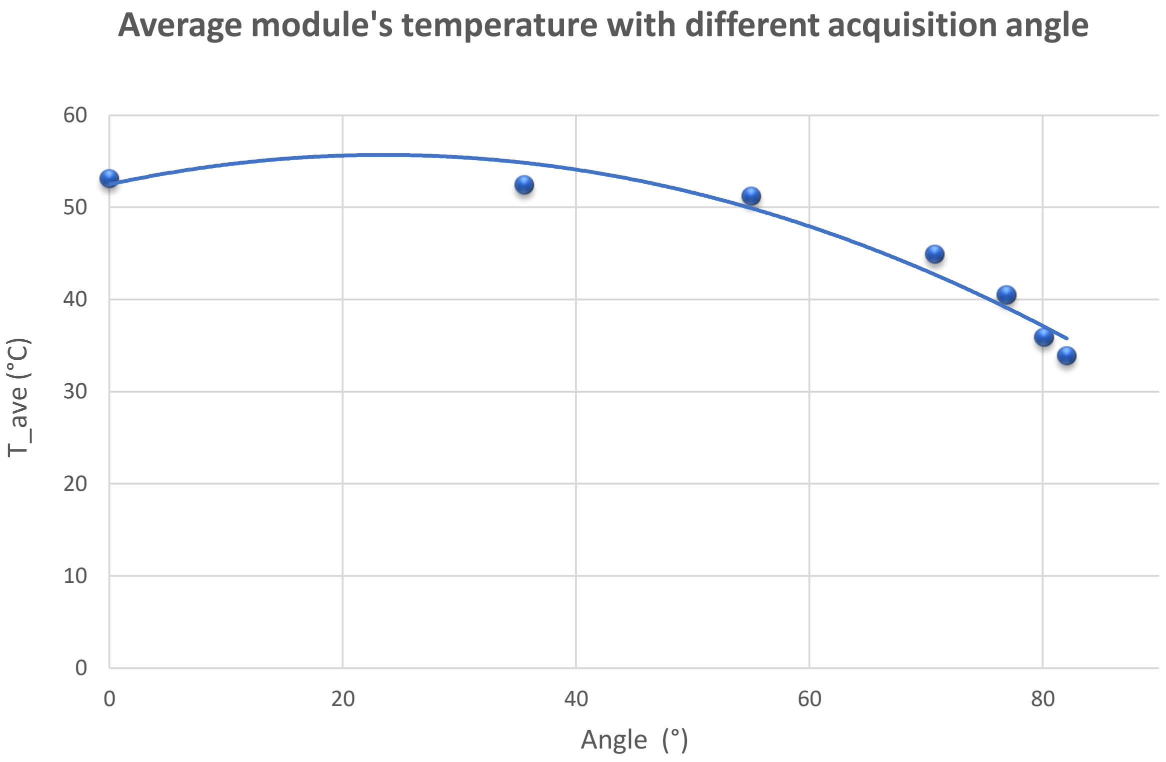

Figure 4.17 - Average module temperature obtained with thermo-graphic analysis, with different acquisition angles

The graph highlights how the acquisition angle can affect IR analysis. In general, within the range of acquisition 0-50°, the expected result is quite constant, with variations smaller than 3%. Furthermore, it is better not to adopt small angles so as to avoid possible reflections of the camera and the operator on panel's surface. An acceptable angle, used for all the following measurements, is around 30°-40°.

Integrating Entec past analysis, it has been possible to carry out the complete mapping of cell's hotspots of the case study plant, adopting the previous mentioned precautions for the thermography campaigns (Tav. III).

Results have highlighted the presence of 268 modules seriously affected by hot-spot problems, out of a total of 3920 installed modules. Despite being a relative small number, the problem is that these defective modules are widespread all over the plant, i.e. they are affecting an elevated number of strings, with at least one defective module (157 out of a total of 196 strings).

As said in ch.1.3.7., dealing with mismatch problems, the consequent “bottleneck effect” is a serious problem also in case of series of modules. In this case, it is necessary also a single defective module to negatively affect the whole string in terms of output power.

4.4. I-V curve definition

Through a professional curve tracer, the I-V and P-V ("Power Voltage") curves of some modules within the plant were traced.

The professional curve tracer allows, through the measurement of solar irradiance, ambient and cell's temperature, to trace the complete I-V curve of the generator. A solarimeter, equipped with two solar cells (p-Si and m-Si), has been placed parallel to the plane of modules; the measured solar irradiance depends on the solar cell considered for the measure (which should be set equal to the one characterizing the analysed panel), because of the different spectral response (ch.1.3.3).

A thermocouple is then connected to the back sheet of the module; results are significant only if the meter is allowed to reach thermal equilibrium with the module.

Finally, terminals exiting from the junction box are connected to the curve tracer, creating a capacitive circuit. Through the variation of the value of capacitance, which resembles the variation of a resistance, the tracer can exploit the whole I-V curve, highlighting crucial points, such as MPP current and voltage, short-circuit current, open-circuit voltage and fill factor.

The instrument is able to directly convert the ambient conditions in STC conditions, and to compare the nominal I-V curve with the real one, always at STC, according to IEC 891 standard (eq.1.12 & 1.13), adopting the appropriate temperature coefficients for current and voltage, set at the beginning of the operation, according to the type and model of panel considered.

Measures were taken considering both defective and non-defective modules; each of them is then put in comparison with the nominal (ideal curve), given from the datasheet.

4.4.1. Faultless module

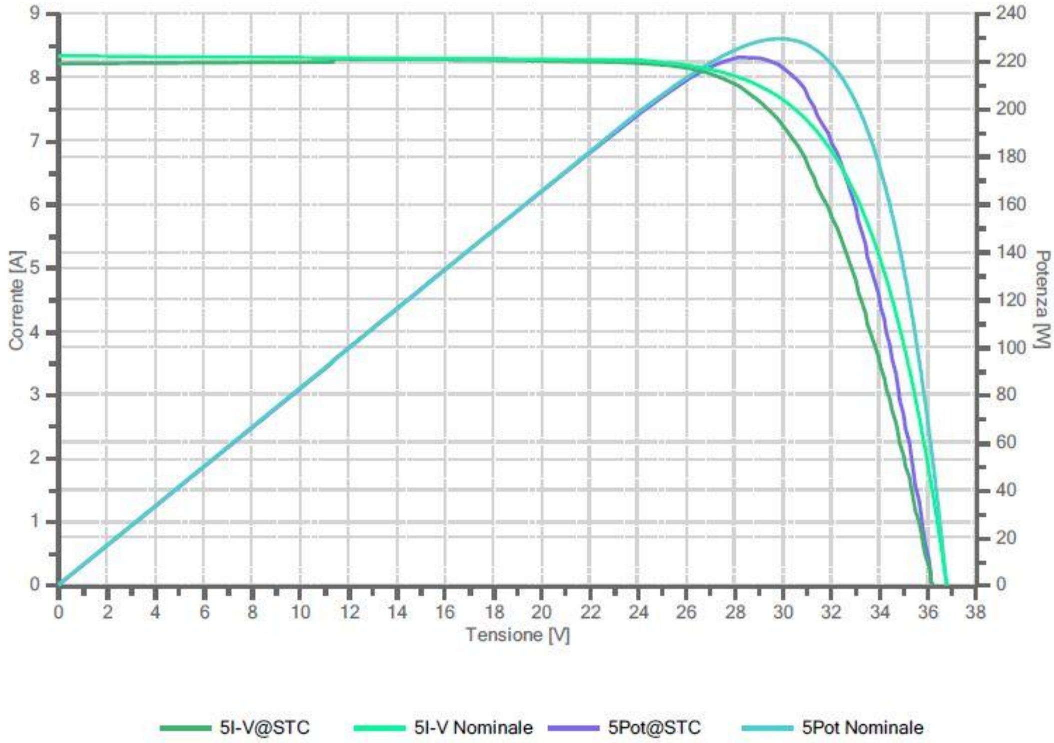

Figure 4.18 - Comparison between nominal curves and faultless module's curves (reported at STC)

	P_{max} (W)	V_{OC} (V)	V_{MPP} (V)	I_{SC} (A)	I_{MPP} (A)	G (W/m^2)	T_{AVE} (°C)
MEASURE	131.31	32.45	25.81	5.49	5.09	658	51.0
CONVERSION TO STC	221.67	36.22	28.19	8.23	7.86	1000	25.0
NOMINAL (STC)	230.00	36.80	29.90	8.34	7.68	1000	25.0

Table 4.3 - Comparison faultless - nominal values

Inevitable differences with nominal and real I-V curve are also present for faultless modules. In particular, the I-V curve is shifted towards left as well as the MPP, which presents a lower value. The percentage reduction in output power is of 3.6 %.

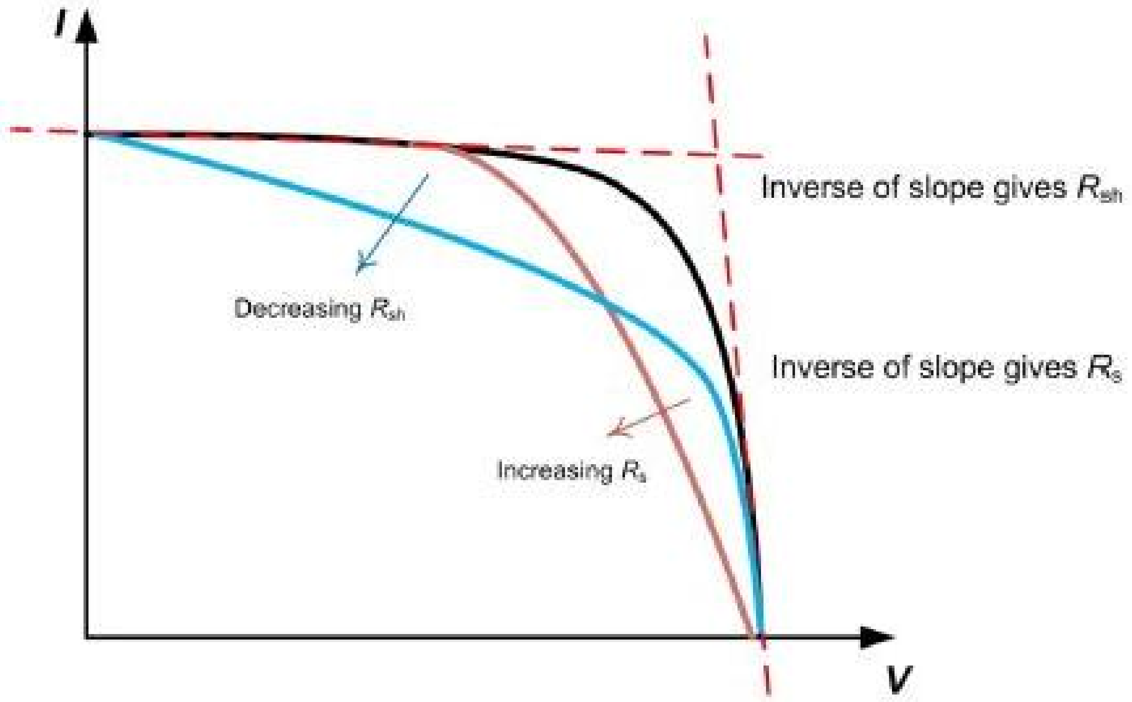

Figure 4.19 - Schematic I-V curve of an illuminated PV module and influence of series resistance R_s and shunt resistance R_{sh} on the I-V curve – IEA (Report PVPS 2014)

According to fig.4.19, the main reason for the curve shape is due to the increment in R_S (series resistance, see ch.1.3.4.), which essentially accounts for cell's mismatch and Ohmic losses.

Consequently, also the power voltage curve results reshaped and lowered according to the I-V curve modifications. Globally, the power loss is quite limited, and therefore the module can be considered, to all effects, devoid from main defects.

4.4.2. Faulty module

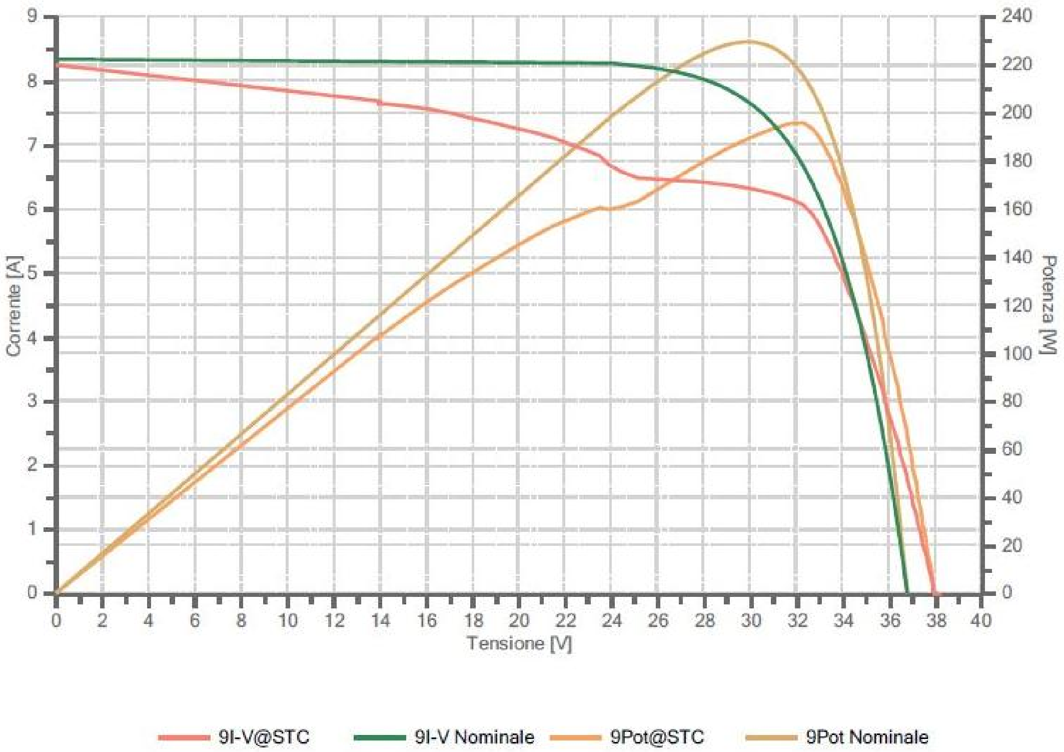

Figure 4.20 - Comparison between nominal curves and faulty module's curves (reported at STC)

	P_{max} (W)	V_{OC} (V)	V_{MPP} (V)	I_{SC} (A)	I_{MPP} (A)	G (W/m^2)	T_M (°C)
MEASURE	152.49	33.90	28.24	7.36	5.40	874	57.9
CONVERSION TO STC	195.64	38.04	32.31	7.79	6.06	1000	25.0
NOMINAL (STC)	230.00	36.80	29.90	8.34	7.68	1000	25.0

Table 4.4 - Comparison faulty - nominal values

The module considered is affected by hot-spot problems; as said before, hot-spot can be caused by a reduction of the shunt resistance of the modules, due, in turn, to several causes. This is exactly the situation depicted in fig. 4.20, in which its clearly evident the reduction of the shunt parameter, represented by the shifting towards bottom of the upper part of the curve. Modules' problems can be therefore associated to low shunt resistance (ch.4.2.1). Indeed, LDK solar modules are well-known to present process-induced defects; experts in the sector confirmed that the not perfect adhesion between EVA and cells causes localized preferential paths for current and, consequently, localized heating. In this case, power reduction due to shunt paths is of 14.9 % with respect nominal value.

4.5. Estimation of PR– OLD configuration

According to what described in ch.2.1.5., a testing procedure for the case study plant has been set in order to determine the performance ratio PR, following what established by the Italian guide CEI 82-25.

4.5.1. Final aim

Through the following verification, the goal is to test if the ratio between the energy produced in alternating current and the theoretical energy produced in alternating current, determined according to the solar irradiation incident on the plan of the modules, the nominal power of the system and the operating temperature of the modules, is at least higher than 0.80, in compliance with the measurement and calculation conditions described below and taken from the guide CEI 82-25.

4.5.2. Guideline procedure

The following is an excerpt from the guide CEI 82-25:

"The performance verification of the photovoltaic systems during plant start-up is carried out in terms of energy by evaluating the PR_e performance index (or energy performance index, corrected in temperature). The performance index PR_e highlights the overall effect of the losses on the energy generated in alternating current by the photovoltaic system, due to the incomplete exploitation of solar irradiance, the inverter conversion efficiency and the inefficiencies or failures of the components (including the decoupling between strings and any shadowing on the modules)."

$$PR_e = \frac{Eca}{Eca\_theoretical\_(Hi,Pn,Tcel)} \tag{4.5}$$

, where:

- **Eca**: energy (in kWh) produced in alternating current from the photovoltaic system, measured at the exchange counter;
- **Eca_theoretical**: energy produced in alternating current, determined according to the solar irradiation incident on the plane of the modules (Hi), the nominal power of the system (Pn) and the operating temperature of the photovoltaic cell (Tcel).

The index is related to the PR introduced in ch3.1, and equal to:

$$PR_e = \frac{PR}{(1-\gamma\cdot(T_{cell}-25°C))} \tag{4.6}$$

Therefore,

$$PR_e > PR \ if \ T_{cell} > 25\ °C$$

Essentially, PR_e does not take into account the negative effect of temperature in estimating plant performances.

For the evaluation of Eca, the following formulation is proposed:

$$Eca = Rinv \cdot Rfv \cdot \frac{Hi}{G_{STC}} \cdot Pn \tag{4.7}$$

, where:

- **Rinv**: concerns losses for DC to AC power conversion;
- **Rfv**: takes into account losses on the energy generated in DC from the photovoltaic system, due to the temperature of the modules, to the incomplete exploitation of solar irradiation and to the inefficiencies or failures of the components in DC.
  The parameter can be further decomposed in:

  $$Rfv = Rfv_1 \cdot Rfv_2 \tag{4.8}$$

  Rfv_1 takes into account all possible energy losses, with the exception of those due to variation of solar irradiation and of cell's temperature (above 40 °C); Rfv_2 takes into account the loss of energy due to the temperature of the cell, Tcel, greater than 40 ° C and can be evaluated with the following expression:

  $$\begin{cases} Rfv2 = 1 \rightarrow \ if \ Tcel < 40\ °C \\ Rfv2 = 1-(Tcel-40)\cdot\frac{|\gamma|}{100} \rightarrow if \ Tcel \geq 40\ °C \end{cases} \tag{4.9}$$

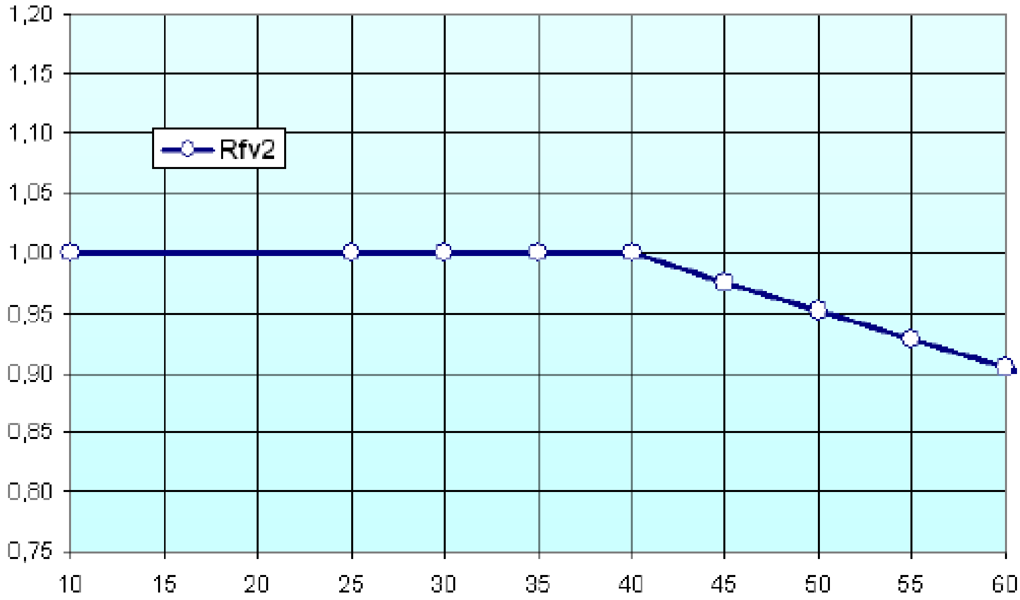

Figure 4.21 - Rfv2 piecewise behaviour (CEI 82-25)

- **Hi**: global solar irradiation [kWh/m^2] measured on the plan of the modules (integral of Gp in a given period).

The verification of the PR_e is therefore carried out by checking if the parameter satisfies or not the following constraints, in operating conditions:

$$PRe = \frac{Eca}{Eca\_theoretical\_(Hi, Pn, Tcel)} = \frac{Eca}{Rfv2 \cdot \frac{Hi}{G_{STC}} \cdot Pn} > 0.80$$

4.5.3. Instrumentation

Necessary procedures for the verification of the performance index Pr_e of the plant are the following:

- Hi integral measurement using a solarimeter;
- Measurement of Eca, reading the production counter signers;
- Tcel as average measurement over the time interval.

Conditions of validity of each measure are now considered:

- Measurements with solar irradiance greater than 200 W/m^2;
- Distributor network available;
- All the inverters of the system or of the examination section correctly in service.

The instrumentation requested to carry out the experimental test includes:

- <u>Solarimeter</u>

The solarimeter adopted for the irradiance measurement is the MacSolar solarimeter. Following, main technical characteristics:

Figure 4.22 - MacSolar solarimeter

Parameter	Units	Range	Resolution	Max.deviation	Notes
G_n (Normal in-plane irradiance)	W/m^2	0 – 1’500	1 W/m^2	<3 %	AM=1.5 T = 0-50 °C
T_a	°C	-40 - +85	0.1 °C	< 3 K	/
Power of the integrated solar cell	mW	180	/	/	/
Maximum relative humidity	%	95	/	/	/
Weight	g	170	/	/	/
Dimensions	mm	130x90x30	/	/	/
Certifications	CE/EN50081, EN50082, EN60068				
Calibration	IEC904/3				

Table 4.5- MacSolar solarimeter technical specifications

- Thermographic camera

In order to determine cell's temperature, it has been adopted a IR camera useful to rapidly check the average temperature of a solar module. The camera adopted for the module's temperature is the FLIR T4. Main specifications are now stated:

Parameter	Units	Range	Resolution	Max.deviation	Notes
Object temperature range	°C	-20 – 650	0.1 °C	±2%	/
IR resolution	Pixels	320x240	/	/	/
Minimum focus distance	m	0.4	/	/	/
Spectral range	µm	7.5-13	/	/	/
Operating temperature range	°C	-15 – 50	/	/	/
Maximum relative humidity	%	95			
Weight	kg	0.88	/	/	/
Dimensions	mm	106x201x125	/	/	/
Emissivity correction	Variable from 0.01 to 1.0, or selected from internal list of materials				
Measurements corrections	Reflected temperature, optics transmission and atmospheric transmission				
Certifications	EN/UL/CSA/PSE 60950-1, IEC 60068-2-30, IEC 60068-2-6, IEC 60529				
Calibration	IEC904/3				

Table 4.6- FLIR T4 Thermo-camera technical specifications

Figure 4.23 & 4.24: FLIR thermo camera

- <u>**P**roduction counter</u>

Useful to determine the actual energy production of the plant in the time interval considered. The value furnished by the counter should be multiplied by a constant k, since measurement is carried out through a voltage transducer; through the measurement of voltage, the counter determines consequently the energy produced. Input voltage is lowered according to the transformation ratio k of the transformer; in the specific case, the value of k is 300.

4.5.4. Experimental procedure

The test has been carried on between 12:30 PM and 14:00 PM, during a clear sky day, without evident clouds, and with 50 % of relative humidity.

The solarimeter is positioned in a plane parallel to the modules; at time t=0, solarimeter starts averaging solar irradiance.

Figure 4.25 - Solarimeter placed on the plane of solar modules

Through production counter, the reading value of the produced energy at time 0 has been recorded.

During the period of a test, whose duration has been set equal to 13 minutes, through the thermographic camera, some pictures of modules were taken, to identify roughly mean cell's temperature.

A set of 4 photos per test was made; average cell's temperature was defined. The camera has been positioned not exactly perpendicular to the modules, but within a range of 5-50 ° from the perpendicular to the plane of the modules, in order to avoid reflections of the operator and the camera itself on the frontal glass (ch.4.3.1).

A proper value of emissivity[30] of modules, suggested by literature, has been set equal to 0.87, which is in within the range of emissivity of the module's frontal glass.

During all the tests, it has been observed that, averagely, module's temperature was around 60 °C; attention has been posed to avoid hot-spot locations.

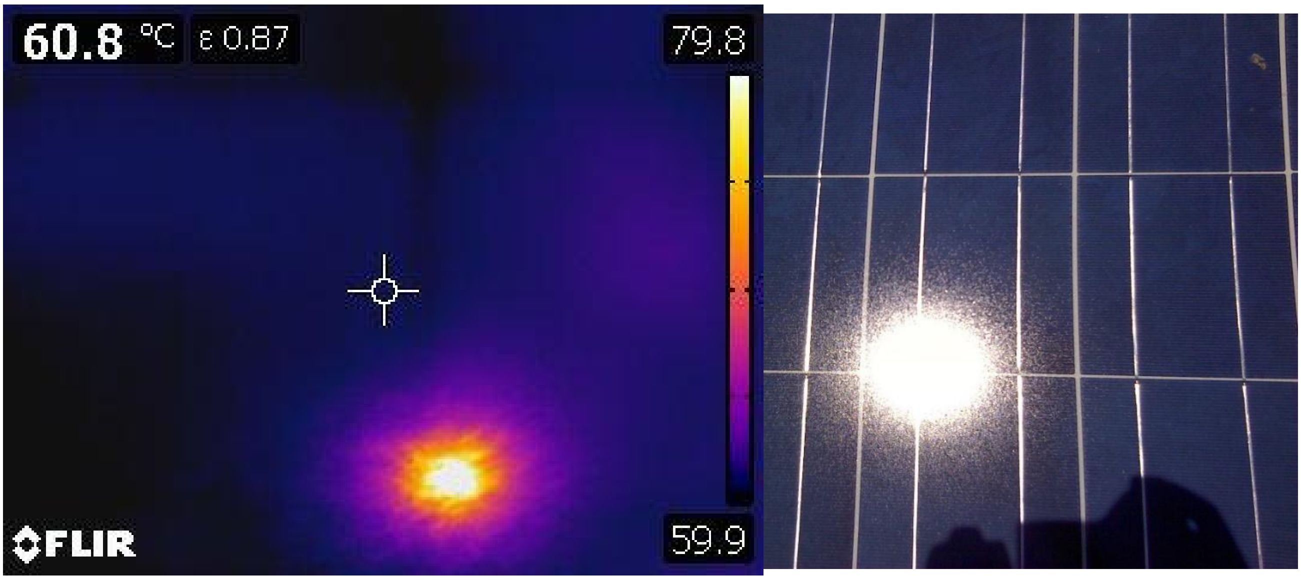

Figure 4.26 & 4.27 - IR and visible images

In the pictures reported above, on the left it is present the IR rendering of the right image. The temperature spotted in the point circled by camera objective is 60.8 °C. qualitatively, except for the location of the Sun reflex, the colorimetry of the whole module indicates that 60 °C can be reasonably considered as the average temperature.

The procedure has been repeated for four different modules, which are not affected by hot-spot problems; every set of four measures has been repeated at every time interval of 13 minutes, always on the same four modules.

[30] The emissivity of a material (usually indicated by ε) is the fraction of energy irradiated by that material with respect to the energy irradiated by a black body that is at the same temperature. It is a measure of the ability of a material to irradiate energy.

The average cell's temperature adopted for the calculation has been determined as the average of the following measures.

Test number	Average temperature (°C)
1	60.32
2	59.98
3	60.78
4	60.23

Table 4.7 - Average cell's temperature for each test

With a totality of 16 measures, a reasonable average temperature of 60 °C can be considered for the calculations. As further proof, result obtained with thermographic camera has been compared positively to the one furnished by temperature sensors (PT) installed in the plants, which show average temperatures across 60 °C.

At the end of every time interval, production counter furnishes a cumulative value of energy; through the difference with the previous step value, it is possible to determine exactly the amount of energy produced on the time interval considered.

The solarimeter furnishes the average value of solar irradiance on the same time interval; for every time interval, solarimeter is reset to 0 and calculates another mean irradiance value, starting to average values only from that time on.

The procedure has been repeated four times, for a total time of 52 minutes.

Average solar irradiance is reported below:

Test number	Average solar irradiance (W/m^2)
1	1'011
2	1'006
3	1'013
4	1'009

Table 4.8 - Average solar irradiance for each test

Solar irradiance detected on the plane of the modules is very similar to the STC value of 1'000 W/m^2, therefore the influence of the value on modules performances is quite limited, as seen in ch.1.3.5.

4.5.5. Final results

To resume, main results and data collected are presented in tabular form:

Test 1			
Eca 00	27057540	/	*Counter marker time t=0 sec*
Eca 01	27057962.00	/	*Counter marker time t=13min- 0 sec*
Eca	126.60	kWh	*Alternate current energy produced by the PV plant*
Hi	0.219	kWh/m^2	*Global solar radiation on the plane of the modules*
Tcel	60	°C	*Cell's temperature*
Rfv2	0.91	-	*Corrective coefficient as a function of cell's temperature*
G_{STC}	1000	W/m^2	*STC solar irradiance*
Pn	901.6	kWp	*PV generator nominal power*
PRe	**0.70**		*Performance ratio (corrected in temperature)*

Test 2			
Eca 00	27057962	/	*Counter marker time t=13 min- 0 sec*
Eca 01	27058382.00	/	*Counter marker time t= 26 min- 0 sec*
Eca	126.00	kWh	*Alternate current energy produced by the PV plant*
Hi	0.218	kWh/m^2	*Global solar radiation on the plane of the modules*
Tcel	60	°C	*Cell's temperature*
Rfv2	0.91	-	*Corrective coefficient as a function of cell's temperature*
G_{STC}	1000	W/m^2	*STC solar irradiance*
Pn	901.6	kWp	*PV generator nominal power*
PRe	**0.70**		*Performance ratio (corrected in temperature)*

Test 3			
Eca 00	27058382.00	/	*Counter marker time t= 26 min- 0 sec*
Eca 01	27058875.00	/	*Counter marker time t= 41min- 15 sec*
Eca	147.90	kWh	*Alternate current energy produced by the PV plant*
Hi	0.257	kWh/m^2	*Global solar radiation on the plane of the modules*
Tcel	61	°C	*Cell's temperature*
Rfv2	0.9055	-	*Corrective coefficient as a function of cell's temperature*
G_{STC}	1000	W/m^2	*STC solar irradiance*
Pn	901.6	kWp	*PV generator nominal power*
PRe	**0.70**		*Performance ratio (corrected in temperature)*

Test 4			
Eca 00	27058875.00	/	*Counter marker time t= 41min- 15 sec*
Eca 01	27059220.00	/	*Counter marker time t= 52min- 0 sec*
Eca	103.50	kWh	*Alternate current energy produced by the PV plant*
Hi	0.181	kWh/m^2	*Global solar radiation on the plane of the modules*
Tcel	60	°C	*Cell's temperature*
Rfv2	0.91	-	*Corrective coefficient as a function of cell's temperature*
G_{STC}	1000	W/m^2	*STC solar irradiance*
Pn	901.6	kWp	*PV generator nominal power*
PRe	**0.70**		*Performance ratio (corrected in temperature)*

Table 4.9 - Test 1,2,3 & 4 main data and results

The acceptability conditions of the measures are always satisfied; for test 3 and 4, the time interval considered results different due to technical problems arisen during the test.

Final result of the test, approximated to the second decimal place, is averagely equal to 0.70; clearly, a value below the acceptability range.

The global PR, considering also the depleting effect of temperature, can be averagely determined reversing eq.4.6:

$$PR = PRe \cdot (1 - \gamma \cdot \Delta T) = 0.70 \cdot \left(1 - \frac{0.45}{100} \cdot (60 - 25)\right) = 0.59$$

The value obtained is very low, considering that standard values belongs to the range 0.75-0.85; this fact is not only linked to the problematic of solar panels, but it can be partially explained by the fact that experimental measure has been performed on a specific day of the year, i.e. it does not have a particular relevance. Since yearly average cell's temperature is lower than what measured during the test, as a result, the relative temperature loss would result to be smaller, giving averagely a higher PR when ambient temperature is lower.

Parameter PR_e, instead, is independent on cell's temperature; therefore, it is more significant for quick tests useful to characterize the plant as a whole.

5. Revamping and optimization: PV plant

In the following chapter, case study plant will be subjected to revamping: it will be reconfigured, and its productivity estimated after the intervention, taking advantage of the main results obtained in chapter 3. Finally, a financial analysis of the investment will be presented.

5.1. Revamping of photovoltaic systems – Italian situation

Revamping is the process of maintenance and "restructuring" of existing photovoltaic systems to make them more efficient and to bring them back to initial or design performances. This practice, related to PV technology, is relatively a newcomer, therefore there is not enough statistic to completely document the phenomenon; however, it can be considered a technique already established in other energy sectors. For instance, in nuclear field, many plants have been subjected to revamping interventions to extend their working life, in complete safety, far beyond their expected limit, avoiding possible environmental impacts connected to the dismissal and to the installation of new plants.

In Italy, as highlighted in chapter 1, the diffusion of photovoltaic was pervasive since the end of the early 2000s, due to the very generous incentive systems. Consequently, many of the plants, designed during that period (ended with V° Conto Energia in 2013), were, in numerous cases, not optimally installed. Indeed, with the time passing, incentive rates have seen a substantial reduction, also from a month to another; this inexorable depreciation of the value of the energy produced with time has pushed designers to fasten up their processes, sometimes causing negative repercussions on the final product, in order to obtain the highest incentives.

In the last years, after the cessations of the incentives, no clear regulation was produced about revamping and repowering matter; many plant owners were afraid of acting on the plant since they could have lost the access to the incentives, dramatically compromising the convenience of the whole investment. Lately, in 2017, Italian authorities (GSE) have introduced new regulations aimed at encouraging a total revamping of a photovoltaic systems, which allow the companies to re-design PV plants that benefit from the incentive tariffs in a way so as not to lose these economic privileges. As will be seen deeply in the next section, these guidelines promoted the necessity of intervention wherever the presence of a premature degradation of the plants cause huge losses, and also where the PV plant design is clearly inadequate.

5.2. Case study

5.2.1. Goal of the work

As highlighted in chapter 3, the plant under analysis presents very moderate values of productivity and the main cause, as emphasized in chapter 4, is the very bad performance of the installed modules, seriously affected by hot-spot problem.

As a consequence, the plant's revamping is the option which will be considered and described. The aim is the complete substitution of the existent modules with newer ones. This solution has been chosen due to the absence of feasibility of the partial solution hypothesis, i.e. the substitution limited to the heavily damaged modules (about 250). Partial substitutions have been performed around the years, but with scarce results, since new defective panels arise every year, being the problem linked to constructive defects characteristics of LDK producer.

The process followed for this purpose will be explained step by step; main results and calculations will be reported.

5.2.2. Determination of the active incentives

Since the plant was built in 2011, it was subject to the support scheme "IV Conto Energia"[31]. The scheme, defined for all the plants entered into operation after the 31/05/2011, forecasted all the criterion for the incentive of electricity production by solar photovoltaic plants, and for the development of innovative technologies for the PV conversion.

The plant under analysis was subject to an incentive of 276 €/MWh, constant for a period of time of 20 years, on the electricity produced and injected into the grid.

Date of entry into service	June 2011
Support scheme	IV Conto Energia
Incentive tariff on electricity fed into the grid	276 €/MWh

Table 5.1 - Support scheme considered

[31] DM 05/05/2011 – Ministero dello sviluppo economico – "Incentivazione della produzione di energia elettrica da impianti solari fotovoltaici".

5.2.3. Compatibility of the interventions with the incentive mechanisms in force

As stated in GSE website, the plant, during the period in which incentives are provided, can be subject to maintenance activities in order to keep it in efficiency, contrasting the inevitable degradation of its components with time.

For activities which involve the variation of relevant characteristic data, such as substitution of principal components, like modules and inverters, it is necessary to send a communication directly to GSE.

In order to maintain the compatibility of the plant with the active support mechanism, GSE has recently published a document ("Impianti fotovoltaici in esercizio. Interventi di manutenzione ed ammodernamento tecnologico – Procedure ai sensi del D.M. 23 giugno 2016", February 2017) which exposes the procedures which should be followed for a maintenance intervention or technological modernization on a plant subject to "Conto Energia".

It is therefore necessary that the planned interventions "*guarantee the durableness of the objective requirements, expected by the D.M. of reference (Conti Energia), regulating over time the incentive for electricity production from solar source […], as well as of the requirements of the sector regulation and of what deliberated in D.M. 23 June 2016*".

5.2.4. Definition of the type of intervention

The intervention under analysis concerns the complete substitution of the existent set of modules with newer and more efficient ones. All the existent support structures (therefore modules tilt angle, azimuth and row distance) are maintained; also, the electrical single-line diagram is not varied.

The intervention falls into the category of significant intervention of maintenance and technological modernization "*to remedy an obvious and untimely degradation of the active components (modules), which limits the energy production […], to pursue the restoration of the expected theoretical yield*", as highlighted in GSE guidelines.

Furthermore, it is said that "*installed or substituted modules must be new or regenerated, and compliant to requirements contained in V° Conto Energia*".

5.2.5. New modules: technical features

The modules chosen for the substitution have a power of 270 W_p and are produced by the company Trina Solar; they consist of 60 polycrystalline silicon cells (156x156 mm). Following, are reported the main features from the datasheet.

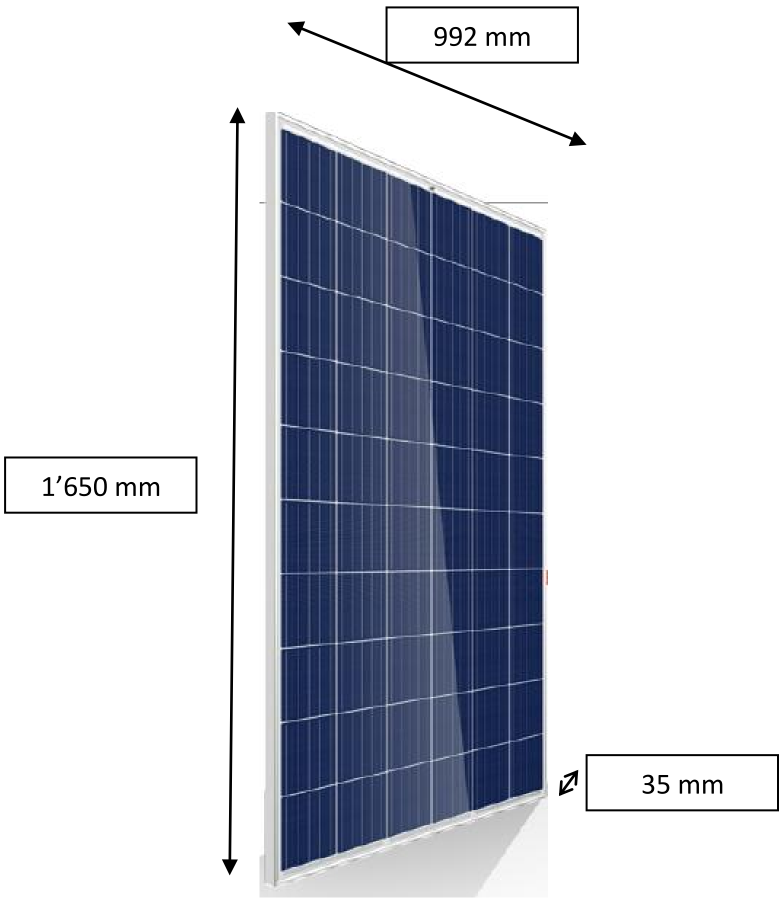

Figure 5.1 - Trina Solar 270 PD05

Brand	Trina Solar
Model	270 PD05
Dimensions	992x1’650x35 mm
Nominal power P_n (W_p)	270 W_p
Module’s efficiency	16.50 %
Weight	18.6 kg
MPP voltage (U_{mpp})	30.9 V
MPP current (I_{mpp})	8.73 A
Open Circuit Voltage (U_{oc})	37.9 V
Short Circuit Current (I_{sc})	9.22 A
Thermal coefficient of P_{mpp}	-0.41 %/°C
Thermal coefficient of I_{sc}	0.050 %/°C

Thermal coefficient of V_{oc}	-0.32 %/°C
Fill Factor FF	76.7%
Power/weight ratio	14.5 W/kg

Table 5.2 – New PV modules

In the figure below, the characteristic curve I-V of the solar cell at different solar irradiance values is reported below.

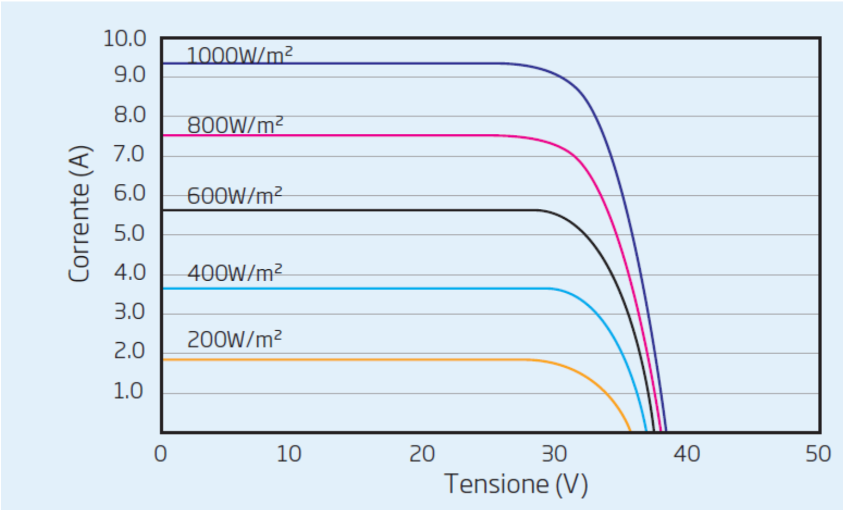

Figure 5.2 - Characteristic curves for different irradiance values

Module model	Trina Solar TSM PD-05
Module technology	Polycrystalline silicon (p-Si)
Module power (W_p)	270
Ten years warranty on product	Present
Adhesion to a consortium of recycling	Present (PV Cycle association)
ISO 9001:2008 certificate	Present
ISO 18001:2007 certificate	Present
ISO 14001 certificate	Present
Factory inspection certificate	Present
IEC 61215	Present
IEC 61730	Present
CEI UNI EN ISO/IEC 17025:2008	Present
ISO 61701	Present

Table 5.3 - Module's certifications

Each of these certificate attests different module's mandatory features and requirements according to V° Conto Energia; in detail:

- ISO 9001: Quality management - evaluates whether the Quality Management System is appropriate and effective, while forcing to identify and implement improvements;
- ISO 18001: Occupational Health and Safety Management Certification -International standard which provides a framework to identify, control and decrease the risks associated with health and safety within the workplace;
- ISO 14001: Environmental Management Systems - Requirements and guidance for use;
- IEC 61215 and IEC 61730: PV module's certification (p-Si);
- IEC 61730: General requirements for the competence of testing and calibration laboratories;
- IEC 61701: PV module certification in corrosive environments.

Through the possession of the certifications introduced before, modules result completely in agreement with GSE requests, since compliant to V° Conto Energia.

5.2.6. Plant's reconfiguration

Having certificated the compatibility of the new type of modules with GSE restrictions, the intervention under study will be briefly summarized.

- **Definition of the intervention**: complete substitution of the original PV modules.
- **Module's number before the intervention**: 3'920
- **Plant's power before the intervention**: 3'920 x 0.230 = 901.6 kW

In order to determine the number of modules which would be present after the intervention, GSE maximum power increment limit must be considered. Indeed, the power of the plant after the revamping process should not overcome the original power plus **1%** of the original power. That is:

$$P_{max} = P_{ante} \cdot (1 + 0.01) = 901.6 \cdot (1 + 0.01) = 910.6\ kW \tag{5.1}$$

Therefore, the number of new modules should be limited to:

$$N_{max} = \frac{P_{max}}{P_{module}} = \frac{910.616}{0.270} = 3'372 \tag{5.2}$$

To correctly determine a suitable number of modules, inverter's datasheet must be considered. As said in chapter 3, the inverter is composed of 6 modules, of 55 kW each, and with MPPT functionality.

The maximum number of modules per string can be analytically determined. The following data are known at STC:

- Peak power of a PV module: 270 W_p;
- Voltage at peak power: 30.9 V;
- Thermal coefficient of voltage at maximum power: -0.121 V/°C;
- MPPT range of work: 485 – 850 V;

The minimum number of series connected modules can be determined at a temperature of 70 °C[32] inverting eq. 2.11:

$$N_{sMIN} = \frac{V_{min}}{U_{MPP} - \beta \cdot (T_{max} - T_{STC})} = \frac{485}{30.9 - 0.121 \cdot (70 - 25)} = 20 \tag{5.3}$$

[32] In general, a value of 75 °C should be adopted. In this case, a lower value can be considered since the plant, being ground mounted, is well ventilated, therefore the maximum temperature attainable is lower.

The maximum number, instead, is determined at a temperature of -10°C, inverting eq. 2.10:

$$N_{sMAX} = \frac{V_{max}}{U_{MPP} - \beta \cdot (T_{min} - T_{STC})} = \frac{850}{30.9 - 0.121 \cdot (-15 - 25)} = 24 \tag{5.4}$$

In order to minimize costs associated to the intervention (i.e. changings with respect the original configuration), considering that strings in old configuration were of 20 modules in series each, also in the new configuration this parameter (N_S), since allowed by mathematical calculations, would be kept constant and equal to 20.

Considering 20 series connected modules, and knowing that each inverter's module has a power of 55 kW, the maximum number of parallel strings of 20 modules each can be determined as:

$$N_{pMAX} = \frac{P_{inv}}{N_S \cdot P_{mod}} = \frac{55000}{20 \cdot 270} = 10 \tag{5.5}$$

In order to check the validity of these calculations, ABB inverter's online configuration tool can be used. The tool gives all the possible configurations in terms of number of modules per string and number of strings per MPPT for the considered inverter's model and the considered module's model. The basic principles of calculations are the same adopted with the numerical calculations performed before; as a result, the couple (N_S;N_P) = (20;10) results verified also from the configurator.

Final adopted configuration, considering the necessity of cost's minimization and GSE upper limit, is then reported:

Module's number after the intervention	3'360
Number of modules per string	20 series connected
Number of strings in parallel per MPPT	- Inv.1: 10 - Inv.2: 9 - Inv.3: 9
Number of strings per inverter	- Inv.1: 6 x 10 = 60 - Inv.2: 6 x 9 = 54 - Inv.3: 6 x 9 = 54
Plant's power after the intervention	3'360 x 0.270 = 907.2 kW

Table 5.4 - Post intervention situation

Since the variation of power is limited to:

$$\Delta P = \frac{907.2-901.6}{901.6} \cdot 100 = 0.62\ \% \tag{5.6}$$

, the intervention can be correctly allowed by GSE, and the plant is not losing the access to the previous mentioned incentives.

The complete modules substitution implies a necessary reconfiguration of the plant, in terms of strings. Since the goal is the minimization of the global cost of intervention, the new string subdivision should minimize the variations with respect the original configuration.

The plant is subdivided in three zones, each of them connected to an inverter. Each single module of inverter has a certain number of strings in parallel, of 20 modules each in series. These strings convey into the 55 kW module after having been put in parallel through a DC switchboard.

In the old configuration, there were installed N_{old} 20 modules each; therefore, the number of strings which must be eliminated N_{elim} is:

$$N_{elim} = N_{old} - N_{new} = 196 - 168 = 28 \tag{5.7}$$

, where:

$$N_{old} = \frac{3'920}{20} = 196\ strings\ in\ the\ old\ configuration$$

$$N_{new} = \frac{3'360}{20} = 168\ strings\ in\ the\ new\ configuration$$

The 28 strings have been eliminated starting from the original ones in the OLD configuration, i.e. the original string subdivision has been maintained constant and the necessary number of strings has been removed starting from that; modifications to the electrical scheme are therefore null except for power related to each inverter, with slightly changes due to the module's power variation.

The global post operam layout is reported, with eliminated modules highlighted in red, in Tav. II.

The criterion adopted for the project of the new configuration is the minimization of costs, which coincides with the minimization of changings with respect the initial configuration.

Eliminated strings are primarily the ones which, in the original layout, were not straight, i.e. which presents a "C" (double) structure, with modules both in the upper and lower part of the structure;

this is because these strings, are the ones which suffer the most eventual reciprocal shading from adjacent rows (each row has two modules in vertical; if the lower part is subject to shading, the whole string would be negatively affected).

The remaining number of eliminated strings, with straight structure, are chosen from the ones which are located in the lower part of the structure, for the same reason of the major probability of shading.

All considered, the 28 eliminated strings were originally located at the ends of the rows. This fact permits to maintain free a certain portion of the structures on the same side, not excluding the possibility of refilling these portions of the structure with other modules in next future, going to make up a new plant.

5.3. Estimation of plant's productivity – NEW configuration

In chapter 3, preliminary estimations of plant's productivity and expected yearly final yield increase after the intervention have been furnished.

Determined the new configuration (Tav.II), it is now possible to apply main results obtained in chapter 3 to estimate the new configuration's yearly productivity.

5.3.1. Comparison with real plants of the same area

With this estimation, it has been obtained a 10% (k_1) rise in final yield with respect the old configuration.

Consequently, the new expected yearly final yield is given by:

$$P_{new}\left[\frac{kWh}{kW_p}\right] = P_{old} \cdot (1 + k_1) = 1'308 \cdot (1 + 0.1) = \mathbf{1'438.8}\,\frac{\boldsymbol{kWh}}{\boldsymbol{kW_p}} \tag{5.8}$$

5.3.2. Computational simulation

Having defined the structure of the new plant, it is then possible to simulate the new configuration on PV*SOL and estimate the yearly final yield.

The simulation gives the following result:

$$P_{new\_simulated}\left[\frac{kWh}{kW_p}\right] = 1'360.22\,\frac{kWh}{kW_p}$$

It is then necessary to apply, to the found result, the correction coefficient obtained by modelling several plants and comparing results with real data. This coefficient, determined in ch.3.3.2, results equal to 8.1 % (k_2)

Finally, the final yield obtained through the simulation is:

$$P'_{new} = P_{new_{simulated}} \cdot (1 + k_2) = 1'360.22 \cdot (1 + 0.081) = \mathbf{1'470.40}\,\frac{\boldsymbol{kWh}}{\boldsymbol{kW_p}} \tag{5.9}$$

5.3.3. Literature formulas

Adopting the same meteorological data of chapter 3, it is then possible to determine the yearly final yield of the plant in the new configuration, adopting the following formula (eq.3.4):

$$P_{AC} = P_N \cdot \frac{G}{1000} \cdot (1 + \gamma \cdot \Delta T) \cdot \eta_{PCU} \cdot 0.92$$

The coefficients present are:

	Plant 1 (NEW)
Power coefficient (%/°C)	*-0.41*
PCU efficiency	*0.98*
Nominal power P_N (kW)	*907.2*

Table 5.5 - Adopted coefficients

The yearly final yield determined in this case results is equal to **1'517 kWh/kW$_p$**. Not surprisingly, the value obtained is the highest, as already determined in ch.3.3.3.

Yearly final yield of the plant after revamping will be cautiously considered equal to the lowest estimation, i.e. 1'439 kWh/kW$_p$. This value will be useful for the successive financial analysis.

Extending the analysis on a period of 15 years, it is possible to represent the productivity trend of the plants in the two cases. The decay rate, i.e. the annual percentage decrease in productivity of the two plants, as determined in ch.3.3.1, will be assumed as 0.8%/year. In the case of the plant in new configuration, as suggested by PV modules datasheet, only for the first year, it will be assumed a decay rate of 2.5%/year.

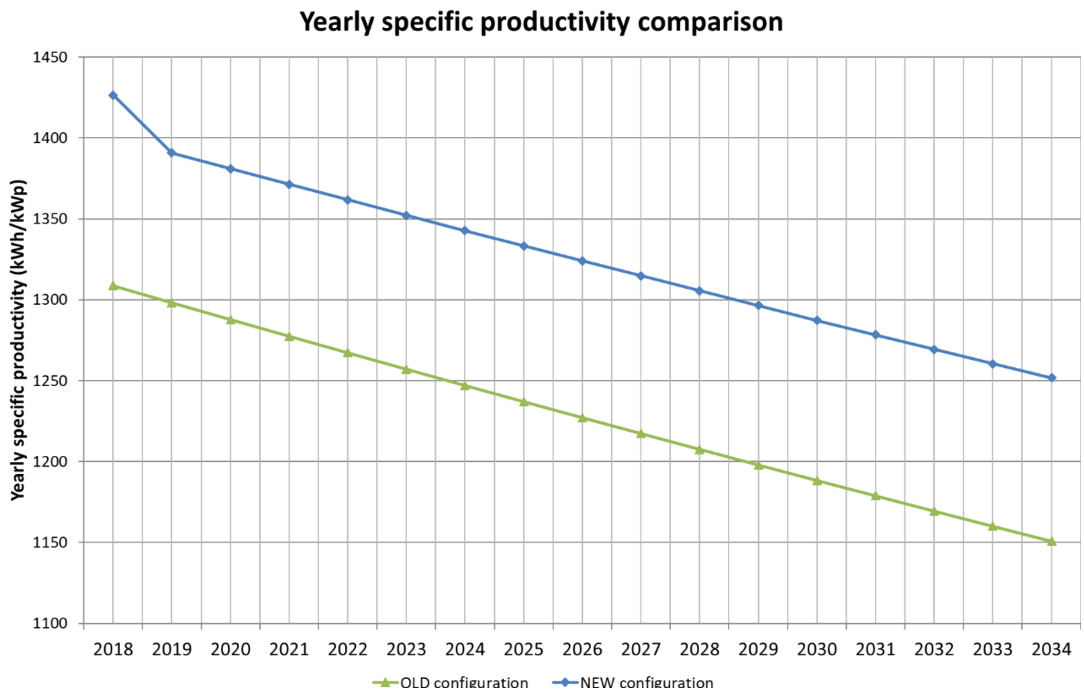

Figure 5.3 - Comparison of final yield (plant 1 OLD vs. NEW) with time

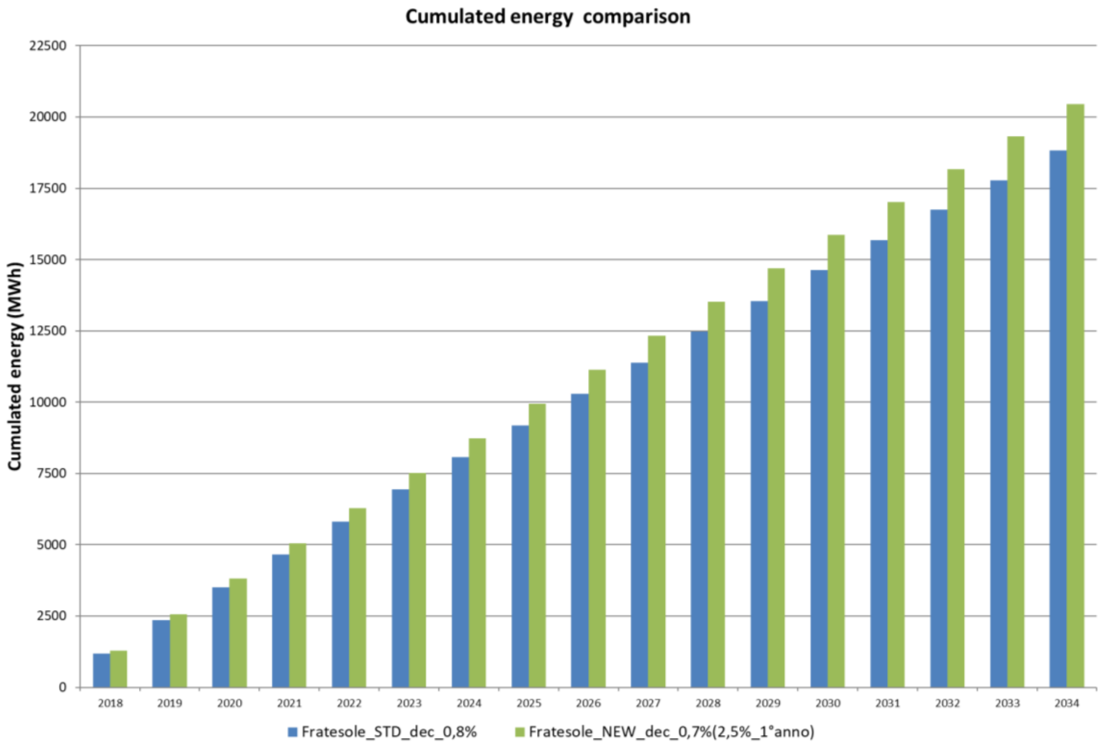

Figure 5.4 Cumulated energy (Plant 1 OLD vs. NEW)

At the end of the period considered, the actual gain in energy exceeds 2 GWh; this is a crucial parameter in order to evaluate the convenience or not of the investment sustained, being directly linked to the economical profits. In the next paragraph, this aspect will be further analysed.

5.4. Economic analysis

The aim of this part is the economic evaluation of the investment discussed before. The goal is the determination of the cumulated cash flow of the investment, and its comparison with the same parameter considering not to apply the revamping intervention to the PV plant.

5.4.1. Input parameters

	Plant 1 – OLD configuration	Plant 1 – NEW configuration
Installed power (kW)	901.6	907.2
Yearly final yield (kWh/kW$_p$)	1’309	1’439
Annual production decay rate (%/y)	0.8	0.8
Basic energy value (€/MWh)	50	
Energy value’s growth (%/y)	0	
Time period for analysis (y)	15	

Table 5.6 - Input parameters (Plant 1 OLD vs. NEW)

The two plants present a different installed power and yearly final yield, as estimated before. The decay rate of production has been assumed equal and constant for both.

The basic energy value regards the value of electrical energy sold to the grid, without incentives. It can be estimated for the present day by analysing the trend reported in ch.2.1.2. As an assumption, the growth rate of electrical energy value with time will be set to 0; since the main incomes derives from the incentives, the value of the growth rate of basic energy price results not particularly influent, therefore it can be neglected.

The time period considered for the analysis is 15 years, assuming to carry out the intervention in the calendar year 2018, starting from June (the period considered is 06/2018-06/2033).

5.4.2. Revenues and incentives

The basic value of the incentive on the electrical energy produced is 276 €/MWh. According to the Italian law *lg. 116 11/08/2014 ("Legge Spalma-incentivi*"), changes were introduced regarding the methods for providing incentive tariffs. In particular, for PV plants under "Conto Energia" scheme, with nominal power greater than 200 kW, a remodulation of incentive rates has been introduced.

Depending on the choice of the plant's owner, three possible solutions for remodulation were proposed. The scheme adopted for the case study plant concerns the maintenance of the twenty-year payment period, against a reduction in the incentive for a first period, and a corresponding increase in the same for a second period, according to percentages defined by the Italian Ministry of Economic Development with the D.M. 17/10/14.

If $\mathbf{I_{OLD}}$ is the original value of the incentive, $\mathbf{I_{NEW}}$ can be determined, for every year starting from 2015, as:

$$I_{NEW} = I_{OLD} \cdot (1 - X_i) \qquad (5.10)$$

, where $\mathbf{X_n}$ is the remodulation percentage coefficient, which varies for every year **n** of the residual incentive period according to the following formula:

$$X_n = \begin{cases} -X_o,\ 2015 < n \leq 2019 \\ -X_o + K \cdot (n - 2019),\ 2020 \leq n \leq (2015 + a - 6) \\ +X_o,\ (2015 + a - 5) \leq n \leq (2015 + a - 1) \\ 0,\ n = 2015 + a \end{cases} \qquad (5.11)$$

$\mathbf{X_o}$, in turn, can be determined adopting the following equation:

$$X_o = F_a + [F_{a+1} - F_a] \cdot \frac{m}{12} \qquad (5.12)$$

a and **m** are, respectively, the remaining years and months of the incentive period, calculated from December 31st, 2014.

F_a is calculated as a function of parameter **a** according to the following table:

a	F_a
11	-31.39 %
12	-26.43 %
13	-22.59 %
14	-19.54 %
15	-17.08 %
16	-15.05 %
17	-13.37 %
18	-11.95 %
19	-10.74 %
20	-9.70 %

Table 5.7 - Fa coefficient with varying a (number of years of incentive left)

Coefficient **K** can be determined as:

$$K = \frac{2 \cdot Xo}{a-9} \tag{5.13}$$

The plant under analysis started to produce officially in June of 2011. Therefore, the analysis starts in the 6.5 year of life of the plant (2018). It is important to stress that also the revamped configuration will see the same methodology of support, since authoritatively the plant remains the same.

The remaining years **a** of incentive, from 31/12/14, are 16 (till 2031), while remaining months are 197 (till May 2031).

Coefficients **X_o** and **K** can be found as:

$$X_o = -15.05 + [-13.37 + 15.05] \cdot \frac{197}{12} = 14.21\ \% \tag{5.14}$$

$$K = \frac{2 \cdot 14.21}{16-9} = 4.06 \tag{5.15}$$

Final percentages reductions and increment can be briefly resumed:

Year	# Year	% variation on base value	Incentive (€/MWh)
2018	6.5	-14.21	0.237
2019	7.5	-14.21	0.237
2020	8.5	-10.15	0.248
2021	9.5	-6.09	0.259
2022	10.5	-2.03	0.270
2023	11.5	2.03	0.282
2024	12.5	6.09	0.293
2025	13.5	10.15	0.304
2026	14.5	14.21	0.315
2027	15.5	14.21	0.315
2028	16.5	14.21	0.315
2029	17.5	14.21	0.315
2030	18.5	14.21	0.315
2031	19.5	/[33]	0.000

Table 5.8 - Incentive's value variation, according to "Spalma Incentivi"

The reduction coefficient applied to the base value of the incentive will be then multiplied for the yearly energy produced for the year to which it is referred.

Revenues, both for the OLD and NEW configurations, can be determined through the multiplication of the value of the incentive plus the basic energy value times the yearly energy production. Numerically:

$$Rev = E_{year} \cdot (I_{new} + C_e) \quad (5.16)$$

[33] For the year 2031, it is assumed that, starting from January, the incentive decays.

5.4.3. Costs

Financial analysis must take into account both investment costs, which have to be sustained only the first year of life of the plant, and O&M ("Operation and Maintenance") costs, which are yearly costs, incurring every year for all the years of life of the plant. Disposal costs are not considered in the following analysis.

Cost's weight is very different for the plant in the two configurations: if, in the OLD configuration, the main voice are periodical costs which has to be sustained every year, and there are no investment costs (since the analysis starts with the plant already built), for the NEW configuration, initial investment is the major contributor, while periodical costs can be considered less relevant with respect the other configuration, since the plant is assumed to be less maintenance addicted.

An estimation of costs, in the two cases, can now be made, exploiting also Entec experience in the field.

- OLD configuration:

$$INV_{OLD} = 0 \text{ €}$$

Only costs present are periodical costs. Part of these costs are linked to the problematic behavior of the plant and the need of partial substitution of very defective modules.

In detail, the following yearly cost items can be distinguished:

COST TYPE	UNIT COST	UNIT QUANTITY	€
Inverter's maintenance	3 €/kW	901.6 kW	2'705
Technical and administrative management	/	/	1'500
Extra-ordinary maintenance - unexpected	/	/	2'500
Insurance against vandalism, theft, weathering	/	/	1'500
IMU (on terrain)	/	/	3'000

Yearly module substitution[34]	600 €/kW	23 kW	13’800
TOTAL		**25’005**	

Table 5.9 - Costs (OLD configuration)

$$O\&M_{OLD} = 25'005 \frac{€}{y}$$

- <u>NEW configuration</u>:

An estimation on the investment cost will now be proposed:

COST TYPE	UNIT COST	UNIT QUANTITY	€
Preliminary design	/	/	1’500
Executive project	/	/	1’500
Module cost	325 €/kW	907.2 kW	294’800
Module substitution[35]	3 €/mod	3’640	10’900
Mechanical equipment for the operation	/	/	4’800
Cost of new modules disposal contract	0.06 €/kg	63’054 kg	3’800
Surveillance	/	/	7’500
Other	/	/	32’480
Unexpected	2%	/	6’500
TOTAL		**363’780**	

Table 5.10 - Investment costs (NEW configuration)

To this value, the amount of gains deriving from the sale of old modules must be subtracted:

$$Rev'_{NEW} = C_{sold} \cdot N_{sold} \tag{5.17}$$

[34] 100 per year -average value sustained all over the years of work of the plant, from 2011 to 2016.
[35] Physical substitution, extracting old modules from structures and mounting the new ones. Since this cost depends on the number of modules both mounted (3920) and to be mounted (3360), it has been assumed an average value between the two.

Due to the high inefficiency of the panels, the selling price is inevitably very low:

$$C_{sold} = 11 \frac{€}{mod}$$

Consequently, the revenues deriving from the operation are determined as:

$$Rev'_{NEW} = 11 \cdot 3'920 = 43'120 \text{ €}$$

Therefore, investment costs are definitely:

$$Inv_{NEW} = 363'780 - 43'120 = 320'660 \text{ €}$$

For what concerns O&M costs, those are the same as in the OLD configuration, except for the yearly module substitution cost, which is set to 0.

$$O\&M_{NEW} = 25'005 - 13'800 = 11'205 \frac{€}{y}$$

5.4.4. Economic evaluation

The evaluation of the cumulated cash flow for the two configurations would allow to underline the eventual economic benefit of the investment.

In detail:

$$Cash_{CUM,i} = -Inv - n \cdot O\&M + n \cdot Rev\ [€] \quad (5.18)$$

, where **n** is the year number (n=0 for 2018).

Plotting results for the two configurations:

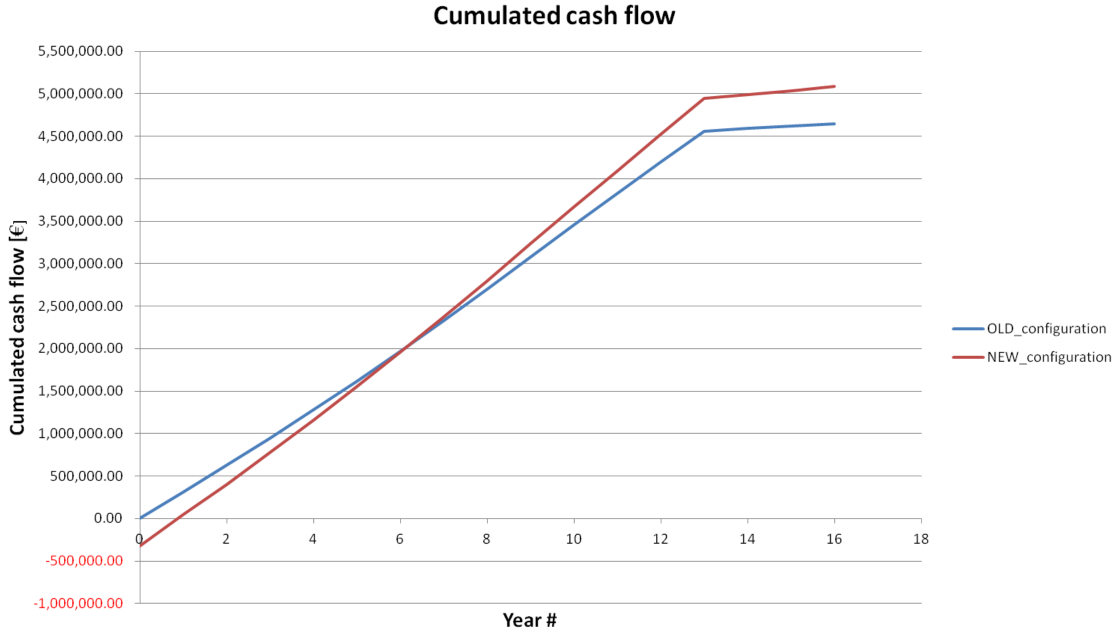

Figure 5.5 - Cumulated cash flow (Plant 1 OLD vs. NEW)

Differently from other kinds of investments, in which the goal is the minimization of the pay-back time (ch.2.1.2), the aim here is focused on the time in which the new investment starts to be advantageous.

Graphically, that value can be seen as the intersection of the two curves of the cumulated cash flows; it means that the new configuration, from that time on, has become more advantageous than the old one, i.e. it has started to produce capital.

In order to estimate more clearly the intersection, the two curves have been linearly approximated as straight lines. The two equations are the following:

$$OLD: \quad 306'570x + 139'094, where\ x = \#\ years$$

$$NEW: \quad 355'793x - 166'706, where\ x = \#\ years$$

Solving the system of two equations for x equal to the number of years corresponding to the same cumulated cash flow for the two layouts, final result is:

$$Eq_{CF}\ [y] = \frac{139'094 + 166'706}{355'793 - 306'570} = 6.20\ y$$

After almost 6 years, the NEW configuration starts to become more fruitful than the OLD.

At the end of the period considered, the cumulated cash flow for the two configurations is:

Plant configuration	**Cumulated cash flow [M€]**
OLD	4.64
NEW	5.08

Table 5.11 – Cumulated cash flow: final results at 2033

The NEW configuration is expected to produce an increase in capital of the 9.45%, which means almost 440'000 €.

A deeper analysis can be performed adopting the NPV ("Net Present Value") concept, which includes also interest rate.

The formulation adopted is the following:

$$NPV = -Inv + \frac{(1+i')^n - 1}{i'(1+i')^n} \cdot Rev - \frac{(1+i)^n - 1}{i(1+i)^n} * O\&M \qquad (5.19)$$

, where **i** is the interest rate, which can be assumed equal to 6%, **e** is the energy's value growth, which has been assumed equal to 0%/year; therefore, coefficient **i'**, which can be calculated as:

$$i' = \frac{i-e}{i+e} = i \qquad (5.20)$$

, results coincident with the interest rate i.

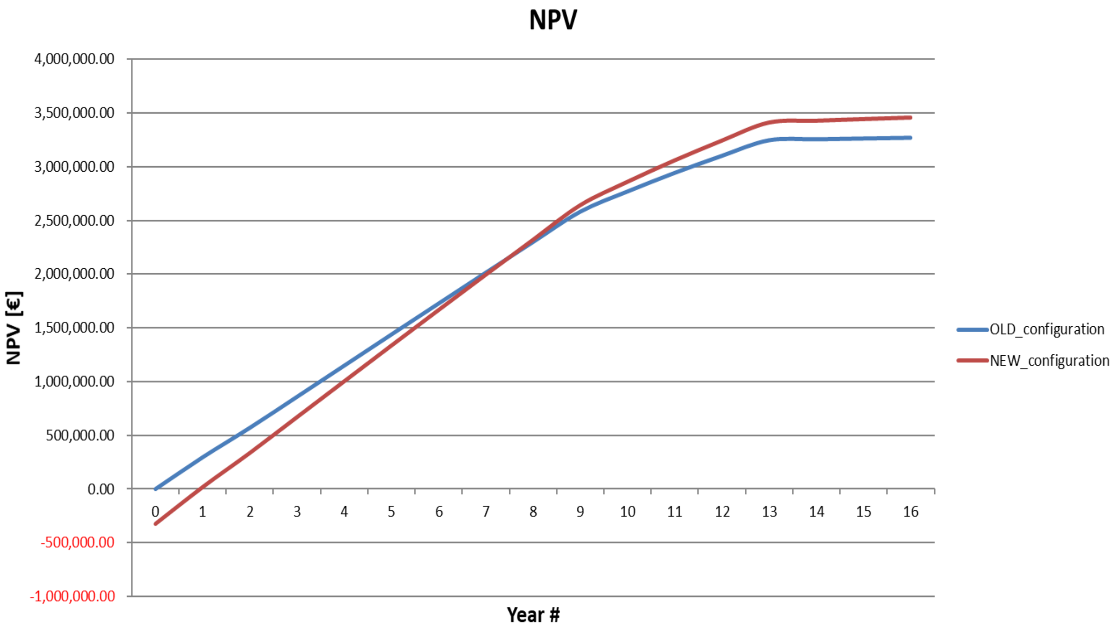

Figure 5.6 - Cumulated cash flow (Plant 1 OLD vs. NEW)

Considering also inflation, final results can be considered more affordable. The behavior of the two curves is almost the same compared to the previous case.

As in the previous case, the intersection between the two lines gives the time in which the new plant starts to be fruitful compared to the previous configuration. Numerically:

$$Eq_{NPV}[y] = 7.20\ y$$

At the end of the period considered, the Net Present Value for the two configurations is:

Plant configuration	**NPV [M€]**
OLD	3.27
NEW	3.46

Table 5.12 – Net Present Value (NPV): final results at 2033

The NEW configuration is expected to produce an increase in NPV of the 6,00%, which means almost 200’000 €.

5.4.5. Comments

Economic analysis has shown how to determine the pay-back time of such an investment; differently from new plant's installations, for reconfiguration's cases the time of return should be determined by the comparison between ante and post operam solutions.

Considering a return time of 7 years, and an average plant lifetime of 20 years, which is mainly determined by modules lifetime, the investment results convenient because it permits to extend the life of the plant and to avoid dramatic productivity problems, exploiting at best the remaining incentive time. Indeed, due to the variation of the incentive rates, the last years of the analyzed period are the ones with the highest rates, therefore the convenience of the investment is far more evident.

5.5. A possible energy optimization

The goal of the final part of this chapter is the optimization of the PV plant previously studied. Optimization concept will be presented and then applied to the case study plant.

Energy Optimization

Optimization is the action of making the best or the most effective use of a situation or resource. In the case of energy systems, such as PV plants, the aim of the optimization could be considered the maximization of the energy productivity.

Usually, the typical problem to solve in the case of industrial energy systems is a constrained optimization problem:

$$\min\ f(x)$$

$$x_i^{LI} \le x_i \le x_i^{LS} \quad i = 1, \dots, . N \tag{5.21}$$

where:

- f is the objective function;
- x are the N decision variables, which values are constrained between minimum and maximum values.

The objective function can be of various types:

- <u>Thermodynamic:</u> minimum exergy destruction and losses, minimum primary energy consumption, maximum efficiency;
- <u>Economical</u>: minimum cost of products, minimum investment cost, maximum net revenue;
- <u>Environmental</u>: minimum environmental impact, minimum life cycle impact;
- <u>Technical</u>: minimum weight, maximum life, maximum reliability.

Three optimization levels can be considered in energy systems:

1) <u>Optimal synthesis</u>: search for the optimal system configuration (i.e. components to be installed and how they are linked together);

2) <u>Optimal design</u>: search for the optimal values of design parameters of a system or component, which configuration is defined;

3) Optimal operation: search for the optimal operating of a system (or component), which configuration and design are already defined. This typically involves the analysis of off-design conditions.

There are several classes of optimization methods:

- Graphical methods: the objective function is calculated for various values of the decision variable. The minimum (or maximum) is obtained from graphical representation;

- Direct methods: the objective function is iteratively calculated for various values of the decision variable;

- Indirect methods: the first derivative of the objective function is calculated and then the points where the derivative is zero are obtained;

For the optimization procedure linked to the case study plant:

- **Objective function**: yearly final yield (kWh/kW_p);

- **Design variables**: Tilt angle (°) and Azimuth angle (°);

- **Optimization level**: optimal design (plant is already defined and cannot shift these parameters during operation);

- **Optimization method**: graphical method. The optimization will involve two design variables together. A range of both variables will be exploited, the objective function evaluated for each couple of variables. Results will be given in a matrix form.

The optimization process, in this case, coincides with a maximization process; therefore, the aim of the analysis will be the maximization of the design energy productivity through the optimal tilt and azimuth angles.

The optimization process will be carried on using PV*SOL program, whose modeling procedure was explained in ch.3.3.2.

The plant modeled is the new version of the case study plant, after the revamping process. The general layout of the plant is reported in Tav.II and described in ch.5.3.

Not to complicate the analysis, row distance will be fixed to the actual value of 6.5 m; since the power of the plant should remain almost constant, and the area occupied does not vary, it is pointless trying to vary also the row distance. Indeed:

- An increase in row distance, with equal area, will diminish sensibly the installable power, although it can reduce reciprocal shadings and improve energy productivity;

- A decrease in row distance, with equal area, will increase sensibly the installable power, increasing reciprocal shading and reducing productivity.

Therefore, a row distance variation will change installable power beyond permitted limits.

In general, with fixed area, the optimal row distance has to be a trade-off between power installed and final yield, i.e. the one which minimizes reciprocal shading and maximizes energy productivity and installed power. For the case study plant, the choice was performed according to this criterion. A parameter useful to check the correct row distance is the profile angle (ch.2.2.4). According to Entec past experience, the optimal profile angle is included in the range 10-20°; the optimal row distance can be found consequently.

As a further simplification, it has been supposed that changing in tilt and azimuth have a negligible effect on mutual spacing of rows, therefore the same structure of the plant can be proposed always in the same occupational area.

Main results, in terms of yearly final yield (kWh/kW$_p$) are reported for a series of azimuth and tilt angles.

	Azimuth (°)	175 °	180 °	185 °
Tilt (°)				
10°		1’278.97	1’279.61	1’281.51
15°		1’311.05	1’311.05	1’313.41
20°		1’334.29	1’332.50	1’336.35
25°		1’351.82	1’348.75	1’348.98
30°		1’360.07	**1’360.22**	1’359.82
35°		1’358.19	1’353.47	1’354.75
40°		1’343.96	1’342.28	1’341.89
45°		1’320.77	1’319.16	1’308.49

Table 5.13 - Yearly final yield (kWh/kW$_p$) for different values of tilt and azimuth (row distance = 6.5 m)

The optimal result is in correspondence with adopted values of azimuth and tilt; therefore, the original project was correctly performed in this sense, and there is no point in varying these parameters in case of revamping.

Optimal design parameters are 30° tilt angle and South orientation (180° Azimuth), i.e. equal to the ones suggested by literature in case of single rows of modules, without mutual shading. The fact can be explained easily considering that a row distance of 6.5 m guarantees a very low profile angle (13.88 °, fig.2.17); therefore, the effect of mutual shading is very limited.

The effect of mutual shading in the optimal configuration can be visualized thanks to PV*SOL program, able to show the annual direct irradiance reduction, on the basis of the seasonal shade frequency, on the areas of the coverable objects. For every grid point on the current PV area, irradiance reduction is calculated as an annual average and it can then be graphically evaluated.

An extract from the graphical result given by the program is reported:

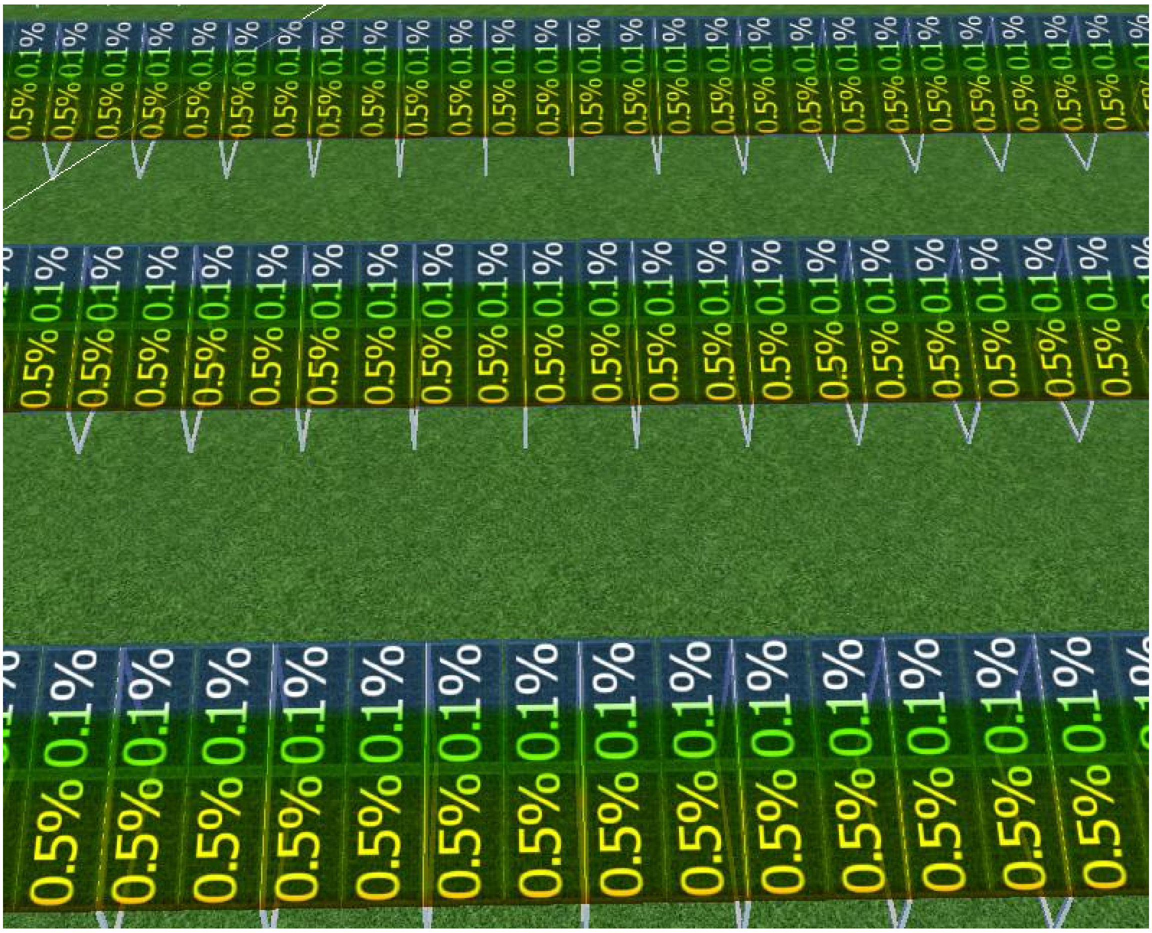

Figure 5.7 - Shade frequency (PV*SOL model) on module's rows (case study plant)

The shade frequency analysis confirms what highlighted before; due to significant row distance, mutual shading effect is almost negligible, since causes, in the inferior and more problematic part of the row, a maximum direct irradiance reduction of only 0.5% per year.

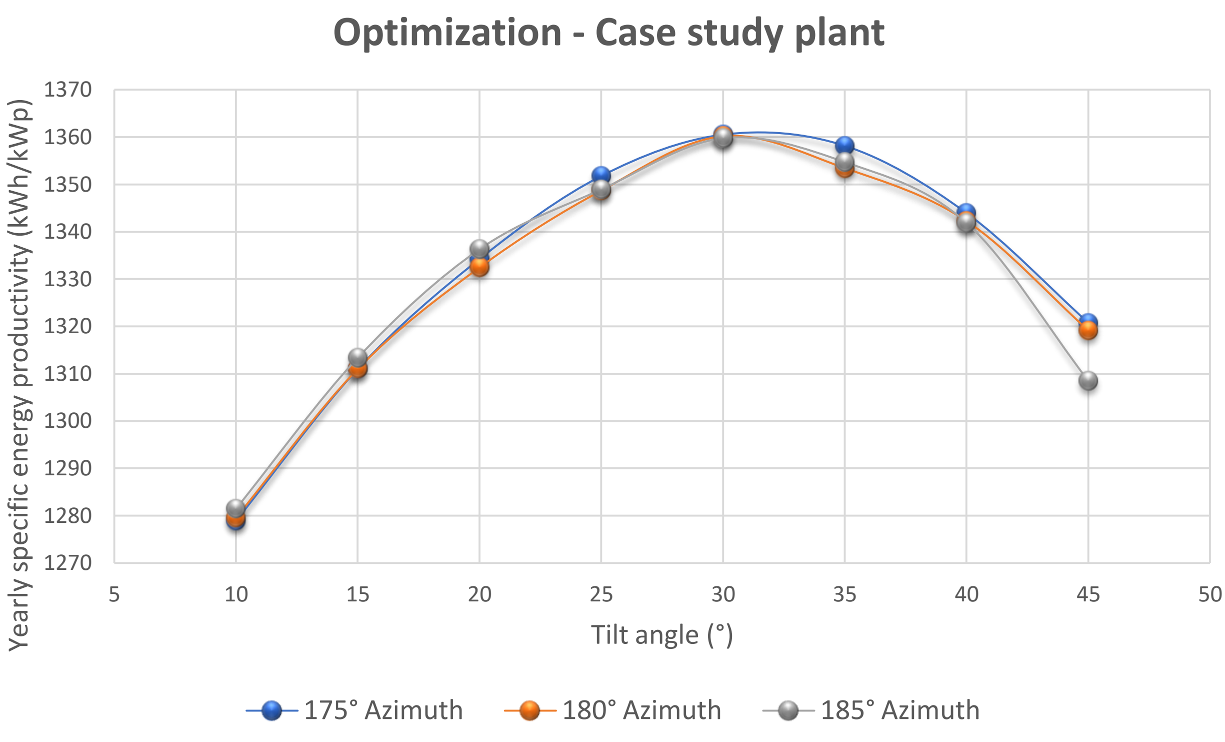

Figure 5.8 - Graphical optimization with respect tilt and azimuth angles

Near the optimal values, variations are very small. For a 5° variation of azimuth angle, considering the optimal tilt, final yield variation is less than 0.1 %.

Reducing tilt below optimal value, productivity reduces because of reduction of in-plane irradiance getting on modules; the consequent decrease in mutual shading is not sufficient to compensate this decrement. The limit case is with 0° tilt modules, i.e. horizontal modules. This solution is suitable when occupied space is low and installed power should be relatively high compared to the surface at disposal; tilt null, indeed, allows to reduce down to 0 m the acceptable row distance, permitting to install far many modules (no mutual shading present).

On the contrary, increasing tilt above optimal value, productivity decreases because of reduction of in-plane irradiance and increase in mutual shading. Higher tilt angles are generally suitable in cases of necessity of maximization of winter productivity, when sun is lower above the horizon.

Varying azimuth both in increase or decrease means respectively exploit more evening or morning radiation. The choice can be performed in case of obstacles' presence, limiting radiation in a specific part of the day.

Conclusions

Ending dependence on solid fuels will not be an easy process. The level of development achieved by our civilization is such thanks to the intensive exploitation of fossil resources that took place over the last two centuries and which will continue for many decades. The exit strategy cannot be drastic and rigid: small steps must be taken both towards renewable sources and energy saving. Some of these small steps are represented by photovoltaic plants.

The present work wanted to give an outline of the design process of a PV plant and on the ways of estimation of its performance, in terms of energy production and Performance Ratio (PR). Different methods of calculation have been presented, all based on the necessity of valuable meteorological data to be applied; several experimental measures have been performed to characterize both the plant as a whole and its singular components.

The deficiency of modules has been associated to hot-spot presence; the cause of this localized heating, in the specific case analysed, have been related to a reduction of the shunt (parallel) resistance of the equivalent solar cell circuit, caused by constructive defects, which induces the rise of superficial dispersion currents and lead to relevant thermal loads on the module, difficult to dissipate. The presence of hot-spots causes an average module's nominal power reduction of almost 15% with respect its nominal value. For the case study PV plant, the connection of several modules with hot-spot problems (the 7% of the whole number installed) in the 80% of the strings installed has brought yearly productivity below 1'300 kWh/kW$_p$, value under average for optimally set PV plants of northern Italy (around 1'400 kWh/kW$_p$).

The hearth of the discussion was certainly linked to the process of revamping of an existent plant. In general, the identification of the installations which, for a reason or another, mainly economical, were not designed optimally is crucial for revamping operation because it allows to exploit already existent sites, avoiding the occupation of different areas (reducing consequently all possible environmental impacts consequent to new installations), and it permits to return the original plant performant and economically interesting.

For the case considered, indeed, the estimated +10% increase in productivity with respect the original situation, allows to recover the investment in around 6 years; being the remaining incentive period longer, after the PBT period, the plant starts producing economic benefits estimated to be, at the end of the considered period, 9% higher than the expected value if the plant had not been modified.

In general, design, construction and operation of a plant must not only follow economic considerations, but the scrupulous management of available resources must lead to careful choices for the protection of the environment. And it is precisely in this context that it is inserted one of revamping's targets: reducing the environmental impact connected to new installations by improving or renewing existing ones. Since environmental concerns are prominent aspects to consider for each project, especially in Italy (where the legislation is quite twisted), personally, I believe that operations aimed at improving already existent installations will be more and more relevant and frequent in the future.

Bibliography and sitography[36]

Abstract

1. GSE, “Rapporto statistico”,2016.
2. *GSE, “Rapporto statistico”,2016 – fig.7.*
3. Ministero dello Sviluppo Economico, Ministero dell’Ambiente e della Tutela del Territorio e del Mare, “Strategia energetica nazionale”, 2017.
4. *Ministero dello Sviluppo Economico, Ministero dell’Ambiente e della Tutela del Territorio e del Mare, “Strategia energetica nazionale”, 2017 – fig. 1,3,6,8,9.*
5. IEA (“International energy agency), “World energy outlook”,2016,2017.
6. *IEA (“International energy agency), “World energy outlook”,2016,2017 – fig.2,4,5.*

Chapter 1

7. F.Spertino, Notes and slides from the course “Power generation from renewable sources” ,2017.
8. *F.Spertino, Notes and slides from the course “Power generation from renewable sources” ,2017 – fig.7-17,19-21.*
9. G.V. Fracastoro, Notes and slides from the course “Technology for renewable energy sources”, 2017.
10. *G.V. Fracastoro, Notes and slides from the course “Technology for renewable energy sources”, 2017 – fig.1-4.*
11. *GSE, “Rapporto statistico”,2016 – fig.5-6, 28-34.*
12. *Canfailla, Ciabatti, Del Corto, Satti, “Progettazione ed esecuzione di impianti fotovoltaici: manuale operativo per il cantiere”,Dei editore, 2012 – fig.18, 22-27.*
13. F.Califano, V.Silvestrini, G.Vitale, “La progettazione di sistemi fotovoltaici”, Liguori, 1988.
14. F.Lasnier, T.G.Ang, “Photovoltaic Engineering Handbook”, A. Hilger, 1990.
15. T.Markvart, “Solar electricity”, J. Wiley&Sons, 1994, 2nd Ed. 2001.
16. Lorenzo, “Solar electricity”, Progensa, 1994.
17. F.Sick, T.Erge, “Photovoltaics in Buildings: a Design Handbook for Architects and Engineers”, James&James, 1995.
18. A.Goetzberger, J.Knobloch, B.Voss, "Crystalline silicon solar cells", J. Wiley&Sons, 1998.
19. A.Abete, F.Spertino, “Generatori e Impianti Fotovoltaici”, Dip. Ingegneria Elettrica, Politecnico di Torino, CELID, 2001.
20. M.Archer, R.Hill, “Clean Electricity from Photovoltaics”, Series on Photoconversion of Solar Energy, Imperial College Press, 2001.
21. T.Markvart, L.Castaner, "Practical handbook of photovoltaics: fundamentals and applications", Elsevier Science, 2003.
22. F.Groppi, C.Zuccaro, “Impianti solari fotovoltaici a norme CEI: guida per progettisti e installatori”, Ed. Delfino, 2005.

[36] List of figures and relative source in italic.

23. N.Aste, “Il fotovoltaico in architettura: l’integrazione edilizia dei sistemi per la generazione di elettricità solare”, Gruppo Editoriale Esselibri Simone, 2005.
24. F.Groppi, "Il fotovoltaico per tutti: manuale pratico per esperti e meno esperti" Ed. Delfino, 2005.
25. PVeducation.it

Chapter 2

26. Canfailla, Ciabatti, Del Corto, Satti, “Progettazione ed esecuzione di impianti fotovoltaici: manuale operativo per il cantiere”,Dei editore, 2012.
27. *Canfailla, Ciabatti, Del Corto, Satti, “Progettazione ed esecuzione di impianti fotovoltaici: manuale operativo per il cantiere”,Dei editore, 2012 – fig. 2-9*
28. Pepe, Del Zotto, Dignani, “Impianti fotovoltaici: manuale pratico per la progettazione e la manutenzione”, Dei editore, 2012.
29. F.Spertino, Notes and slides from the course “Power generation from renewable sources” ,2017.
30. *Eurostat.eu – fig. 1*
31. G.V. Fracastoro, Notes and slides from the course “Technology for renewable energy sources”, 2017.
32. *G.V. Fracastoro, Notes and slides from the course “Technology for renewable energy sources”, 2017 – fig.10-11*

Chapter 3

- G.V. Fracastoro, Notes and slides from the course “Technology for renewable energy sources”, 2017.
- F.Spertino, Notes and slides from the course “Power generation from renewable sources” ,2017.

Chapter 4

- Zhang Z, Wang L, et alia., “Study of bypass diode reliability under non-uniform irradiance distribution on PV module surface”, Acta Energiae Solaris Sinica,2016.
- *Zhang Z, Wang L, et alia., “Study of bypass diode reliability under non-uniform irradiance distribution on PV module surface”, Acta Energiae Solaris Sinica,2016, fig. 10, 12-14.*
- Shifeng D, Zhen Z, et alia, “Research on hot-spot risk for high-efficiency solar module”, SNEC 11th International Photovoltaic Power Generation Conference & Exhibition, 2017, Shanghai, China.
- O. Breitenstein, J.P. Rakotoniaina, M.H. Rifai, M. Werner, “Shunt types in crystalline silicon solar cells”, Progress in Photovoltaic: Research and applications 12, 2004.
- *O. Breitenstein, J.P. Rakotoniaina, M.H. Rifai, M. Werner, “Shunt types in crystalline silicon solar cells”, Progress in Photovoltaic: Research and applications 12, 2004, fig.11.*

- IEA ("International energy agency), "Review of Failures of Photovoltaic Modules" – Photovoltaic Power system programme – Report IEA-PVPS T13-01:2914.
- *IEA ("International energy agency), "Review of Failures of Photovoltaic Modules" – Photovoltaic Power system programme – Report IEA-PVPS T13-01:2914 – fig. 2-3,9,19*
- F.Spertino, Notes and slides from the course "Power generation from renewable sources" ,2017.
- *F.Spertino, Notes and slides from the course "Power generation from renewable sources" ,2017 – fig. 21*

Chapter 5

- G.V. Fracastoro, Notes and slides from the course "Technology for renewable energy sources", 2017.
- F.Spertino, Notes and slides from the course "Power generation from renewable sources" ,2017.
- P.Leone, Notes and slides from the course "Thermal design and optimization" ,2017.
- E.Bellini, "Revamping Italian PV", PV magazine, 2017.

APPENDIX A

PV*SOL uses some dedicated models to perform calculations:

1) Irradiance:

   In the supplied climate files, radiation to the horizontal plane is given in watts per square meter of active solar surface (radiation to the horizontal plane). The program converts the value to the tilted surface during the simulation in the radiation processor and multiplies it by the total active solar surface.

   From time t, sun's position is computed as length, width and time zone (according to DIN5034-2[37]); the incident angle θ of the irradiance on the PV modules is computed with trigonometric calculations.

   The global horizontal irradiance is separated into is direct and diffuse components, adopting specific models for decomposition:

- **Reindl** with reduced correlation - Reindl, D.T.; Beckmann, W. A.; Duffie, J.A.: Diffuse fraction correlations; Solar Energy; Vol. 45; No. 1, S.1.7; Pergamon Press; 1990.
- **Orgill & Hollands** - Orgill, J. F., & Hollands, K. G. T. (1977). Correlation equation for hourly diffuse radiation on a horizontal surface. Solar Energy, 19(4), 357–359.
- **Erbs, Klein & Duffie** - Erbs, D. G., Klein, S. A., & Duffie, J. A. (1982). Estimation of the diffuse radiation fraction for hourly, daily and monthly-average global radiation. Solar Energy, 28(4), 293–302.
- **Boland, Ridley & Laurent** - Ridley, B., Boland, J., & Lauret, P. (2010). Modelling of diffuse solar fraction with multiple predictors. Renewable Energy, 35(2), 478–483.
- **Perez & Ineichen** - Perez, R. R., Ineichen, P., Maxwell, E. L., Seals, R. D., & Zelenka, A. (1992). Dynamic global-to-direct irradiance conversion models. In ASHRAE Transactions (Vol. 98, pp. 354–369).
- **Hofmann** - Hofmann, M., & Seckmeyer, G. (2017). A New Model for Estimating the Diffuse Fraction of Solar Irradiance for Photovoltaic System Simulations. Energies, 10(2), 248.
- **Skartveit** - Skartveit, A., Olseth, J. A., & Tuft, M. E. (1998). An hourly diffuse fraction model with correction for variability and surface albedo. Solar Energy, 63(3), 173–183.

For diffuse radiation determination, the program adopts the following models:

[37] German norm about Sun's lighting.

- **Hay & Davies** - Hay, J. E., & Davies, J. A. (1980). Calculation of the Solar Radiation Incident on an Inclined Surface. In Proceedings of First Canadian Solar Radiation Data Workshop. Toronto.

- **Liu & Jordan** - Liu, B. Y. H., & Jordan, R. C. (1960). The interrelationship and characteristic distribution of direct, diffuse and total solar radiation. Solar Energy, 4(3), 1–19.

- **Klucher** - Klucher, T. M. (1979). Evaluation of models to predict insolation on tilted surfaces. Solar Energy, 23(2), 111–114.

- **Perez -** Perez, R., Seals, R., Ineichen, P., Stewart, R., & Menicucci, D. (1987). A new simplified version of the perez diffuse irradiance model for tilted surfaces. Solar Energy, 39(3), 221–231.

- **Reindl -** Reindl, D. T., Beckman, W. A., & Duffie, J. A. (1990). Evaluation of hourly tilted surface radiation models. Solar Energy, 45(1), 9–17.

2) PV modules temperature:

   Module temperature has a strong influence on the characteristic curve of PV modules, as seen in ch.1.3.5.

   With a simulation interval of one hour, the module temperature is calculated statically from the irradiance and a temperature offset depending on the installation type.

   This static temperature model is unsuitable for a simulation in minute intervals with variable irradiance, since it does not take into account the thermal inertia of the module. Therefore, a dynamic temperature model is used for a simulation interval of one minute, introducing a thermal capacitance factor for the modules.

3) PV modules characteristic curve:

   PV*SOL model for characteristic curves is primarily a mathematical model that requires absolute input values in the form of an additional set of electrical data with a partial load point near 20% of the STC irradiance in addition to the electrical data supplied by the manufacturer.

4) <u>Losses</u>:

-Conversion to DC and AC and MPP tracking: via the efficiency characteristic curve of each inverter in database, PV*SOL® calculates the output power depending on the input power;

-Cable losses: Ohm's law;

-Shading: PV*SOL simulates on substring level the PV modules so that the losses due to partial shading, and so to active bypass diodes, are considered. Each substring is checked whether there is a shadow or not. If there is a shadow, the bypass diode is active.

PV*SOL assumes from this that the shaded substrings are never completely in shadow, but that there is always diffused radiation on the shaded parts. There is therefore a I-V-curve with lower current for these cells as well.

APPENDIX B – PVGIS values for irradiance and ambient temperature

Hour	January		February		March		April		May		June	
	G (W/m^2)	Ta (°C)	G (W/m^2)	Ta (°C)	G (W/m^2)	Ta (°C)	G (W/m^2)	Ta (°C)	G (W/m^2)	Ta (°C)	G (W/m^2)	Ta (°C)
04:45	0	-1.7	0	-2.7	0	2.7	13	8.2	51	12.7	63	17.2
05:00	0	-1.6	0	-2.6	0	2.9	28	8.4	65	13	72	17.5
05:15	0	-1.5	0	-2.4	0	3.1	40	8.7	85	13.4	100	17.8
05:30	0	-1.4	0	-2.2	11	3.5	69	9	116	13.7	131	18.2
05:45	0	-1.2	0	-1.9	34	3.9	100	9.4	150	14.1	166	18.5
06:00	0	-1	0	-1.6	62	4.3	134	9.8	186	14.5	204	18.8
06:15	0	-0.8	11	-1.2	102	4.8	171	10.3	224	14.8	243	19.2
06:30	0	-0.6	44	-0.7	143	5.3	210	10.8	263	15.2	283	19.5
06:45	0	-0.3	79	-0.3	186	5.8	249	11.2	302	15.6	324	19.8
07:00	42	0	124	0.2	232	6.3	288	11.7	341	16	364	20.2
07:15	74	0.3	167	0.7	278	6.9	328	12.2	380	16.4	405	20.5
07:30	114	0.6	211	1.1	323	7.4	366	12.6	418	16.7	445	20.8
07:45	149	1	255	1.6	368	7.9	404	13.1	455	17.1	483	21.1
08:00	184	1.3	297	2.1	411	8.4	440	13.5	491	17.4	520	21.4
08:15	217	1.7	338	2.6	453	8.9	474	13.9	524	17.7	556	21.7
08:30	248	2.1	377	3	493	9.3	506	14.2	556	18	590	22
08:45	277	2.5	414	3.4	530	9.6	537	14.6	586	18.3	621	22.3
09:00	304	2.8	448	3.8	564	10	565	14.9	613	18.5	650	22.5
09:15	329	3.2	480	4.2	596	10.3	590	15.1	638	18.7	677	22.7
09:30	351	3.6	508	4.6	624	10.6	613	15.4	661	18.9	701	22.9
09:45	371	4	533	4.9	649	10.8	633	15.6	681	19.1	722	23.2
10:00	388	4.4	555	5.3	671	11.1	650	15.8	698	19.3	740	23.3
10:15	402	4.7	573	5.6	689	11.3	665	16	712	19.5	756	23.5
10:30	413	5	588	5.9	704	11.5	677	16.1	724	19.6	768	23.7
10:45	422	5.3	599	6.1	715	11.7	685	16.3	732	19.8	777	23.8
11:00	427	5.6	606	6.4	722	11.9	691	16.4	738	19.9	784	24
11:15	430	5.8	610	6.6	726	12	694	16.6	741	20	787	24.1
11:30	430	6	610	6.9	726	12.2	694	16.8	741	20.1	787	24.2
11:45	427	6.2	606	7	722	12.4	691	16.9	738	20.2	784	24.3
12:00	422	6.3	599	7.2	715	12.6	685	17	732	20.3	777	24.4
12:15	413	6.4	588	7.4	704	12.7	677	17.1	724	20.4	768	24.5
12:30	402	6.4	573	7.5	689	12.8	665	17.2	712	20.5	756	24.5
12:45	388	6.4	555	7.5	671	12.9	650	17.3	698	20.5	740	24.6
13:00	371	6.4	533	7.6	649	13	633	17.4	681	20.5	722	24.6
13:15	351	6.3	508	7.6	624	13	613	17.4	661	20.5	701	24.6
13:30	329	6.2	480	7.5	596	13	590	17.4	638	20.5	677	24.6
13:45	304	6.1	448	7.4	564	12.9	565	17.3	613	20.5	650	24.6
14:00	277	5.9	414	7.2	530	12.8	537	17.2	586	20.4	621	24.6
14:15	248	5.6	377	7	493	12.6	506	17.1	556	20.4	590	24.6
14:30	217	5.4	338	6.7	453	12.4	474	16.9	524	20.3	556	24.5
14:45	184	5.1	297	6.4	411	12.1	440	16.6	491	20.1	520	24.4
15:00	149	4.8	255	6	368	11.7	404	16.4	455	20	483	24.3
15:15	114	4.4	211	5.6	323	11.4	366	16.1	418	19.8	445	24.2
15:30	74	4.1	167	5.2	278	11	328	15.7	380	19.6	405	24
15:45	20	3.8	124	4.7	232	10.6	288	15.4	341	19.3	364	23.9
16:00	0	3.4	79	4.3	186	10.2	249	15	302	19.1	324	23.7
16:15	0	3	44	3.8	143	9.8	210	14.7	263	18.8	283	23.4
16:30	0	2.7	11	3.4	102	9.4	171	14.3	224	18.5	243	23.2
16:45	0	2.4	0	3	62	9	134	13.9	186	18.2	204	22.9
17:00	0	2.1	0	2.6	27	8.6	100	13.5	150	17.9	166	22.7
17:15	0	1.8	0	2.2	11	8.2	69	13.2	116	17.6	131	22.3
17:30	0	1.6	0	1.9	0	7.9	40	12.8	85	17.2	100	22
17:45	0	1.4	0	1.6	0	7.6	28	12.5	65	16.9	72	21.7
18:00	0	1.2	0	1.4	0	7.3	13	12.2	51	16.5	63	21.3
18:15	0	1	0	1.1	0	7.1	0	11.9	36	16.1	50	20.9
18:30	0	0.9	0	0.9	0	6.9	0	11.6	22	15.8	37	20.5

Hour	July		August		September		October		November		December	
	G (W/m^2)	Ta (°C)	G (W/m^2)	Ta (°C)	G (W/m^2)	Ta (°C)	G (W/m^2)	Ta (°C)	G (W/m^2)	Ta (°C)	G (W/m^2)	Ta (°C)
04:45	54	19.6	29	18.6	0	14.1	0	8.9	0	3.7	0	-1.3
05:00	58	19.9	42	18.9	0	14.3	0	9.1	0	3.8	0	-1.2
05:15	89	20.2	57	19.1	14	14.6	0	9.3	0	4	0	-1
05:30	124	20.6	89	19.5	32	14.9	0	9.5	0	4.2	0	-0.9
05:45	164	20.9	126	19.8	61	15.3	0	9.8	0	4.5	0	-0.7
06:00	206	21.3	166	20.2	95	15.6	20	10.2	0	4.8	0	-0.4
06:15	250	21.6	210	20.5	133	16.1	45	10.6	0	5.1	0	-0.2
06:30	296	22	254	20.9	175	16.5	76	11	0	5.5	0	0.1
06:45	342	22.3	300	21.4	219	17	115	11.4	28	5.9	0	0.5
07:00	388	22.7	346	21.8	264	17.4	152	11.8	56	6.3	0	0.8
07:15	434	23.1	391	22.2	309	17.9	190	12.2	89	6.7	53	1.2
07:30	479	23.4	436	22.6	353	18.3	227	12.7	127	7.1	87	1.5
07:45	523	23.8	479	23	397	18.7	264	13.1	162	7.5	130	1.9
08:00	565	24.1	520	23.3	439	19.2	299	13.4	195	7.9	167	2.3
08:15	605	24.4	560	23.7	479	19.5	333	13.8	228	8.3	202	2.7
08:30	643	24.7	598	24	517	19.9	365	14.1	259	8.7	236	3.1
08:45	679	25	633	24.3	553	20.2	394	14.4	288	9	267	3.5
09:00	711	25.2	665	24.6	586	20.5	422	14.6	314	9.3	296	3.9
09:15	742	25.5	694	24.8	616	20.7	447	14.8	339	9.6	322	4.3
09:30	769	25.7	721	25.1	644	21	469	15	361	9.9	346	4.7
09:45	793	25.9	744	25.3	668	21.2	489	15.2	380	10.1	367	5
10:00	813	26.1	765	25.5	688	21.4	506	15.4	397	10.4	385	5.4
10:15	831	26.3	782	25.7	706	21.6	521	15.5	411	10.6	400	5.7
10:30	845	26.5	795	25.9	720	21.8	532	15.7	423	10.8	413	6
10:45	855	26.7	806	26.1	731	22	541	15.8	431	10.9	422	6.2
11:00	862	26.8	813	26.3	738	22.1	547	15.9	437	11.1	428	6.4
11:15	866	27	816	26.4	741	22.3	550	16.1	440	11.2	431	6.6
11:30	866	27.1	816	26.6	741	22.5	550	16.2	440	11.4	431	6.8
11:45	862	27.2	813	26.8	738	22.6	547	16.3	437	11.5	428	6.9
12:00	855	27.4	806	26.9	731	22.8	541	16.5	431	11.5	422	6.9
12:15	845	27.5	795	27.1	720	22.9	532	16.6	423	11.6	413	7
12:30	831	27.6	782	27.2	706	23	521	16.6	411	11.6	400	7
12:45	813	27.6	765	27.3	688	23.1	506	16.7	397	11.6	385	6.9
13:00	793	27.7	744	27.3	668	23.2	489	16.7	380	11.6	367	6.9
13:15	769	27.7	721	27.4	644	23.2	469	16.8	361	11.5	346	6.8
13:30	742	27.7	694	27.4	616	23.2	447	16.7	339	11.4	322	6.6
13:45	711	27.7	665	27.4	586	23.1	422	16.7	314	11.3	296	6.4
14:00	679	27.7	633	27.3	553	23	394	16.6	288	11.1	267	6.2
14:15	643	27.6	598	27.2	517	22.9	365	16.4	259	10.9	236	6
14:30	605	27.6	560	27.1	479	22.7	333	16.2	228	10.7	202	5.7
14:45	565	27.5	520	26.9	439	22.4	299	16	195	10.4	167	5.5
15:00	523	27.3	479	26.7	397	22.1	264	15.8	162	10.1	130	5.2
15:15	479	27.2	436	26.4	353	21.8	227	15.5	127	9.8	87	4.8
15:30	434	27	391	26.2	309	21.4	190	15.2	89	9.5	53	4.5
15:45	388	26.8	346	25.9	264	21.1	152	14.8	56	9.2	0	4.2
16:00	342	26.6	300	25.6	219	20.7	115	14.5	16	8.8	0	3.8
16:15	296	26.3	254	25.2	175	20.3	76	14.2	0	8.5	0	3.5
16:30	250	26.1	210	24.9	133	19.9	45	13.9	0	8.2	0	3.1
16:45	206	25.8	166	24.6	95	19.6	15	13.5	0	7.9	0	2.8
17:00	164	25.5	126	24.2	61	19.2	0	13.2	0	7.6	0	2.5
17:15	124	25.2	89	23.9	32	18.9	0	13	0	7.4	0	2.2
17:30	89	24.8	57	23.5	14	18.5	0	12.7	0	7.2	0	2
17:45	58	24.4	42	23.2	0	18.3	0	12.5	0	7	0	1.7
18:00	54	24.1	29	22.9	0	18	0	12.3	0	6.8	0	1.5
18:15	42	23.7	15	22.6	0	17.7	0	12.1	0	6.7	0	1.3
18:30	29	23.3	0	22.3	0	17.5	0	12	0	6.5	0	1.1